Oklahoma Department of Transportation
200 NE 21st Street, Oklahoma City, OK 73105-3204

FINAL REPORT ~ FHWA-OK-14-10

ENERGY DISSIPATION IN THIRTY-FOOT BROKEN-BACK CULVERTS USING LABORATORY MODELS

Avdhesh K. Tyagi, Ph.D., P.E.
Abdelfatah Ali, Ph.D.
Matthew Hamilton
School of Civil and Environmental Engineering
College of Engineering, Architecture and Technology
Oklahoma State University

September 2014

Oklahoma Department of Transportation

DISCLAIMER

The contents of this report reflect the views of the author(s) who is responsible for the facts and the accuracy of the data presented herein. The contents do not necessarily reflect the views of the Oklahoma Department of Transportation or the Federal Highway Administration. This report does not constitute a standard, specification, or regulation. While trade names may be used in this report, it is not intended as an endorsement of any machine, contractor, process, or product.

ENERGY DISSIPATION IN THIRTY-FOOT BROKEN-BACK CULVERTS USING LABORATORY MODELS

FINAL REPORT ~ FHWA-OK-14-10

ODOT SP&R ITEM NUMBER 2254

Submitted to:

John R. Bowman, P.E.
Director of Capital Programs
Oklahoma Department of Transportation

Submitted by:

Avdhesh K. Tyagi, Ph.D., P.E.
Director
Abdelfatah Ali, Ph.D.
Matthew Hamilton
Research Associates
School of Civil Engineering and Environmental Engineering
Oklahoma State University

September 2014

TECHNICAL REPORT DOCUMENTATION PAGE

1. REPORT NO. FHWA-OK-14-10	**2. GOVERNMENT ACCESSION NO.**	**3. RECIPIENTS CATALOG NO.**
4. TITLE AND SUBTITLE ENERGY DISSIPATION IN THIRTY-FOOT BROKEN-BACK CULVERTS USING LABORATORY MODELS		**5. REPORT DATE** September 2014 **6. PERFORMING ORGANIZATION CODE**
7. AUTHOR(S): Avdhesh Tyagi, Ph.D., P.E., Abdelfatah Ali, Ph.D., Matthew Hamilton		**8. PERFORMING ORGANIZATION REPORT**
9. PERFORMING ORGANIZATION NAME AND ADDRESS Oklahoma Infrastructure Consortium School of Civil & Environmental Engineering Oklahoma State University 207 Engineering South Stillwater, OK 74078		**10. WORK UNIT NO.** **11. CONTRACT OR GRANT NO.** ODOT SP&R Item Number 2254
12. SPONSORING AGENCY NAME AND ADDRESS Oklahoma Department of Transportation Planning and Research Division 200 N.E. 21st Street, Room 3A7 Oklahoma City, OK 73105		**13. TYPE OF REPORT AND PERIOD COVERED** Final Report October 2013 –September 2014 **14. SPONSORING AGENCY CODE**

15. SUPPLEMENTARY NOTES
Oklahoma Transportation Center

16. ABSTRACT: This research investigates the reduction in scour downstream of a broken-back culvert by forming a hydraulic jump inside the culvert. A broken-back culvert is used in areas of high relief and steep topography as it has one or more breaks in profile slope. A broken-back culvert in the laboratory represents a 1 (vertical) to 2 (horizontal) slope after the upstream inlet and then continuing 90 feet at a 1 percent slope in the flat part of the culvert to the downstream outlet. The prototypes for these experiments were either a two barrel 10-foot by 10-foot, or a two barrel 10-foot by 20-foot reinforced concrete culvert. The drop between inlet and outlet was selected as 30 feet. Three flow conditions were simulated, consisting of 0.8, 1.0 and 1.2 times the culvert depth. This report represents Phase V of broken-back culverts with a drop of 30 feet. The first phase of this research was performed with a drop of 24 feet, the second phase of this research was carried with for a drop of 6 feet, the third phase of this research, performed was a drop of 18 feet, and the fourth phase of this research was performed with a drop of 12 feet.

The Froude number (F_{r1}) of the hydraulic jump created in the flat part of the culvert ranged between 2.53 and 5.66. This F_{r1} classifies the jump as an oscillating to steady jump. The jump began nearly at the toe by placing sills and friction blocks of different sizes in the flat part. For new culvert construction, the best option to maximize energy dissipation under open channel flow conditions is to use one 5.83-foot sill located 33.33 feet from the outlet. The maximum length of the culvert can be reduced from 25 feet to 30 feet that was for middle sill. For existing and new culverts, the best option is to use one end sill with height of 6.67-foot. In pressure flow conditions, the optimal location was determined at a distance of 31.67 feet from the outlet for 4.17-foot sill. The length of the culvert can be reduced by 25 feet to 30 feet. Also, for new and existing culverts, the optimal end sill is to use one 4.17-foot sill height under pressure flow conditions. Such a scenario is important where right-of-way problems exist for culvert construction. Also examined was a slotted sill which has a cut in the middle for cleanup purposes. In open channel flow conditions, the best option to maximize energy dissipation is to use one 5.83-foot slotted sill located 33.33 feet from the outlet, and for end slotted sill is to use 7.5-foot height. In the pressure flow conditions, the optimal slotted sill was 5-foot at a distance of 41.67 feet from the outlet, and for end slotted sill is to use 4.17-foot height. The regular and slotted sills contain two small orifices at the bottom to allow the culvert to completely drain. The impact of friction blocks was found to be minimal. No friction blocks were used to further dissipate the energy.

17. KEY WORDS Hydraulic jump, broken-back culvert, energy dissipation, pressure flow, open-channel flow	**18. DISTRIBUTION STATEMENT** No restrictions. This publication is available from the Planning and Research Division, Oklahoma DOT.		
19. SECURITY CLASSIF. (OF THIS REPORT) unclassified	**20. SECURITY CLASSIF. (OF THIS PAGE)** unclassified	**21. NO. OF PAGES** 170 pages	22. PRICE N/A

SI* (MODERN METRIC) CONVERSION FACTORS

APPROXIMATE CONVERSIONS TO SI UNITS				
SYMBOL	**WHEN YOU KNOW**	**MULTIPLY BY**	**TO FIND**	**SYMBOL**
LENGTH				
in	inches	25.4	millimeters	mm
ft	feet	0.305	meters	m
yd	yards	0.914	meters	m
mi	miles	1.61	kilometers	km
AREA				
in^2	square inches	645.2	square millimeters	mm^2
ft^2	square feet	0.093	square meters	m^2
yd^2	square yard	0.836	square meters	m^2
ac	acres	0.405	hectares	ha
mi^2	square miles	2.59	square kilometers	km^2
VOLUME				
fl oz	fluid ounces	29.57	milliliters	mL
gal	gallons	3.785	liters	L
ft^3	cubic feet	0.028	cubic meters	m^3
yd^3	cubic yards	0.765	cubic meters	m^3
NOTE: volumes greater than 1000 L shall be shown in m^3				
MASS				
oz	ounces	28.35	grams	g
lb	pounds	0.454	kilograms	kg
T	short tons (2000 lb)	0.907	megagrams (or "metric ton")	Mg (or "t")
TEMPERATURE (exact degrees)				
^oF	Fahrenheit	5 (F-32)/9 or (F-32)/1.8	Celsius	^oC
ILLUMINATION				
fc	foot-candles	10.76	lux	lx
fl	foot-Lamberts	3.426	candela/m^2	cd/m^2
FORCE and PRESSURE or STRESS				
lbf	poundforce	4.45	newtons	N
lbf/in^2	poundforce per square inch	6.89	kilopascals	kPa

APPROXIMATE CONVERSIONS FROM SI UNITS				
SYMBOL	**WHEN YOU KNOW**	**MULTIPLY BY**	**TO FIND**	**SYMBOL**
LENGTH				
mm	millimeters	0.039	inches	in
m	meters	3.28	feet	ft
m	meters	1.09	yards	yd
km	kilometers	0.621	miles	mi
AREA				
mm^2	square millimeters	0.0016	square inches	in^2
m^2	square meters	10.764	square feet	ft^2
m^2	square meters	1.195	square yards	yd^2
ha	hectares	2.47	acres	ac
km^2	square kilometers	0.386	square miles	mi^2
VOLUME				
mL	milliliters	0.034	fluid ounces	fl oz
L	liters	0.264	gallons	gal
m^3	cubic meters	35.314	cubic feet	ft^3
m^3	cubic meters	1.307	cubic yards	yd^3
MASS				
g	grams	0.035	ounces	oz
kg	kilograms	2.202	pounds	lb
Mg (or "t")	megagrams (or "metric ton")	1.103	short tons (2000 lb)	T
TEMPERATURE (exact degrees)				
^oC	Celsius	1.8C+32	Fahrenheit	^oF
ILLUMINATION				
lx	lux	0.0929	foot-candles	fc
cd/m^2	candela/m^2	0.2919	foot-Lamberts	fl
FORCE and PRESSURE or STRESS				
N	newtons	0.225	poundforce	lbf
kPa	kilopascals	0.145	poundforce per square inch	lbf/in^2

*SI is the symbol for the International System of Units. Appropriate rounding should be made to comply with Section 4 of ASTM E380.
(Revised March 2003)

Acknowledgments

This project was funded by the Federal Highway Administration and sponsored by the Oklahoma Department of Transportation. We would like to thank Mr. Robert Rusch, P.E., Bridge Division Engineer, Oklahoma Department of Transportation for his active participation in incorporating ideas to make this research more practical to field conditions.

In addition, Dr. Sherry Hunt and Kem Kadavy, P.E., Hydraulic Engineers of the U.S. Department of Agriculture, Agricultural Research Service, each contributed their ideas in the early stages of this project regarding ways to improve the physical construction of the model.

TABLE OF CONTENTS

List of Figures

List of Tables

Executive Summary

This research investigated the reduction in scour downstream of a broken-back culvert by forming a hydraulic jump inside the culvert. A broken-back culvert is used in areas of high relief and steep topography as it has one or more breaks in profile slope. A broken-back culvert in the laboratory represents a 1 (vertical) to 2 (horizontal) slope after the upstream inlet and then continues 90 feet at a 1 percent slope in the flat part of the culvert to the downstream outlet. The prototype for these experiments was either a two-barrel 10-foot by 10-foot, or a two-barrel 10-foot by 20-foot reinforced concrete culvert. The drop between the inlet and outlet was designated to be chosen to be 30 feet. Three flow conditions were simulated, consisting of 0.8, 1.0 and 1.2 times the culvert depth.

The Froude number of the hydraulic jump created in the flat part of the culvert ranged between 2.53 and 5.56. This Froude number classified a jump from an oscillating jump to steady jump. The jump in the experiments began nearly at the toe by placing sills and friction blocks of different sizes in the flat part. For new culvert construction, the best option to maximize energy dissipation under open channel flow conditions was to use one 5.83-foot sill located 33.33 feet from the outlet. The maximum length of the culvert can be reduced by 25 feet to 30 feet. Also, for existing and new culverts, the best option for end sill is to use 6.67-foot end sill height under open channel conditions. In pressure flow conditions, the optimal location was determined to be a distance of 31.67 feet from the outlet for a 4.17-foot sill. The length of the culvert can be reduced by 25 to 30 feet.

For a modified slotted sill, the best option to maximize energy dissipation under open channel flow conditions was to use one 5.83-foot slotted sill located 33.33 feet from the outlet. The maximum length of the culvert can be reduced by 25 to 30 feet. For sill placement at the end of the culvert a 7.5-foot sill is optimal. In pressure flow conditions, the optimal location was determined to be at a distance of 41.67 feet from the outlet for a 5-foot sill. The length of the culvert can be reduced by 25 to 30 feet, and

for the end slotted sill is to use 4.17-foot height under pressure flow conditions. Such a scenario is important where right-of-way problems exist for culvert construction.

The sills contain two small orifices at the bottom to allow the culvert to completely drain. The slotted sill has a cut in the middle and contains two small orifices at the bottom of the other parts to allow the culvert to completely drain and to use the middle cut to clean up the sedimentation behind the slotted sill. The impact of friction blocks was found to be minimal. Different friction blocks examined experimentally. It was found that a big size of friction blocks could make more impact in the energy dissipation.

It was found that slotted sill experiments yielded results most applicable to the new and existing construction of culverts for open and pressure flow conditions. Adding friction blocks to a slotted sill did not significantly increase the energy dissipation with these experiments. It was found that the friction blocks represented only a 2% increase in the energy dissipation; therefore they are not economical or practical to the culvert design. Also, the culvert barrel could be shortened by reducing a section at the end of the channel where the water surface profile is more uniform.

1 Introduction

A recent research study conducted by the Oklahoma Transportation Center at Oklahoma State University indicated that there are 121 scour-critical culverts on the Interstate System (ISTAT), the National Highway System (NHS), and the State Transportation Program (STP) in Oklahoma (Tyagi, 2002). The average replacement cost of these culverts is about $121M. A survey of culverts in Oklahoma indicates that the drop in flowline between upstream and downstream ends ranges between 6 and 30 feet. Tyagi et al. (2009, 2011, and 2012) carried out five phases of these projects; the first phase of this research was performed for a drop of 24 feet, the second phase of this research was performed for a drop of 6 feet, the third phase of this research was performed for a drop of 18 feet, the fourth phase of this research was performed for a drop of 12 feet. The fifth and final phase was 30-foot drop. Each drop has its own optimum characteristics. Since the 30-foot drop height is different from the other heights, there will be a difference in the optimum sill location and sill height from other drop heights.

This report represents Phase V of broken-back culverts with a drop of 30 feet. A drop of 30 feet was used in the laboratory model because it is highest drop within the project scope. Results of this research targeted maximizing the energy loss within the culvert, thus minimizing the scour around the culvert and decreasing the degradation in the downstream channel. This will reduce the construction and rehabilitation costs of culverts in Oklahoma. The project is supported by the Bridge Division, Oklahoma Department of Transportation (ODOT).

The purpose of this project was to develop a means for energy dissipation in broken-back culverts. Once created, energy dissipaters were experimented and analyzed to find the optimal energy dissipation, so that degradation could be minimized downstream. The purpose of a culvert is to safely pass water underneath the roadways constructed in hilly topography or on the side of a relatively steep hill. A broken-back culvert is used in areas of high relief and steep topography as it has one or more breaks in the profile slope. Culvert dimensions and hydraulic parameters for the scale model

were provided by the Bridge Division, ODOT (personal communication with R. Rusch, 2007).

The research investigation included the following tasks: 1) Obtaining and reviewing existing research currently available for characterizing the hydraulic jump in culverts; 2) Building a scale model representing a prototype of a broken-back culvert 150 feet long, with two barrels of 10 X 10 feet, and a vertical drop of 30 feet; 3) Simulating different flow conditions for 0.8, 1.0 and 1.2 times the culvert depth (d) In the scale model; 4) Evaluating the energy dissipation between upstream and downstream ends of the broken-back culvert with and without friction blocks of different shapes; 5) Refining the sill design for easy drainage of water from the broken-back culverts using regular and slotted sills; 6) Observing in physical experiments the efficiency of the hydraulic jump with and without friction blocks between the upstream and downstream ends of the culvert and the location of the hydraulic jump from the toe of the drop in the culvert; and 7) Preparing a final report incorporating the analysis of the hydraulic jump and the devices to create the jump and energy loss. These tasks are presented in the following sections.

2 Literature Review

The literature search was performed for hydraulic jump and Acoustic Doppler Velocimeter and the results are discussed in the following sections.

2.1 HYDRAULIC JUMP

The hydraulic jump is a natural phenomenon of a sudden rise in water level due to a change from supercritical flow to subcritical flow, i.e., when there is a sudden decrease in the velocity of the flow. This sudden change in velocity causes considerable turbulence and loss of energy. Consequently, the hydraulic jump has been recognized as an effective method for energy dissipation for many years. There have been many studies carried out to explain the characteristics of the hydraulic jump. Some of these studies are summarized in the following paragraphs.

There are four basic regimes of flow: subcritical-laminar, supercritical-laminar, subcritical-turbulent, and supercritical-turbulent (Chow, 1959). Smith and Oak (1994) conducted experiments to determine the inlet efficiency of a culvert. They found that projecting a slightly larger frame of the culvert upstream increased inlet efficiency. This study was done on circular culverts and showed the relationship between inlet styles and inlet efficiency.

Pegram et al. (1999) conducted various experiments looking at skimming flow over stepped spillways. The turbulence associated with this study and the examination of model versus prototype scale impacts make it especially interesting in view of anticipated hydraulic jump. They found that a scale of down to 1:20 can accurately give results in a model highly indicative of prototype reactions.

Campbell et al. (1985) found that for supercritical flows the mass flow rate is controlled by the inlet conditions; but for subcritical flows the mass flow rate becomes controlled by the material properties of the flow and the channel declination. This indicates that sedimentation will be more likely in the subcritical flow after the induced hydraulic jump in the culverts of this study.

Chanson (1996) discussed the occurrence of undular jump characteristics in culverts. He concluded that in standard culverts the flow can reasonably be predicted by using critical flow assumptions. He warned that this could not accurately predict all parameters in the culvert, but can be used for reasonable approximations in undular flow conditions. His study indicated the lack of experimental data in culvert studies at that time.

Stahl and Hager (1998) conducted various experiments analyzing hydraulic jump in circular conduits. They note that in jump conditions where the surface is not allowed to be free but becomes pressurized the characteristics begin to deviate from those in classical hydraulic jump. This deviation from classical hydraulic jump has prompted the study of extended height culverts as well as the observation of incomplete jump formation in typical box culverts with induced jump.

Ohtsu et al. (1996) evaluated incipient hydraulic jump conditions on flows over vertical sills. They identified two methods of obtaining an incipient jump: 1) increasing the sill height, or 2) increasing the tailwater depth until a surface roller forms upstream of the sill. For wide channels, predicted and experimental data were in agreement, but in the case of narrow channels, incipient jump was affected by channel width.

Mignot and Cienfuegos (2010) focused on an experimental investigation of energy dissipation and turbulence production in weak hydraulic jumps. Froude numbers ranged from 1.34 to 1.99. Mignot and Cienfuegos observed two peak turbulence production regions for the partially developed inflow jump, one in the upper shear layer and the other in the near-wall region. The energy dissipation distribution in the jumps was measured and revealed a similar longitudinal decay of energy dissipation, which was integrated over the flow sections and the maximum turbulence production values from the intermediate jump region towards its downstream section. It was found that the energy dissipation and the turbulence production were strongly affected by the inflow development. Turbulence production showed a common behavior for all measured jumps. It appeared that the elevation of maximum Turbulent Kinetic Energy (TKE) and turbulence production in the shear layer were similar.

Alikhani et al. (2010) conducted many experiments to evaluate the effects of a continuous vertical end sill in a stilling basin. They measured the effects of sill position on the depth and length of a hydraulic jump without considering the tailwater depth. In the experiments, they used five different sill heights placed at three separate longitudinal distances in their 1:30 scaled model. The characteristics of the hydraulic jump were measured and compared with the classic hydraulic jump under varied discharges. They proposed a new relationship between sill height and position, and sequent depth to basin length ratio. The study concluded that a 30% reduction in basin length could be accomplished by efficiently controlling the hydraulic jump length through sill height.

Finnemore et al. (2002) stated that the characteristics of the hydraulic jump depend on its Froude number (F_{r1}). The Froude number is the ratio between inertia force and gravity force. They added that in order for the hydraulic jump to occur, the flow must be supercritical, i.e. a jump can occur only when the Froude number is greater than 1.0. The hydraulic jump is classified according to its Froude number. When F_{r1} is between 1.7 and 2.5, the flow is classified as a weak jump and will have a smooth rise in the water surface with less energy dissipation. A F_{r1} between 2.5 and 4.5 results in an oscillating jump with 15-45% energy dissipation. A steady jump will occur when F_{r1} ranges from 4.5 to 9.0, and results in energy dissipation from 45% to 70%. When F_{r1} is above 9.0, a strong jump will occur with energy losses ranging from 70% to 85%.

Ohtsu et al (2001) investigated undular hydraulic jump conditions in a smooth rectangular horizontal channel. They found that the formation of an undular jump depends only on the inflow Froude number and the boundary-layer development at the toe of the jump. At its Froude number ranges, they found that the effects of the aspect ratio and the Reynolds number on the flow characteristics were negligible. Under experimental investigation, it was found that the upper limits of the Froude numbers range between 1.3 and 2.3 at the inflow. Furthermore, a Froude number of 1.7 was found to be the critical velocity point at which inflow was fully developed. They calculated the ratio thickness of the boundary layer to the depth of the toe of the jump to be 0.45 to 1.0, which agreed with predicted values from experimental results.

Bhutto et al. (1989) provided analytical solutions for computing sequent depth and relative energy loss for a free hydraulic jump in horizontal and sloping rectangular channels from their experimental studies. They used the ratio of jump length to jump depth and the Froude number to compute the length of the free jump on a horizontal bed. Jump factor and shape factor were evaluated experimentally for the free jump on a sloping bed. To check the efficiency of the jump, they made comparisons with previous solutions by Ludin, Bakhmateff, Silvester and Chertoussove and found that the equations they derived could be used instead of their equations.

Gharanglk and Chaudhry (1991) presented three models for the numerical simulation of hydraulic jumps in a rectangular channel while factoring in the considerable effect of nonhydrostatic pressure distribution. The one-dimensional Boussinesq equations are solved in time subject to appropriate boundary conditions which numerically simulate the hydraulic jump. The results were compared to experimental data which indicate that four-order models with or without Boussinesq terms gave similar results for all Froude numbers tested. The Froude numbers ranged from 2.3 to 7.0. The MacCormack scheme and a dissipative two-four scheme were used to solve the governing equations subject to specified end conditions until a steady state was achieved.

Hotchkiss and Donahoo (2001) reported that the Broken-back Culvert Analysis Program (BCAP) is a simple but powerful analysis tool for the analysis of broken-back culverts and hydraulic jumps. The program is easy to understand, explain, and document, and is based on the energy equation and momentum equation for classical jumps. It is able to plot rating curves for the headwater, outlet depth and outlet velocity. Hotchkiss and Donahoo described a computer code capable of analyzing hydraulic jumps in the broken-back culvert.

Hotchkiss et al. (2003) described the available predictive tools for hydraulic jumps, the performance of the Broken-Back Culvert Analysis Program (BCAP) in analyzing the hydraulics of a broken-back culvert, and the current applications and distribution of BCAP. They conducted tests on the Broken-Back culvert made of Plexiglas® to assess the performance of BCAP in predicting headwater rating curves,

the locations of hydraulic jumps, and the lengths of hydraulic jumps. Hotchkiss et al. concluded that accounting for the losses within the jumps because of friction in corrugated metal pipes and more accurately predicting the locations of hydraulic jumps may both be improved by predictions of flow hydraulics within the culvert barrel.

The Utah Department of Transportation (UDOT) addresses aspects of broken-back culverts and hydraulic jumps in the state's *Manual of Instruction – Roadway Drainage (US Customary units), Culverts (2004)*. This manual illustrates steps for the design of broken-back culverts which include: 1) Establishing a flow-line profile, 2) Sizing the culvert, 3) Beginning to calculate a supercritical profile, 4) Completing profile calculations, and 5) Considering hydraulic jump cautions. Section F of Appendix 9 of the manual covers aspects of hydraulic jumps in culverts, including: cause and effect, momentum friction, comparison of momentum and specific energy curves, and the potential occurrence of hydraulic jumps. The manual also takes into account the sequent depth of jump for rectangular conduits, circular conduits, and conduits of other shapes.

Larson, (2004), in her Master's thesis entitled *Energy Dissipation in Culverts by Forcing a Hydraulic Jump at the Outlet,* suggested forcing hydraulic jumps to reduce the outlet energy. She considered two design examples to create a hydraulic jump within a culvert barrel: (1) a rectangular weir placed on a flat apron and (2) a vertical drop along with a rectangular weir. These two designs were used to study the energy reduction in the energy of the flow at the outlet. From these experiments, she found that both designs were effective in the reducing of outlet velocity, momentum, and energy. These reductions would decrease the need for downstream scour mitigation.

Hotchkiss et al. (2005) proposed that by controlling the water at the outlet of a culvert, water scour around the culvert can be reduced. The effectiveness of a simple weir near the culvert outlet was compared to that of a culvert having a weir with a drop upstream in the culvert barrel. These two designs were intended to reduce the specific energy of the water at the outlet by inducing a hydraulic jump within the culvert barrel, without the aid of tailwater. The design procedure was proposed after studying the geometry and effectiveness of each jump type in energy reduction. In this research,

they found the Froude number ranged from 2.6 to 6.0. It was determined that both forms of outlets are effective in reducing the velocity of water; hence the energy and momentum thus reduced the need for downstream scour mitigation.

The *Hydraulic Design of Energy Dissipators for Culverts and Channels* (July, 2006), from the Federal Highway Administration, provides design information for analyzing and mitigating problems associated with the energy dissipation at culvert outlets and in open channels. It recommends the use of the broken-back culvert design as an internal energy dissipator. The proposed design for a broken-back culvert is limited to the following conditions: 1) the slope of the steep section must be less than or equal to 1.4:1 (V: H) and 2) the hydraulic jump must be completed within the culvert barrel.

According to this report, for situations where the runout section is too short and/or there is insufficient tailwater for a jump to be completed within the barrel, modifications may be made to the outlet that will induce a jump. The design procedure for stilling basins, streambed level dissipaters, riprap basins and aprons, drop structures and stilling wells is also discussed.

Pagliara et al. (2008) analyzed the hydraulic jump that occurs in homogeneous and nonhomogeneous rough bed channels. They investigated the sequent flow depth and the length of the jump which are the influence parameters of the hydraulic jump. In this research, they drew on the general jump equation to analyze the jump phenomenon. In analyzing the rough bed data, they were able to formulate a representative equation to explain the phenomenon. The equations found in their study may be used to design stilling basins downstream of hydraulic structures.

Hotchkiss et al. (2008) analyzed the accuracy of the following seven programs on culvert hydraulics: HY-8, FishXing, Broken-back Culvert Analysis Program (BCAP), Hydraflow Express, CulvertMaster, Culvert, and Hydrologic Engineering Center River Analysis System (HEC-RAS). The software was tested on the accuracy of three calculations: headwater depths, flow control, and outlet velocities. The software comparison was made between software output values and hand calculations, not from laboratory experimental data. The hand calculations used were derived from laboratory

experiments done by the National Bureau of Standards (NBS). Hotchkiss et al. concluded HEC-RAS is the most comprehensive program for both accuracy and features for culverts affected by upstream structures.

Tyagi et al. (2009) investigated hydraulic jumps under pressure and open channel flow conditions in a broken-back culvert with a 24-foot drop. It was found that for pressure flow, a two-sill solution induced the most desirable jump, and for open channel a single sill close to the middle of the culvert was most desirable. The investigation was funded by the Oklahoma Transportation Center, Research and Innovative Technology Administration, Federal Highway Administration, and Oklahoma Department of Transportation.

Tyagi et al. (2010a) performed many experiments for open channel culvert conditions. Optimum energy dissipation was achieved by placing one sill at 40 feet from the outlet for 24-foot drop. Friction blocks and other modifications to the sill arrangement were not as effective.

Tyagi et al. (2011b) carried out many experiments with a 24-foot drop to optimize flow condition and energy dissipation in a broken-back culvert under pressure flow. It was found that two sills, the first 5 feet high at 25 feet from the outlet and the second 3.34 feet high at 45 feet from the outlet, gave the best results. The culvert could not be shortened since it was full under the tested conditions.

Tyagi et al. (2011) studied the energy dissipation in six-foot broken-back culverts using laboratory models. They stated that the Froude number for the experiments was 1.8 – 2.3, which classified the hydraulic jump as a weak jump. For open channel flow conditions, the best option to maximize energy dissipation is to use 3-foot sill located at 69 feet from the outlet of the culvert. The maximum length of the culvert can be reduced between 42 – 56 feet. Also, for pressure flow conditions, the optimal placement of one 2.1-foot sill was located 42 feet from the outlet face of the culvert.

Tyagi et al. (2012) examined energy dissipation in eighteen-foot broken-back culverts using laboratory models. For open channel flow conditions, it was found that one 5-foot sill located 43.3 feet from the outlet was the best option to maximize energy dissipation. Also, the maximum length of the culvert can be reduced by 30 – 43 feet

(Tyagi et al. (2013)). For pressure flow conditions, the optimal location of two sills was determined to be 62 feet from the outlet for a 2.5-foot sill and 45 feet from the outlet of culvert for a 3.3-foot sill. The culvert length can be reduced by 40 – 45 feet.

Moawad et al. (1994) found that culverts are more susceptible to damage when fully submerged due to uplift around the inlet. They concluded that scour mitigation measures such as aprons should be placed at the inlet of the culvert due to the increase in deterioration of the culvert possible from this uplift aggravated by scour.

Nettleton and McCorquodale (1989) studied the hydraulic jump induced in stilling basins by way of baffle blocks. They concluded that there is an optimal placement for the jump inducers: too close and a large hump will form, too far back and the jump length increases. They determined that a continuous end sill would produce better results, but their scope only covered the baffle blocks.

Acoustic Doppler Velocimeter (ADV) is a sonar device which tracks suspended solids (particles) in a fluid medium to determine an instantaneous velocity of the particles in a sampling volume. In general, ADV devices have one transmitter head and two to four receiver heads. Since their introduction in 1993, ADVs have quickly become valuable tools for laboratory and field investigations of flow in rivers, canals, reservoirs, the oceans, around hydraulic structures and in laboratory scale models (Sontek, 2001).

The flow rate was measured by an orifice plate between which measures the pressure difference in a fixed pipe opening size. An orifice plate is a device used for measuring the volumetric flow rate. It uses the same principle as a Venturi nozzle, namely Bernoulli's principle that states that there is a relationship between the pressure of the fluid and the velocity of the fluid. When the velocity increases, the pressure decreases and vice versa.

2.2 EFFECT OF FRICTION BLOCKS AND SILL IN BROKEN-BACK CULVERT

Eloubaidy et al. (1999) found that in order to provide better stability and after running multiple series of tests to determine which floor block dissipates the most

energy, the curved blocks work the best. Different experiments tested various sizes, curvatures, and locations of the blocks. By choosing these blocks, optimum flow conditions are created lowering the capacity for erosion of the downstream bed. The curved blocks range from 3.2% to 33.3% more effective in dissipating excessive kinetic energy.

Bessaih and Rezak (2002) tried to determine how to shorten the length of a hydraulic jump; experiments were run with different cut ratios of baffled blocks. The blocks' shapes will create strong vortices, which then shorten the lengths of the jumps. After completing the tests, it was shown that baffle blocks with a sloping face reduce the length of a jump up to 48% relative to the free jump, as well as up to 18% relative to USBR basin II. However, only an additional 5% decrease in length was observed when adding a second row, therefore adding an additional row is not very effective.

Oosterholt (1947) found that the total amount of heat generated and the decrease of the energy transport deviated greatly due to friction blocks. The surface roller dissipates the most energy in the lower part; energy dissipation also takes place in the upper part of the main stream. Continuing downstream, the energy dissipation slowly decreases. The surface roller's upper part only contributes to a small amount of the energy dissipation. The bottom friction also makes only a small contribution to energy dissipation.

According to Habibzadeh et al. (2012), observed two flow regimes: the deflected surface jet and the reattaching wall jet, during the study. In order to get the best results, various block arrangements and submerged factors were tested, as well as a wide range of different Froude numbers. In order to determine the maximum submergence factor (S_1) and minimum submergence factor (S_2), empirical equations were derived. Using the empirical equations that were developed it was found that 85% of the time the flow regime was able to be predicted. It was found also that adding more blocks and adjusting their heights did not play a strong role in the energy dissipation. In order to create energy dissipation from baffle blocks, the flow needs to be in the deflected surface jet regime.

According to Baylar et al. (2011), stepped chutes have become more popular over the years and are being used for gabion weirs, river training, and storm waterways. Not only are they low-cost but they have a speedy construction process. It was observed that aeration efficiency increases with the increasing energy-loss ratio. Nappe flow regime leads to greater aeration efficiency and has higher energy dissipation than the skimming flow regime. From their results came the conclusion that using the genetic expression programming method will result in a high rate when predicting aeration efficiency.

Meselhe and Hebert (2007) stated that culverts are very useful and common when trying to control hydraulic systems. In order to collect water level and discharge measurements a laboratory apparatus was used to simulate flow through culverts. In conducting the experiments, Meselhe and Hebert used circular culvert barrels as well as square culvert barrels. While measuring the stage-discharge relationship and the rising and receding limbs of a hydrograph, a noticeable difference was observed.

Jamshidnia et al. (2010) used a three-dimensional acoustic doppler velocimeter to investigate the effect of an intermediate standing baffle in a rectangular open channel. In the upstream baffle region, a peak structure was observed after analyzing the spaced-averaged power spectra of stream velocity. They also observed that a peak structure existed both up and downstream of the baffle.

Noshi (1999) determined that spillways, regulating structures, and outlet works often require stilling basins to achieve energy dissipation. His study estimates the maximum downstream velocity for near the bed, which is vital to know before construction in order to know what and how much materials are needed. For the flow conditions that were investigated, Noshi concluded that a sill height of .15 the tailwater depth can improve energy dissipation. It was concluded that using a greater end-sill height does not increase energy dissipation. The recirculation length is estimated to be about 2.3 times that of the water depth.

Varol et al. (2009) investigated hydraulic jumps in horizontal channels and the effects a water jet has. During the experiments, five different water jet discharges were used as well as Froude numbers ranging from 3.43 to 4.83. A high-speed SVHS camera

was used to analyze the jumps with jets and the free jumps. According to their findings, whenever the water jet flow increased this caused the hydraulic jump to move farther upstream. They also observed an increase in downstream depth (y_2) and energy loss when they increased the water jet discharge. Furthermore, roller length increased with increased water jet discharge. It was found that forced hydraulic jumps initiated by water jets had higher energy losses than free jumps.

Habibzadeh et al. (2011) conducted a preliminary study of the effects baffle blocks and walls have on submerged jumps. When testing the baffle block series, a range of submerged factors and five Froude numbers were tested on one configuration of baffle blocks. They found that the maximum energy dissipation efficiency of submerged jumps was greater than that of the free jump efficiency.

Debabeche and Achour (2007) researched the effect of placing a sill in a horizontal symmetrical triangular channel of 90° central angle. Using various flow conditions, they investigated the sill-controlled jump and the minimum-B jump using either a thin-crested or a broad-crested sill. In order to detect the effect of the inflow Froude number relative to the sill height, the data was fitted to empirical relations. They concluded that a reduced length is needed and a lower tailwater level is required when comparing it to a triangular jump basin.

2.3 EFFECT OF SLOPES IN BROKEN-BACK CULVERT

Numerous studies have observed the characteristics of the hydraulic jump in sloping open channels. Husain et al. (1994) performed many experiments on the sloping floor of open rectangular channels with negative and positive step to predict the length and depth of hydraulic jumps and to analyze the sequent depth ratio. They found that the negative step has advantages over the positive with respect to the stability and compactness of the hydraulic jump. They developed a set of non-dimensional equations in terms of profile coefficient, and they used multiple linear regression analyses on jumps with or without a step. Using Froude numbers between 4 to 12 and slope, S, between 1 and 10 percent, the length and sequent depth ratio can be accurately predicted.

Defina and Susin (2003) investigated the stability of a stationary hydraulic jump situated over a lane with sloping topography in a rectangular channel of uniform width with assuming inviscid flow conditions. On the upslope flow, it was found that the hydraulic jump is unstable and if the jump is slightly displaced from its stationary point, it will move further away in the same direction. In the channel with adverse slope, they indicated that a stationary jump can be produced. Defina and Susin calculated the ratio of bed to friction slope such as energy dissipation per unit weight and unit length, and the result was quite large. They found that the equilibrium state is weakly perturbed when the theoretical stability condition was inferred in terms of the speed adopted by the jump.

Li (1995) studied how to find the location and length of the hydraulic jump in 1^o through 5^o slopes of rectangular channels. He carried out many experimental laboratory models to get the relationship between upstream flow Froude numbers and ratios of jump length and sequent after jump L/y_2. Li used the HEC-2 software to locate the heel of a hydraulic jump to get the length of the jump and toe of the jump. The scale between the models and the prototypes was 1:65. Research concluded that an estimation of sequent depth for a hydraulic jump had to take the channel bed slope into account if the bed slope was greater than 3^o. He found out that y_2/y_1 and F_{r1} had linear relation and could be used to estimate the sequent depth. Also, Li recommended some rules such as using a solid triangular sill which could be arranged at the end of the basin apron to lift the water and reduce the scour from the leaving flow. He stated that if the Fr_1 ranged between 4.5 and 9, the tailwater depth was lowered by 5% of the sequent water depth.

2.4 ACOUSTIC DOPPLER VELOCIMETER

Acoustic Doppler Velocimeter (ADV) is a sonar device which tracks suspended solids (particles) in a fluid medium to determine an instantaneous velocity of the particles in a sampling volume. In general, ADV devices have one transmitter head and two to four receiver heads. Since their introduction in 1993, ADVs have quickly become valuable tools for laboratory and field investigations of flow in rivers, canals, reservoirs, oceans, around hydraulic structures and in laboratory scale models (Sontek, 2001).

Wahl (2000) discusses methods for filtering raw ADV data using a software application called WinADV. Wahl suggests that ADV data present, unique requirements compared to traditional current-metering equipment, due to the types of data obtained, the analyses that are possible, and the need to filter the data to ensure that any technical limitations of ADV do not adversely affect the quality of the results. According to Wahl, the WinADV program is a valuable tool for filtering, analyzing, and processing data collected from ADV. Further, this program can be used to analyze ADV files recorded using the real time data acquisition programs provided by ADV manufacturers.

Goring and Nikora (2002) formulated a new-post processing method for despiking raw ADV data. The method combines three concepts, including: 1) That differentiation of the data enhances the high frequency portion of a signal which is desirable in sonar measurements; 2) That the expected maximum of a random series is given by the Universal threshold function; and 3) That good data clusters are a dense cloud in phase space maps.

These concepts are used to construct an ellipsoid in three-dimensional phase space, while points lying outside the ellipsoid are designated as spikes (bad data). The new method has superior performance over various other methods with the added advantage of requiring no parameters. Several methods for replacing sequences of spurious data are presented. A polynomial fitted to good data on either side of the spike event then interpolated across the event is preferred by Goring and Nikora.

Mori et al. (2007) investigated measuring velocities in aerated flows using ADV techniques. ADV measurements are useful and powerful for measurements of mean and turbulent components of fluids in both hydraulic experimental facilities and fields. However, it is difficult to use the ADV in bubbly flows because air bubbles generate spike noise in the ADV velocity data. This study described the validity of the ADV measurements in bubbly flows. The true three-dimensional phase space method is significantly useful for eliminating the spike noise of ADV recorded data in bubbly flow as compared to the classical low correlation method (Goring and Nikora, 2002). The results of the data analysis suggested that:

1. There is no clear relationship between velocity and ADV's correlation/signal-to-noise ratio in bubbly flow.
2. Spike noise filtering methods based on low correlation and signal-to-noise ratio are not adequate for bubbly flow.
3. The true 3D phase space method significantly removes spike noise of ADV velocity in comparison with the original 3D phase space method.

In addition, the study found that ADV velocity measurements can be valid for 1% to 3% air void flows. The limitations of the ADV velocity measurements for high void fractions were not studied.

Chanson et al. (2008) investigated the use of ADVs to determine the velocity in turbulent open channel flow conditions in both laboratory and field experiments. They demonstrated that the ADV is a competent device for measuring velocity in steady and unsteady turbulent open channel flows. However, in order to accurately measure velocity, the ADV raw data must be processed and the unit must be calibrated to the suspended sediment concentrations. Accurately processing ADV data requires practical knowledge and experience with the device's capabilities and limitations. Chanson concluded that turbulence properties should not be derived from unprocessed ADV signals and that some despiking methods were not directly applicable to many field and laboratory applications.

2.5 IDEALIZED BROKEN-BACK CULVERTS

A culvert is a channel or drain passing under an embankment, usually for the purpose of draining water from one side of the embankment to the other. Lately, culverts have come to mean more than just simple drainage pipes as the culvert has developed into concrete structures of many shapes and many types. Also, the culvert is used to divert water from beneath and away from an area, usually a driveway. It is used to prevent water from pooling and causing erosion, which can damage the existing surfacing and cause extensive costs to repair.

2.6 DIFFERENCE BETWEEN CULVERT, BRIDGE AND OPEN CHANNEL FLOW

The function of a culvert or bridge is to transport storm runoff (or other discharge) from one side of the roadway. Here are a few defining characteristics of specifications for culverts and bridges:

- Bridge-structure must have at least 20 feet of length along the roadway centerline (National Bridge Inspection Standards, NBIS). Culvert structures that are 20 feet or greater are called bridge size structures.
- The costs of culverts are less than those of bridges, there are many times more culverts than bridges, and the total investment of public funds for culverts constitutes a substantial share of highway dollars.
- Culverts are usually designed to operate with the inlet submerged if conditions permit. This allows for a hydraulic advantage by increased discharge capacity. Bridges are usually designed for non-submergence during the design flood event, and often incorporate some freeboard.
- Culvert maintenance requirements include efforts to assure clear and open conduits, protection against corrosion and abrasion, repair and protection against local and general scour, and structural distress repair.

Broken-back culverts can be classified as either single or double broken-back. A single broken-back culvert consists only of a steeply sloped section and outlet section whereas a double broken-back culvert is comprised of an inlet section, a steeply sloped section and outlet section as shown in Figures 1 (UDOT, 2004) (Hotchkiss and Shafer, 1998). The elevation view of each culvert is found in Figure 1c and 1d. The layout of either type of broken-back culvert is important due to the nature of how the water behaves. This layout can force a hydraulic jump to form, which in return decreases the water velocity, and consequently decreases the amount of energy present that is available for water scour (Tyagi and Albert, 2008).

Singley and Hotchkiss (2010) studied the differences between open channel flow conditions and flow through a culvert. These differences in flow characteristics were

broken into four categories: geometry, sediment/debris, bed integrity, and aquatic life. Table A33 in the appendices was summarized the comparison between open channel and culverts.

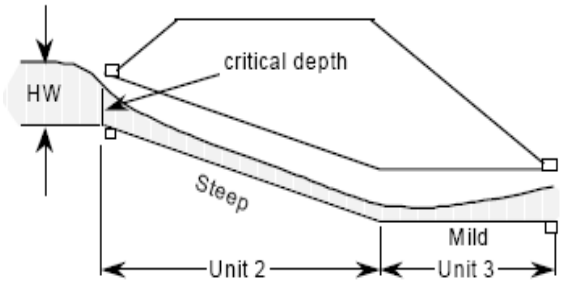

Figure 1a. Two-Unit Broken-Back Culvert

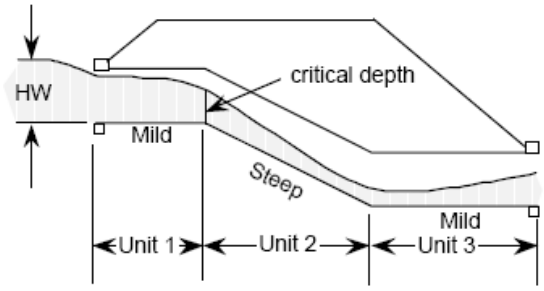

Figure 1b. Three-Unit Broken-Back Culvert.

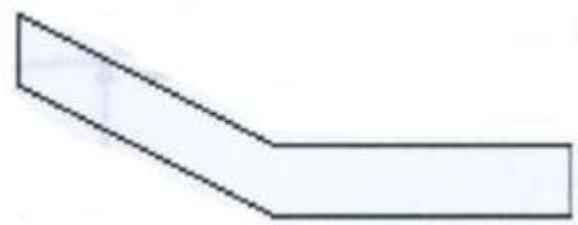

Figure 1c. Elevation view of single Broken-Back culvert

Figure 1d. Elevation view of double Broken-Back culvert

Figure 1. Types of broken-back culverts (Source: UDOT, 2009).

3 Hydraulic Similitude Theory

Similarity between a hydraulic model and a prototype may be achieved through three basic forms: a) geometric similarity, b) kinematic similarity, and c) dynamic similarity (Chow, 1959).

3.1 BROKEN-BACK CULVERT SIMILARITIES

Geometric similarity implies similarity of physical form. The model is a geometric reduction of the prototype and is accomplished by maintaining a fixed ratio for all homologous lengths between the physical quantities involved in geometric similarity: length (L), area (A), and volume (Vol). To keep the homologous lengths in the prototype (p) and the model (m) at a constant ratio (r), they may be expressed as:

$$\frac{L_p}{L_m} = L_r \qquad (1)$$

An area (A) is the product of two homologous lengths; hence, the ratio of the homologous area is also a constant given as:

$$\frac{A_p}{A_m} = \frac{L_p^2}{L_m^2} = L_r^2 \qquad (2)$$

A volume (Vol.) is the product of three homologous lengths; the ratio of the homologous volume can be represented as:

$$\frac{Vol_p}{Vol_m} = \frac{L_p^3}{L_m^3} = L_r^3 \qquad (3)$$

Kinematic similarity implies similarity of motion. Kinematic similarity between the model and the prototype is attained if the homologous moving particles have the same velocity ratio along geometrically similar paths. This similarity involves the scale of time

and length. The ratio of times required for homologous particles to travel homologous distances in a model and prototype is given by:

$$\frac{T_p}{T_m} = T_r \tag{4}$$

The velocity (V) is defined as distance per unit time; thus, the ratio of velocities may be expressed as:

$$\frac{V_P}{V_m} = \frac{\left(L_P/T_P\right)}{\left(L_m/T_m\right)} = \frac{L_r}{T_r} \tag{5}$$

The flow (Q) is expressed as volume per unit time and may be given by:

$$\frac{Q_P}{Q_m} = \frac{\left(L_P^3/T_P\right)}{\left(L_m^3/T_m\right)} = \frac{L_r^3}{T_r} \tag{6}$$

Dynamic Laboratory Model similarity implies similarity in forces involved in motion. In broken-back culverts, inertial force and gravitational (g) force are considered dominant forces in fluid motion. The Froude number is defined as:

$$F_r = \frac{\left[V_P/\left(g_P L_P\right)^{1/2}\right]}{\left[V_m/\left(g_m L_m\right)^{1/2}\right]} = 1 \tag{7}$$

As g_p and g_m are the same in a model and the prototype, these cancel in Equation 7, yielding:

$$\frac{V_r}{\left(L_r\right)^{1/2}} = 1 \tag{8}$$

$$V_r = \frac{V_P}{V_m} = \left(L_r\right)^{1/2} \tag{9}$$

$$V_P = V_m\left(L_r\right)^{1/2} \tag{10}$$

Using the three similarities, a variable of interest can be extrapolated from the model to the prototype broken-back culvert.

4 Model

4.1 LABORATORY MODEL

During the initial period of discussion regarding the construction of a scale model representing a 150 feet long broken-back culvert with 2-10'x10' to 2-10'x20' and a vertical drop of 30 feet, the research group visited the USDA Agricultural Research Service Hydraulic Engineering Research Laboratory in Stillwater, Oklahoma. This was the facility at which testing was done. The group visited with facility personnel and inspected the equipment that would be used to conduct tests. Physical dimensions of the flume that would be used were noted, as well as the flow capacity of the system.

Two scales were considered for the model. A scale of either 1:10 or 1:20 would allow for geometric similitude in a model that could easily be produced. The 1:20 scale model (Figure 2-4) was adopted due to space limitations at the testing facility and in consideration of the potential need to expand the model depending on where the hydraulic jump occurred. If the hydraulic jump did not form within the model, the smaller scale would leave room to double the length of the culvert. In addition, a lower flow rate would be required during testing if a smaller scale were used.

Other considerations included what materials to use in building the model, and what construction methods would be best. The materials considered were wood and Plexiglas®. Plexiglas® was found preferable because it offered visibility as well as durability, and a surface which would closely simulate the surface being modeled. The Manning's roughness value for Plexiglas® is 0.010 which is very close to the roughness of finished concrete at 0.012. The thickness of the Plexiglas® was decided based on weight, rigidity, workability, and the ease with which the material would fit into scale. Half-inch Plexiglas® proved to be sturdy and was thick enough to allow connection hardware to be installed in the edges of the plates. This material also fit well into the proposed scale of 1 to 20 which equated 0.50 inch in the model to one-foot in the prototype. The construction methods included constructing the model completely at the Oklahoma State University campus and moving it to the test facility, creating sections of

the model at the university and assembling them at the test facility, or contracting with the testing facility to construct the model. It was decided that the model would be constructed at the test facility. The entire laboratory model can be seen in Figures 2 and 6. During the course of the test runs, it became apparent that a flow straightener would have to be installed inside the reservoir to calm the inlet flow. A sealed plywood divider was constructed with a series of openings covered with coarse mesh.

In addition to the Plexiglas® model of the culvert, a reservoir was constructed upstream of the model to collect and calm the fluid entering the model. The reservoir was constructed with plywood, because it was not necessary to observe the behavior of the fluid upstream of the model. Within the reservoir, wing walls at an angle of 60 degrees were constructed to channel flow into the model opening. The base of the wingwalls was constructed with plywood and the exposed wingwall models were formed with Plexiglas®. The same design was used for the outlet structure of the culvert (Figure 5-7).

The objective of the test was to determine the effect of sill and friction blocks on the hydraulic jump within the prototype, therefore the model was constructed so that different arrangements of sill and friction blocks could be placed and observed within the model. Friction blocks were mounted in different arrangements on a sheet of Plexiglas® the same width as the barrels, and placed in the barrels (Figure 8-11). The friction block shape selected was a regular flat-faced friction block. Sills were located only on the horizontal portion of the model.

Two sections were constructed and added to the model for several experiments. These sections served two purposes. During initial experimentation, it was observed that the original design was under pressure and that a theoretical hydraulic jump would occur above the confines of the existing culvert ceiling. The additional sections were inverted and mounted to the top of the original model, making a culvert with 2 barrels 6 inches wide by 12 inches high and the original length of 54 inches. Access holes were cut into the top of these sections to allow for the placement of a velocity meter when used as a cover for the expanded height. Figure 12 shows the downstream channel made from plywood, and it connected with a wingwall. Figures 13-14 show the point

gauge that was used to correct the heights of the three flow conditions of 0.8, 1.0, and 1.2 times the culvert depth. The Acoustic Doppler Velocimeter (ADV) can be plugged into the culvert model and connected with the computer as shown in the Figures 15-17. Figures 18-20 show the Pitot tube and the Pitot tube plugged in the culvert model, which illustrates where to measure the velocity upstream and downstream in the model.

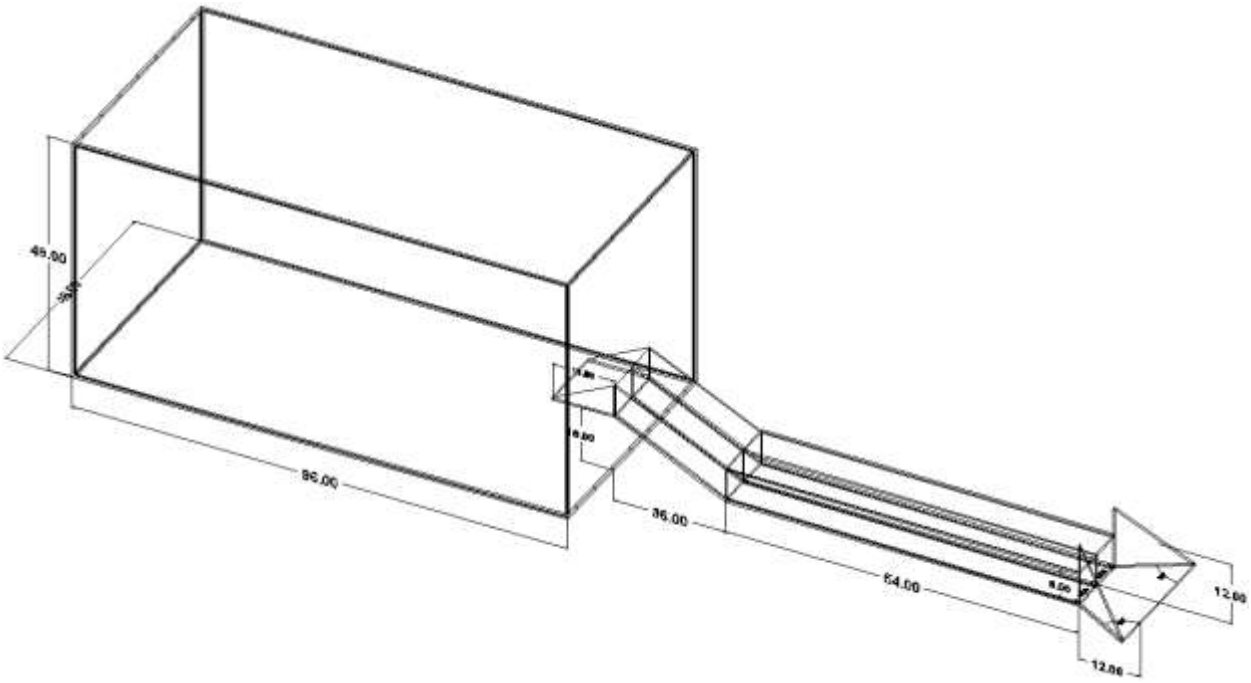

Figure 2. 3-D view of model

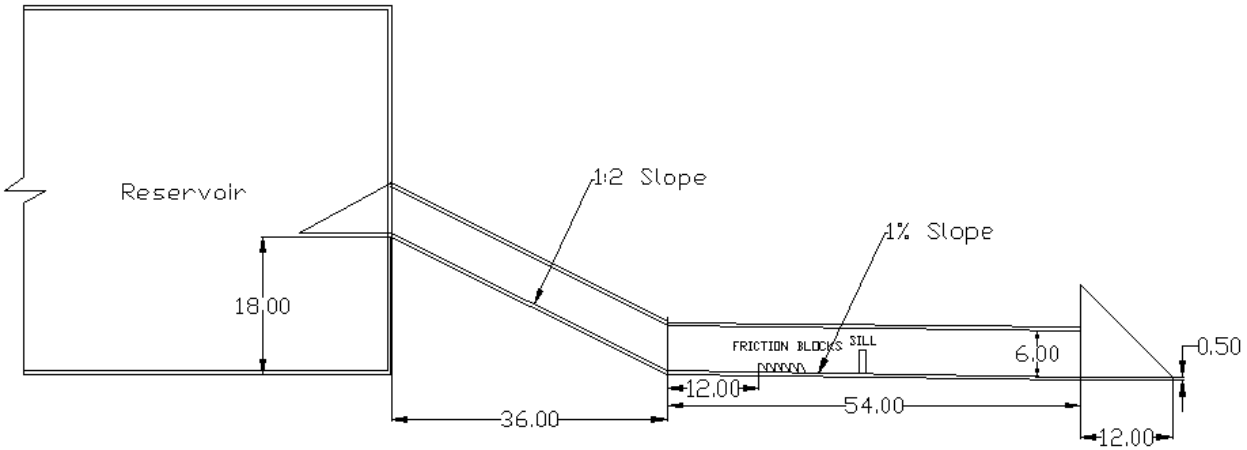

Figure 3. Profile view of model

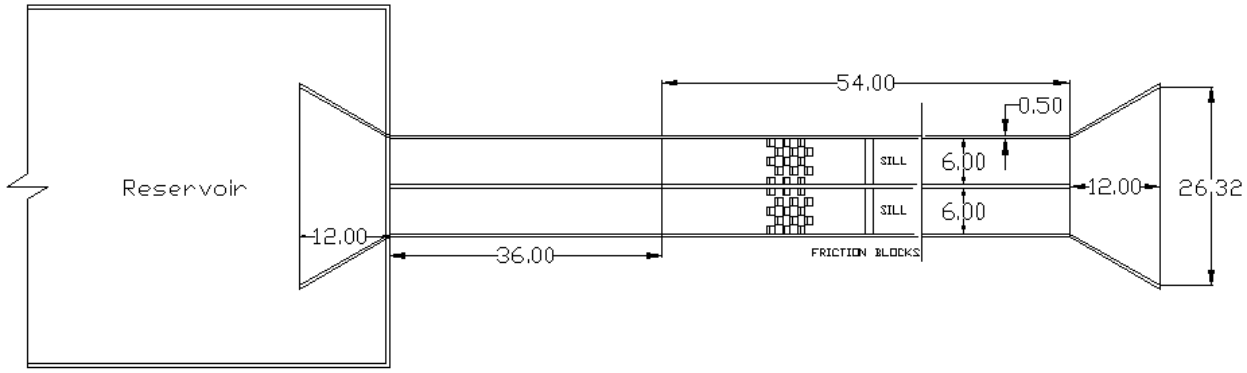

Figure 4. Plan view of model

Figure 5. Front view of laboratory model

Figure 6. Full laboratory model

Figure 7. Reservoir and flow straightener

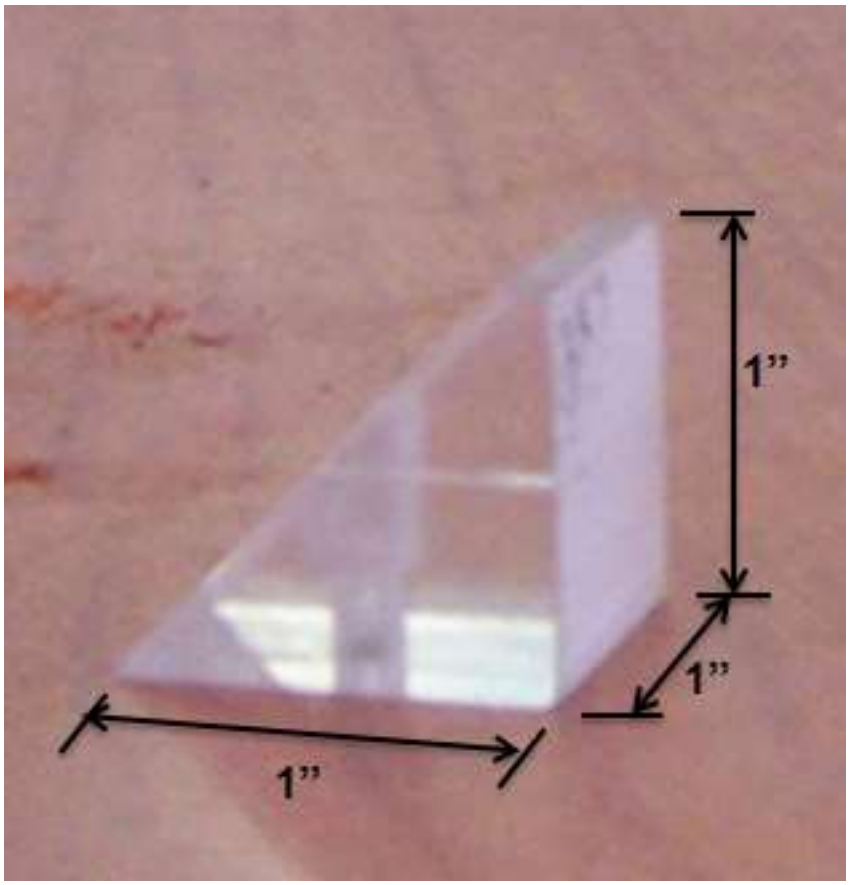

Figure 8. Example of flat faced friction

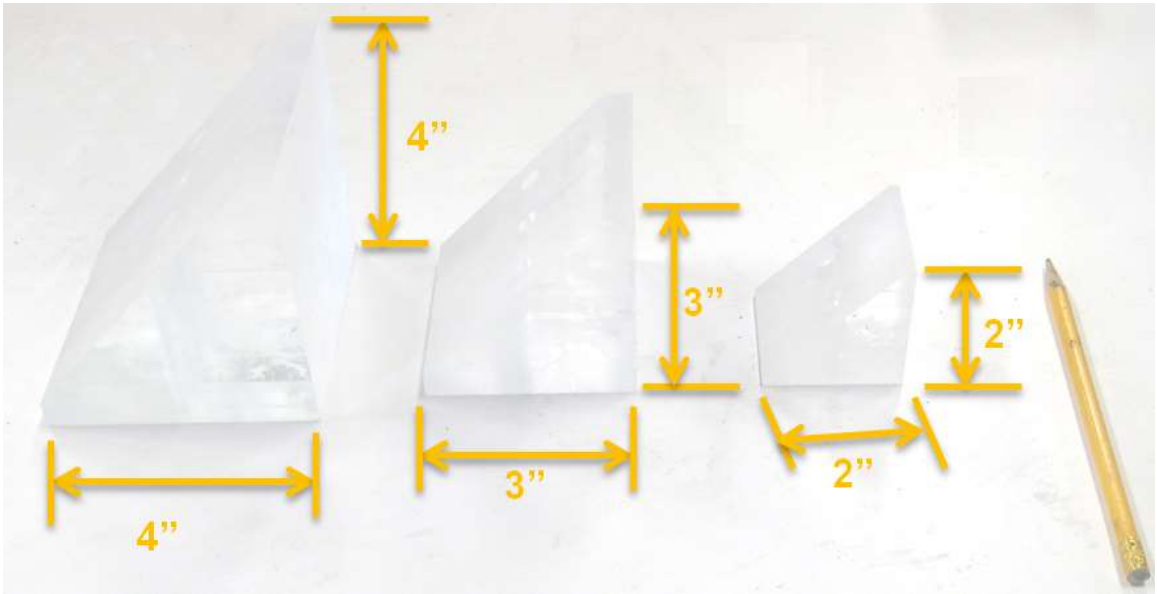

Figure 9. Different size of flat-faced friction blocks

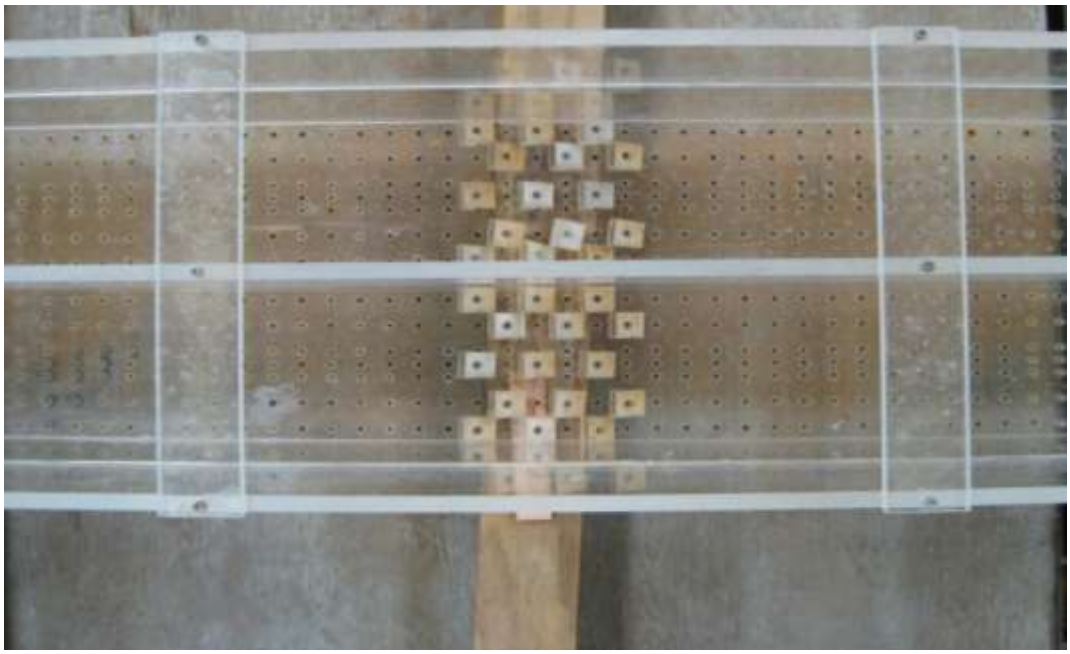

Figure 10. Friction block arrangement

Figure 11. Typical sill dimensions

Figure 12. Downstream plywood channel after wingwall

Figure 13. Point gauge front view

Figure 14. Point gauge side view

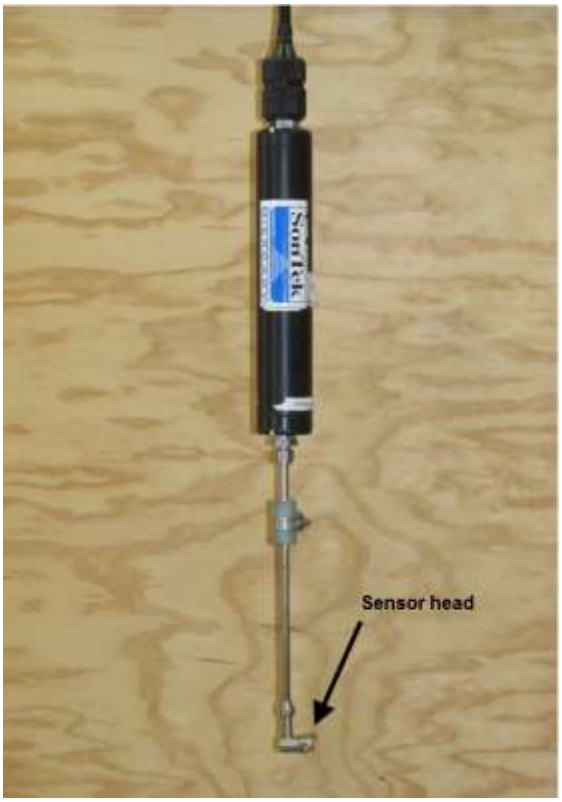

Figure 15. ADV probe and sensor head

Figure 16. ADV plugged to measure the downstream velocity ($V_{d/s}$)

Figure 17. ADV Mounted over Flume

Figure 18. Pitot tube

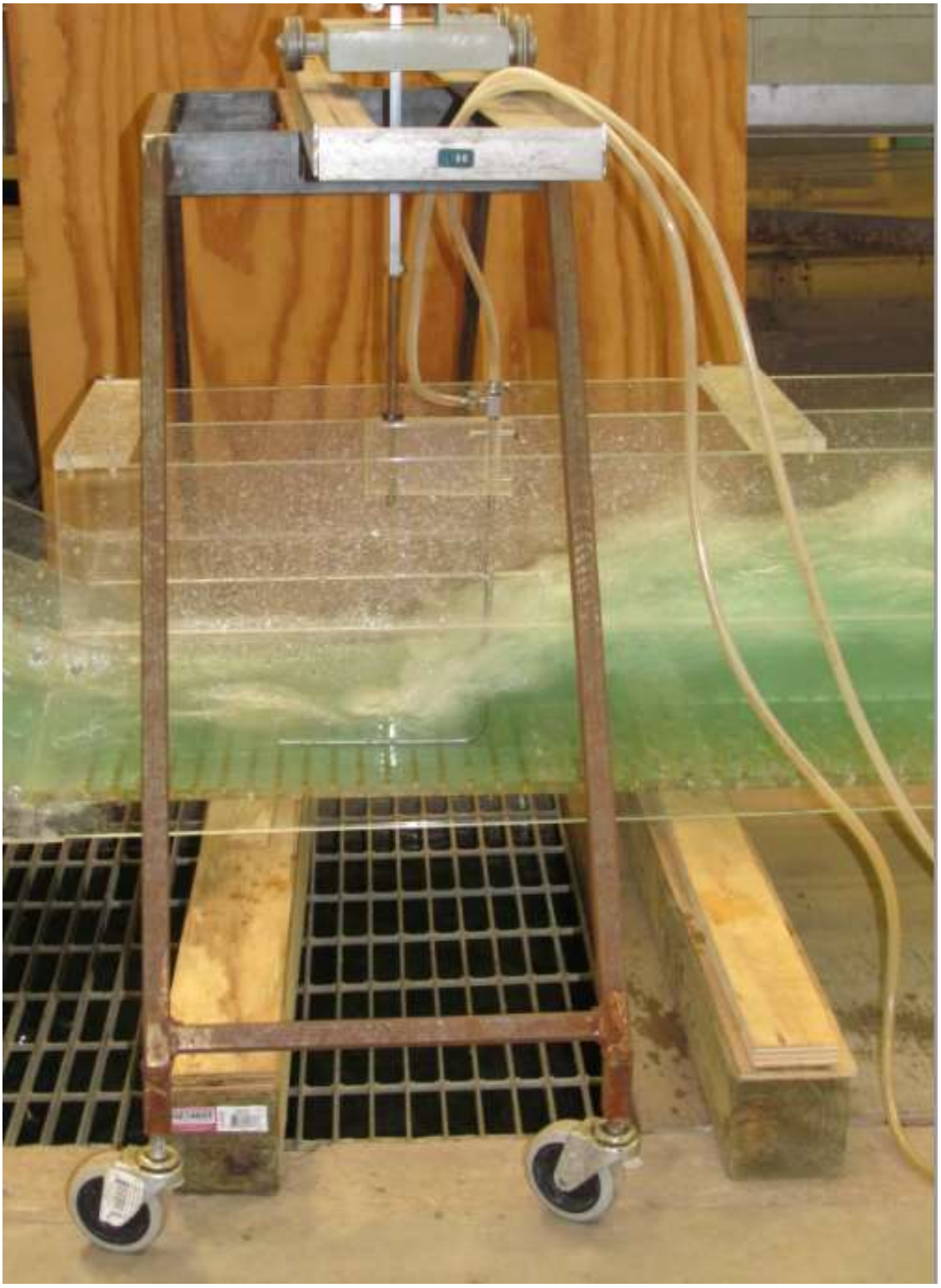

Figure 19. Pitot tube sitting on mount plugged into culvert upstream ($V_{u/s}$)

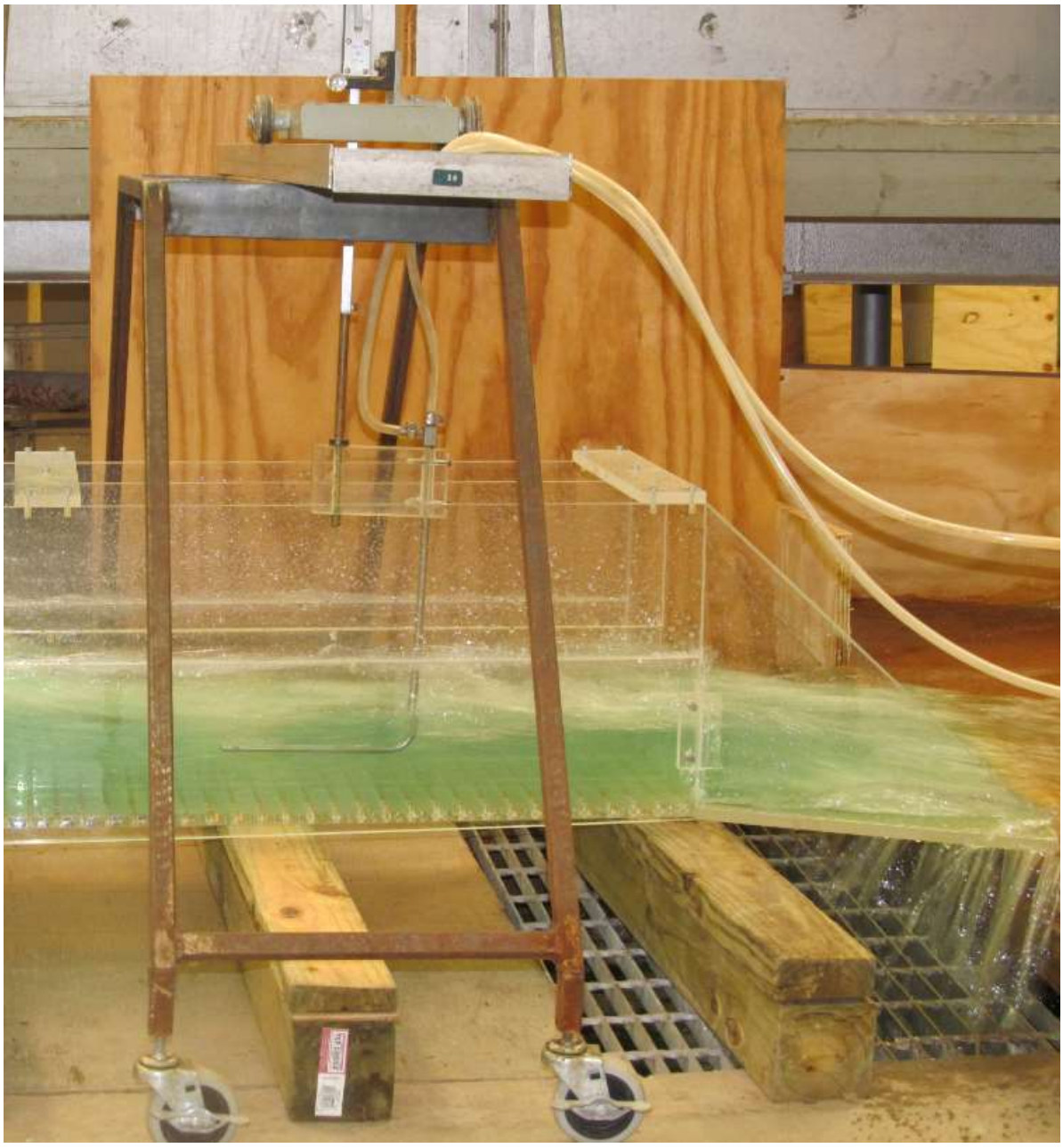

Figure 20. Pitot tube sitting on mount on culvert model downstream ($V_{d/s}$)

5 Data Collection

5.1 OPEN CHANNEL AND PRESSURE FLOW

Many experiments were conducted to create energy dissipation within a broken-back culvert. Thirty-two experiments were completed for this model with variations in length, height, width, and energy dissipators used. Each experiment tested three scenarios. They were run with upstream heads of 0.8d, 1.0d, and 1.2d with each depth denoted by A, B, or C, respectively. In this research, experiments were named according to scenarios. For example, 8A represents Experiment 8 run at 0.8d, 8B represents Experiment 8 run at 1.0d, and 8C represents Experiment 8 run at 1.2d. A SonTek 2D-side looking MicroADV sonar velocimeter was used to measure the velocity at the intake of the structure, after the hydraulic jump, and at the downstream end of the culvert. 2D-side looking denotes it has two receiver arms to give readings in the x and y planes. Also, a Pitot tube was used to measure velocity at the toe before the hydraulic jump. The flow rates for all experiments were measured and used to calculate the velocity at the intake of the structure which is at the inlet of the reservoir.

For open channel flow conditions, Experiment 1 was performed to investigate the possibility of a hydraulic jump occurring without friction blocks or sills. For experiments 2 through 10, the height of the culvert was 12 inches with the original length of 54.00 inches and width of 6 inches representing the open channel condition. Different sill heights were used in the experiments. Experiment 2 was performed with a 4.00-inch sill height located 12 inches from the end. The reason for increasing the sill heights was to produce a hydraulic jump located at the toe of the sloped channel in order to maintain subcritical flow throughout the flat section of the broken-back culvert. In order to get the optimal location of the hydraulic jump with a lower possible sill height, the sill was moved toward the center of the culvert. Therefore, Experiment 3 was performed with a 3.50-inch sill height 20 inches from the end of the culvert. Once this experiment was chosen as a possible solution, further investigation of energy dissipation was necessary. Different configurations and numbers, sizes of friction blocks were utilized in the same sill arrangement. Experiment 4 was performed using fifteen regular flat-faced friction

blocks. Experiment 5 was performed with 30 flat-faced friction blocks. Experiment 6 was performed using 3.50-inch sill with 12, 2 × 2 inches flat-faced friction blocks (FFFBs).

For pressure flow conditions, experiments 11 through 19 were run on a model with 2 barrels measuring 6 inches by 6 inches in area and a length of 54.00 inches, which represented pressure flow conditions. Different configurations of friction blocks and sills were used in the experiments. Experiment 13 was performed with a 2.50-inch sill height 19 inches from the end of the culvert. Once this experiment was chosen as a possible solution, further investigation of energy dissipation was necessary. Different configurations and numbers, sizes of friction blocks were utilized in the same sill arrangement

For the slotted design sill under open channel flow conditions, experiments 23 to 26 were performed to investigate the possibility of a hydraulic jump occurring using the slotted sills and different size of friction blocks. Experiment 23 was performed with 4.50-inch sills at the end of culvert. Experiment 25 was performed with 3.50-inch sills at 20 inches from the end of culvert. Once experiments 23 (with end sill) and 24 (with middle sill) were chosen as a possible solution for the slotted sill, there was a need for further investigation of energy dissipation. Different configurations and numbers, size of friction blocks were utilized in the same sill arrangement. Experiment 24 was performed using Experiment 23 with 6, 2 × 2 inches FFFBs at 18 inches from the toe of culvert. Experiment 26 was performed using Experiment 25 with 6, 2 × 2 inches FFFBs at 31 inches from the toe of culvert.

For slotted sill design under pressure flow conditions, experiments 27 to 30 were performed to investigate the possibility of a hydraulic jump occurring using slotted sill and friction blocks. Experiment 27 was performed with a 2.5-inch sill at the end of the culvert. Once experiment 27 was chosen as a possible solution, further investigation of energy dissipation was necessary. Different configurations and numbers, size of friction blocks were utilized in the same sill arrangement. Experiment 28 was performed using Experiment 27 with 6, 2 × 2 inches FFFBs at 28 inches from the toe of culvert. Experiment 29 was performed with 3.00-inch slotted sill at 25 inches from the end of

culvert. Experiment 30 was performed using Experiment 29 with 6, 2 × 2 inches FFFBs at 18 inches from the toe of culvert.

For open channel and pressure flow conditions, different size of flat-faced friction block were used in order to investigate the significant of FFFBs by itself. The selected experiments are presented in the data analysis, and all experiment photos and results can be seen in Appendix A.

In these experiments, the length of the hydraulic jump (L), the depth before the jump (Y_1), the depth after the jump (Y_2), the distance from the beginning of the hydraulic jump to the beginning of the sill (X), the depth of the water in the inclined channel (Y_s), and the depth of the water downstream of the culvert ($Y_{d/s}$) were measured. All dimensions were measured using a ruler and point gauge. The flow rate was measured by a two-plate manometer which measures the pressure difference in a fixed pipe opening size. As mentioned above, the velocity before the jump (V_1) was measured by a Pitot tube. The velocity at the inlet of the structure ($V_{u/s}$), the velocity after the jump (V_2), and the velocity downstream of culvert ($V_{d/s}$) were all measured by ADV.

The procedure for the experiment is as follows:

1. Install energy dissipation tool (such as sills or friction blocks) in the model.
2. Set point gauge to the correct height in the reservoir (for example, Experiment 1A means the head is equal to 0.8d).
3. Turn on pump in station.
4. Adjust valve and coordinate the opening to obtain the amount of head for the experiment.
5. Record the reading for flow rate (using a two plate manometer).
6. Run the model for 10 minutes before taking measurements to allow flow to establish.
7. Measure Y_s, Y_1, Y_2, L, X, and $Y_{d/s}$.
8. Measure velocities along the channel $V_{u/s}$, V_1, V_2, and $V_{d/s.}$
9. Post-process the raw ADV data to determine final velocity values.

Post-processing the raw ADV data was essential to maintain data validity. A software program from the Bureau of Reclamation called WinADV was obtained to

process the ADV data. The MicroADV was calibrated according to water temperature, salt content, and total suspended solids. The unit was calibrated to the manufacturer's specification for total suspended solids based on desired trace solution water content. At the end of each day of experiments, the reserve was drained to prevent mold growth which could affect the suspended solid concentration of the water. If this change in sedimentation concentration were to occur, it could minimally affect velocity readings.

The variables in a hydraulic jump can be seen in Figure 18 and the following notations are used as variables key in this report:

H. J. = Hydraulic jump

H = Head upstream of culvert, inches

Q = Flow rate, cfs

Y_s = Water depth at inclined channel, inches

Y_t = Water depth at toe of culvert, inches

Y_1 = Water depth before hydraulic jump in supercritical flow, inches

Y_2 = Water depth after hydraulic jump in subcritical flow, inches

$Y_{d/s}$ = Water depth at downstream of culvert, inches

F_{r1} = Froude Number in supercritical flow

$V_{u/s}$ = Velocity at upstream of culvert, fps

V_s = Velocity at inclined channel in supercritical flow, fps

V_1 = Velocity before hydraulic jump in supercritical flow, fps

V_2 = Velocity after hydraulic jump in subcritical flow, fps

$V_{d/s}$ = Velocity downstream of culvert, fps

X = Location of toe of the hydraulic jump to the beginning of the sill, inches

L = Length of hydraulic jump, inches

ΔE = Energy loss due to hydraulic jump, inches

THL = Total head loss for entire culvert, inches

E_2/E_1 = Efficiency of hydraulic jump

N = No hydraulic jump occurred

Y = Hydraulic jump occurred

ADV = Acoustic Doppler Velocimter

FFFBs= Flat-faced friction blocks

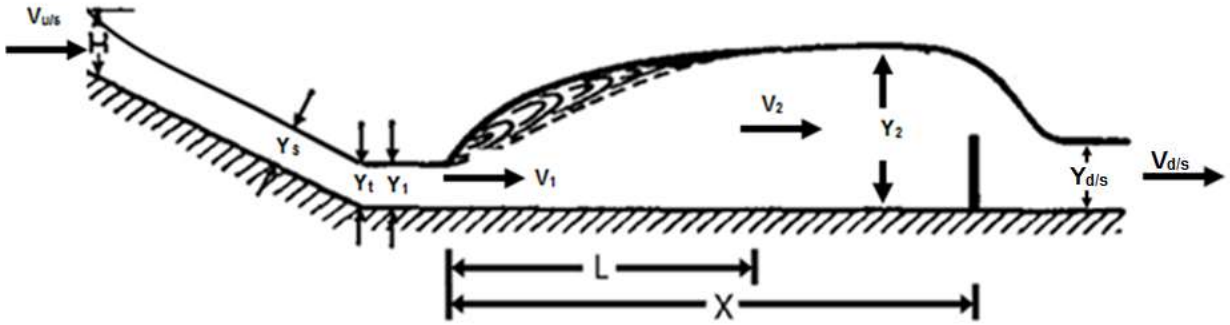

Figure 21. Hydraulic jump variables in a broken-back culvert

6 Data Analysis

6.1 OPEN CHANNEL FLOW CONDITIONS USING REGULAR SILLS

Nine experiments performed using sills only, friction blocks only, and varied height friction block and sill combinations were selected for analysis. Experiment 1 used no sills or friction blocks. Experiment 2 was not selected for analysis because the jump was not located at the toe. Experiment 3 used a sill and no friction blocks. Experiment 4 used a sill and 15 friction blocks. Experiment 5 used a sill and 6 - 2” × 2” flat-faced friction blocks. Experiment 6 used a sill and 12 - 2” × 2” inches flat-faced friction blocks. Experiment 8 used an end sill. Experiment 9 used a sill and 15 flat-faced friction blocks. Lastly Experiment 10 used a sill and 30 flat-faced friction blocks.

Experiment 1 was run without any energy dissipation devices or sill in order to allow evaluation of the hydraulic characteristics of the model, including the Froude number and supercritical flow conditions. This experiment did not produce a hydraulic jump. The results can be found in Table 1, below.

Table 1. Hydraulic parameters for Experiment 1

Scenario	1A	1B	1C
CASE	0.8d	1.0d	1.2d
Q (cfs)	1.16	1.23	1.49
$V_{u/s}$ (fps)	2.91	2.45	2.48
Y_s (in)	2.00	2.75	3.25
Y_t (in)	1.25	1.75	2.00
Y_1 (in)	1.25	1.75	2.00
$Y_{d/s}$ (in)	1.25	1.75	2.00
V_1 (fps)	9.83	10.23	10.23
F_{r1}	**5.37**	**4.72**	**4.42**

The total head loss between upstream of structure and downstream of structure was calculated by applying the Bernoulli equation:

$$THL = \left(H + \frac{V_{u/s}^2}{2g} + Z \right) - \left(Y_{d/s} + \frac{V_{d/s}^2}{2g} \right) \quad (1)$$

Where: THL = Total head loss, inches

H = Water depth upstream of the culvert, inches

Z = Drop between upstream and downstream. The model was 1.5 feet, representing a 30-foot drop in the prototype.

The loss of energy or energy dissipation in the jump was calculated by subtracting the specific energy after the jump from the specific energy before the jump.

$$\Delta E = E_1 - E_2 = \frac{(Y_2 - Y_1)^3}{4Y_1Y_2} \quad (2)$$

The efficiency of the jump was calculated by taking the ratio of the specific energy after and before the jump:

$$\frac{E_2}{E_1} = \frac{\left(8F_{r1}^{\ 2} + 1\right)^{3/2} - 4F_{r1}^2 + 1}{8F_{r1}^2\left(2 + F_{r1}^2\right)} \quad (3)$$

Where the downstream depth was known, the following equation was used to calculate the upstream supercritical flow Froude number (F_{r1}) of the hydraulic jump:

$$F_{r1} = \sqrt{\frac{\left(\frac{2Y_2}{Y_1} + 1\right)^2 - 1}{8}} \quad (4)$$

The following equation was used to calculate the Froude number (F_{r1}) of the hydraulic jump in pressure flow conditions:

$$F_{r1} = \frac{V_1}{\sqrt{gY_1}} \quad (5)$$

Experiment 2 was run using a 4-inch sill located 12 inches from the end of the culvert. A hydraulic jump was observed in all three flow conditions. The results show the Froude number values ranged from 4.06 to 4.11. The hydraulic jump was located far away from the toe of the culvert, so the sill was changed to 3.5 inches and moved forward to the toe in Experiment 3, which was 20 inches from the end of the culvert with 3.5 inches sill. Additional results for Experiment 2 can be seen in Table 2.

Table 2. Hydraulic parameters for Experiment 2

Scenario	2A	2B	2C
CASE	0.8d	1.0d	1.2d
Q (cfs)	0.92	1.23	1.48
$V_{u/s}$ (fps)	2.31	2.45	2.47
Y_s (in)	2.13	2.50	3.35
Y_t (in)	1.75	2.00	2.13
Y_1 (in)	1.75	2.00	2.13
Y_2 (in)	8.5	9.50	9.75
$Y_{d/s}$ (in)	2.80	3.00	4.00
F_{r1}	**4.07**	**4.06**	**4.11**
V_s (fps)	5.34	4.95	7.42
V_1 (fps)	8.82	9.41	9.83
V_2 (fps)	2.07	2.32	3.28
$V_{d/s}$ (fps)	4.33	3.47	2.84
L (in)	23.00	28.00	13.30
X (in)	41.00	41.00	41.00
ΔE (in)	5.17	5.55	5.33
THL (in)	17.49	19.87	20.84
E_2/E_1	**0.60**	**0.60**	**0.60**

Experiment 3 was run with a 3.5-inch sill 20 inches from the end of the culvert, utilizing the increased culvert height of 12 inches. A hydraulic jump was observed in all three flow conditions. The results show that the Froude number values ranged from 3.77 to 5.09. This range of Froude number values indicates between an oscillating and steady type of hydraulic jump. In an oscillating jump, a cyclic jet of water enters the bottom of the jump and then rises to the water surface and sinks back down again with no periodicity in cycles. The energy loss due to the hydraulic jump ranged from 6.35 inches to 7.96 inches and the total head loss for the whole culvert ranged from 15.50 inches to 16.51 inches. Additional results can be seen in Table 3.

Table 3. Hydraulic parameters for Experiment 3

Scenario	3A	3B	3C
CASE	0.8d	1.0d	1.2d
Q (cfs)	0.91	1.22	1.50
$V_{u/s}$ (fps)	2.26	2.43	2.49
Y_s (in)	2.00	2.85	3.50
Y_t (in)	1.35	1.75	2.25
Y_1 (in)	1.35	1.75	2.25
Y_2 (in)	8.50	9.75	10.75
$Y_{d/s}$ (in)	2.50	3.00	3.35
F_{r1}	**5.09**	**4.60**	**3.77**
V_s (fps)	5.33	5.08	4.42
V_1 (fps)	9.69	9.96	9.27
V_2 (fps)	2.83	3.06	6.13
$V_{d/s}$ (fps)	5.56	5.91	5.91
L (in)	18.00	20.00	22.00
X (in)	33.00	33.00	33.00
ΔE (in)	7.96	7.50	6.35
THL (in)	15.57	15.60	16.51
E_2/E_1	**0.50**	**0.55**	**0.64**

Experiment 4 was run with a 3.5-inch sill 20 inches from the end of the culvert with 15 flat-faced friction blocks (FFFBs) at 19” from toe, utilizing the increased culvert height of 12 inches. A hydraulic jump was observed in all three flow conditions. The results show that the Froude number values ranged from 4.53 to 4.83. This range of Froude number values are indicates an oscillating type of hydraulic jump. The energy loss due to hydraulic jump ranged from 4.76 inches to 7.26 inches and the total head loss for the whole culvert ranged from 12.87 inches to 15.75 inches. Additional results can be seen in Table 4.

Table 4. Hydraulic parameters for Experiment 4

Scenario	4A	4B	4C
CASE	0.8d	1.0d	1.2d
Q (cfs)	0.91	1.23	1.50
$V_{u/s}$ (fps)	2.26	2.45	2.50
Y_s (in)	2.25	2.75	3.50
Y_t (in)	1.50	1.50	1.85
Y_1 (in)	1.50	1.75	2.00
Y_2 (in)	8.75	9.00	9.00
$Y_{d/s}$ (in)	2.50	3.25	3.50
F_{r1}	**4.83**	**4.72**	**4.53**
V_s (fps)	7.05	7.45	7.52
V_1 (fps)	9.69	10.23	10.49
V_2 (fps)	3.66	4.17	5.18
$V_{d/s}$ (fps)	5.43	6.95	6.65
L (in)	17.00	16.00	16.00
X (in)	33.00	33.00	33.00
ΔE (in)	7.26	6.05	4.76
THL (in)	15.75	12.87	14.62
E_2/E_1	**0.52**	**0.53**	**0.55**

Experiment 5 was run with a 3.5-inch sill 20 inches from the end of the culvert with 6, 2 by 2 inches flat-faced friction blocks (FFFBs) at 18” from the toe, utilizing the increased culvert height of 12 inches. A hydraulic jump was observed in all three flow conditions. The results show that the Froude number values ranged from 3.46 to 4.28. This range of Froude number values are indicates an oscillating type of hydraulic jump. The energy loss due to hydraulic jump ranged from 2.30 inches to 5.33 inches and the total head loss for the whole culvert ranged from 16.17 inches to 16.29 inches. Additional results can be seen in Table 5.

Table 5. Hydraulic parameters for Experiment 5

Scenario	5A	5B	5C
CASE	0.8d	1.0d	1.2d
Q (cfs)	0.86	1.18	1.44
$V_{u/s}$ (fps)	2.16	2.36	2.39
Y_s (in)	2.00	2.75	3.00
Y_t (in)	2.25	2.50	2.75
Y_1 (in)	2.50	2.00	2.13
Y_2 (in)	8.25	9.25	9.75
$Y_{d/s}$ (in)	2.00	2.50	3.25
F_{r1}	**3.46**	**3.94**	**4.28**
V_s (fps)	6.88	7.22	7.32
V_1 (fps)	8.97	9.12	10.23
V_2 (fps)	2.32	5.05	5.67
$V_{d/s}$ (fps)	5.43	5.79	6.02
L (in)	17.00	19.00	22.00
X (in)	33.00	33.00	33.00
ΔE (in)	2.30	5.15	5.33
THL (in)	16.17	16.29	16.27
E_2/E_1	**0.68**	**0.62**	**0.58**

Experiment 6 was run with a 3.5-inch sill 20 inches from the end of the culvert with 12, 2 by 2 inches flat-faced friction blocks (FFFBs) at 18 inches from the toe, utilizing the increased culvert height of 12 inches. A hydraulic jump was observed in all three flow conditions. The results show that the Froude number values ranged from 2.52 to 2.70. This range of Froude number values are indicates an oscillating type of hydraulic jump. The energy loss due to hydraulic jump ranged from 1.63 inches to 2.24 inches and the total head loss for the whole culvert ranged from 15.82 inches to 15.98 inches. The energy dissipation ranged from 0.79 to 0.82. Additional results can be seen in Table 6.

Table 6. Hydraulic parameters for Experiment 6

Scenario	6A	6B	6C
CASE	0.8d	1.0d	1.2d
Q (cfs)	0.89	1.18	1.47
$V_{u/s}$ (fps)	2.23	2.37	2.45
Y_s (in)	2.00	2.50	3.50
Y_t (in)	3.00	4.00	4.50
Y_1 (in)	2.75	3.75	4.00
Y_2 (in)	8.75	10.00	11.25
$Y_{d/s}$ (in)	2.25	2.85	3.50
F_{r1}	**2.70**	**2.52**	**2.55**
V_s (fps)	5.20	7.74	7.47
V_1 (fps)	7.33	8.03	8.35
V_2 (fps)	4.01	4.63	5.43
$V_{d/s}$ (fps)	5.43	5.79	6.13
L (in)	17.00	18.00	20.00
X (in)	33.00	33.00	33.00
ΔE (in)	2.24	1.63	2.12
THL (in)	15.98	15.94	15.82
E_2/E_1	**0.79**	**0.82**	**0.82**

Experiment 8 was run with a 4-inch sill at the end of the culvert, utilizing the increased culvert height of 12 inches. A hydraulic jump was observed in all three flow conditions. The results show that the Froude number values ranged from 4.29 to 4.90. This range of Froude number values are indicates an oscillating type of hydraulic jump. The energy loss due to hydraulic jump ranged from 6.65 inches to 7.03 inches and the total head loss for the whole culvert ranged from 18.58 inches to 20.26 inches. Additional results can be seen in Table 7.

Table 7. Hydraulic parameters for Experiment 8

Scenario	8A	8B	8C
CASE	0.8d	1.0d	1.2d
Q (cfs)	0.87	1.20	1.43
$V_{u/s}$ (fps)	2.18	2.41	2.39
Y_s (in)	1.85	2.75	3.00
Y_t (in)	1.50	1.75	1.85
Y_1 (in)	1.50	1.85	2.00
Y_2 (in)	8.50	9.65	10.35
$Y_{d/s}$ (in)	1.75	2.50	2.25
F_{r1}	**4.90**	**4.29**	**4.30**
V_s (fps)	6.41	3.59	5.89
V_1 (fps)	9.83	9.55	9.96
V_2 (fps)	2.32	2.59	2.84
$V_{d/s}$ (fps)	4.01	4.63	4.49
L (in)	18.00	19.00	22.00
X (in)	50.00	35.00	36.00
ΔE (in)	6.73	6.65	7.03
THL (in)	18.94	18.58	20.26
E_2/E_1	**0.52**	**0.58**	**0.58**

Experiment 9 was run with a 4-inch sill at the end of the culvert with 15 FFFBs at 25” from the toe. A hydraulic jump was observed in all three flow conditions. The results show that the Froude number values ranged from 4.28 to 4.50. This range of Froude number values are indicates an oscillating type of hydraulic jump. The energy loss due to hydraulic jump ranged from 4.76 inches to 6.37 inches and the total head loss for the whole culvert ranged from 18.66 inches to 18.82 inches. Additional results can be seen in Table 8.

Table 8. Hydraulic parameters for Experiment 9

Scenario	9A	9B	9C
CASE	0.8d	1.0d	1.2d
Q (cfs)	0.94	1.21	1.68
$V_{u/s}$ (fps)	2.34	2.41	2.79
Y_s (in)	2.13	2.75	3.25
Y_t (in)	1.75	1.75	2.25
Y_1 (in)	1.75	1.85	2.13
Y_2 (in)	8.25	9.50	10.25
$Y_{d/s}$ (in)	1.50	2.00	2.50
F_{r1}	**4.34**	**4.50**	**4.28**
V_s (fps)	6.18	6.15	7.52
V_1 (fps)	9.41	10.03	10.23
V_2 (fps)	3.06	4.33	2.84
$V_{d/s}$ (fps)	4.33	4.78	5.43
L (in)	18.00	21.00	22.00
X (in)	47.00	41.00	44.00
ΔE (in)	4.76	6.37	6.13
THL (in)	18.82	18.84	18.66
E_2/E_1	**0.57**	**0.55**	**0.58**

Experiment 10 was run with a 4-inch sill at the end of the culvert with 30 FFFBs at 25” from the toe. A hydraulic jump was observed in all three flow conditions. The results show that the Froude number values ranged from 4.30 to 4.55. This range of Froude number values are indicates an oscillating type of hydraulic jump. The energy loss due to hydraulic jump ranged from 5.97 inches to 6.85 inches and the total head loss for the whole culvert ranged from 19.24 inches to 21.65 inches. Additional results can be seen in Table 9.

Table 9. Hydraulic parameters for Experiment 10

Scenario	10A	10B	10C
CASE	0.8d	1.0d	1.2d
Q (cfs)	0.90	1.24	1.50
$V_{u/s}$ (fps)	2.25	2.48	2.49
Y_s (in)	2.00	2.65	3.00
Y_t (in)	1.50	1.75	2.13
Y_1 (in)	1.50	2.00	2.00
Y_2 (in)	8.50	9.75	10.25
$Y_{d/s}$ (in)	1.50	1.75	2.00
F_{r1}	**4.55**	**4.42**	**4.30**
V_s (fps)	5.84	6.17	7.52
V_1 (fps)	9.12	10.23	9.96
V_2 (fps)	2.01	2.01	3.03
$V_{d/s}$ (fps)	4.01	3.06	5.18
L (in)	18.00	19.00	21.00
X (in)	52.00	40.00	43.00
ΔE (in)	6.73	5.97	6.85
THL (in)	19.24	21.65	19.36
E_2/E_1	**0.55**	**0.56**	**0.58**

6.1.1 OPEN CHANNEL FLOW CONDITIONS USING DIFFERENT SIZE OF FRICTION BLOCKS

Experiment 7 was run with a 12 FFFBs 2 × 2 inches at 26 inches from the end of culvert. A hydraulic jump was observed in all three flow conditions. The results show that the Froude number values ranged from 2.86 to 3.80. This range of Froude number values are indicates an oscillating type of hydraulic jump. The energy loss due to hydraulic jump ranged from 2.59 inches to 4.09 inches and the total head loss for the whole culvert ranged from 16.33 inches to 16.80 inches. Additional results can be seen in Table 10.

Table 10. Hydraulic parameters for Experiment 7

Scenario	7A	7B	7C
CASE	0.8d	1.0d	1.2d
Q (cfs)	0.90	1.20	1.46
$V_{u/s}$ (fps)	2.24	2.40	2.43
Y_s (in)	2.00	2.65	3.00
Y_t (in)	2.50	2.35	3.33
Y_1 (in)	2.50	2.35	3.13
Y_2 (in)	8.85	9.50	10.00
$Y_{d/s}$ (in)	2.50	3.25	3.50
F_{r1}	**2.86**	**3.80**	**3.32**
V_s (fps)	5.44	7.55	8.88
V_1 (fps)	7.42	9.55	9.62
V_2 (fps)	1.64	6.13	4.63
$V_{d/s}$ (fps)	4.91	5.43	5.67
L (in)	16.00	18.00	18.00
X (in)	26.00	26.00	26.00
ΔE (in)	2.89	4.09	2.59
THL (in)	16.74	16.33	16.80
E_2/E_1	**0.76**	**0.63**	**0.69**

Experiment 20 was run with a 4 FFFBs 3 × 3 inches at 20” from the end of culvert. A hydraulic jump was observed in all three flow conditions. The results show that the Froude number values ranged from 4.41 to 4.53. This range of Froude number values are indicates an oscillating type of hydraulic jump. The energy loss due to hydraulic jump ranged from 5.17 inches to 7.31 inches and the total head loss for the whole culvert ranged from 15.38 inches to 15.82 inches. Additional results can be seen in Table 11

Table 11. Hydraulic parameters for Experiment 20

Scenario	20A	20B	20C
CASE	0.8d	1.0d	1.2d
Q (cfs)	0.94	1.20	1.51
$V_{u/s}$ (fps)	2.35	2.40	2.51
Y_s (in)	2.00	2.50	3.50
Y_t (in)	1.75	2.00	2.00
Y_1 (in)	1.75	2.00	2.00
Y_2 (in)	8.50	9.50	10.50
$Y_{d/s}$ (in)	2.75	3.00	4.00
F_{r1}	**4.41**	**4.42**	**4.53**
V_s (fps)	5.63	5.52	5.31
V_1 (fps)	9.55	10.23	10.49
V_2 (fps)	3.84	2.32	6.34
$V_{d/s}$ (fps)	5.43	5.79	6.13
L (in)	20.00	21.00	21.00
X (in)	24.00	25.00	24.00
ΔE (in)	5.17	5.55	7.31
THL (in)	15.58	15.82	15.38
E_2/E_1	**0.56**	**0.56**	**0.55**

Experiment 22 was run with a 3 FFFBs 4 × 4 inches at the end of culvert. A hydraulic jump was observed in all three flow conditions. The results show that the Froude number values ranged from 3.65 to 4.06. This range of Froude number values are indicates an oscillating type of hydraulic jump. The energy loss due to hydraulic jump ranged from 3.80 inches to 7.31 inches and the total head loss for the whole culvert ranged from 19.60 inches to 20.28 inches. Additional results can be seen in Table 12.

Table 12. Hydraulic parameters for Experiment 22

Scenario	22A	22B	22C
CASE	0.8d	1.0d	1.2d
Q (cfs)	0.91	1.22	1.44
$V_{u/s}$ (fps)	2.26	2.43	2.40
Y_s (in)	2.00	2.50	3.50
Y_t (in)	2.25	2.00	2.50
Y_1 (in)	2.25	2.00	2.50
Y_2 (in)	9.00	10.50	11.00
$Y_{d/s}$ (in)	2.50	3.50	4.00
F_{r1}	**3.65**	**4.06**	**3.95**
V_s (fps)	7.14	7.35	6.22
V_1 (fps)	8.97	9.41	10.23
V_2 (fps)	1.16	2.32	2.32
$V_{d/s}$ (fps)	2.32	3.28	3.28
L (in)	20.00	18.00	20.00
X (in)	40.00	40.00	39.00
ΔE (in)	3.80	7.31	5.58
THL (in)	20.25	19.60	20.28
E_2/E_1	**0.65**	**0.60**	**0.61**

6.2 PRESSURE FLOW CONDITIONS USING REGULAR SILLS

Seven experiments were selected from fourteen experiments performed in the hydraulic laboratory for pressure flow conditions. These experiments show model runs without friction blocks, the effect of a sill at the end of the model, slotted sill at the end and the middle of culvert, and with friction blocks as well as the sill. The flat-faced friction blocks (FFFBs) were used 1" × 1", 2"×2", 3"×3", and 4"×4" (see Figure 9). After the effectiveness was evaluated, the numbers of blocks were varied dependent on the size of FFFBs. Experiment 16 was not selected for analysis because the two sills were used and the culvert was not shortened.

In these experiments, the optimum regular and slotted sill height was determined first by placing the sill at the end of culvert and then by raising or lowering the sill height until a good hydraulic jump was created. The optimum sill location was found next by incrementally moving the sill towards the front of the culvert to locate the jump near the toe of the culver. Finally the effectiveness of friction blocks and optimum sill parameters was determined by trying different friction block and sill combinations.

To solve the momentum equation for pressure flow conditions in the culvert hydraulic jump and then to simplify the solution graphically, numerous studies have been done for open channel flow conditions derived from the Belanger equation which expresses the ratio between sequent depths as functions of the upstream Froude number (Chow 1959, Lowe et al. 2011). Chow stated the hydraulic jump will form in the channel if the F_{r1} of the flow, the flow depth Y_1, and the depth after hydraulic jump Y_2 satisfy the following equation:

$$\frac{Y_2}{Y_1} = \frac{\sqrt{1+8F_{r1}} - 1}{2} \tag{6}$$

So, from the above equation, Y_2 can be calculated as following:

$$Y_2 = Y_1 \frac{\sqrt{1+8F_{r1}^2} - 1}{2} \tag{7}$$

The following equation was used to calculate the Froude number (F_{r1}) of the hydraulic jump in the upstream:

$$F_{r1} = \frac{V_1}{\sqrt{gY_1}} \quad (8)$$

where V_1 = velocity before hydraulic jump; g = acceleration due to gravity; and Y_1 = water depth before hydraulic jump.

A complete derivation of momentum theory of incomplete hydraulic jumps can be reviewed in Lowe (2011); the following equations are obtained for sequent depth of incomplete jumps for a rectangular cross-section:

$$Y_2' = \frac{1}{2} + \left(F_{r1}^2 + \frac{1}{2}\right) Y_1'^2 - F_{r1}^2 Y_1'^3 \quad (10)$$

$$Y_1' = \frac{Y_1}{D} \quad (9)$$

The dimensionless form of the sequent depth:

$$Y_2' = \frac{Y_2}{D} \quad (11)$$

where Y_1', and Y_2' are the dimensionless sequent depths before and after the jump, respectively; F_{r1} is approach or supercritical Froude number and D is height of culvert (ft).

According to Lowe (2011), equations to calculate the Froude number in the incomplete hydraulic jump are as follows:

Calculate the Y_2 from Y_2', dimensionless flow depth

$$Y_2 = Y_2' \times D \quad (12)$$

From equation (2), the actual Froude number at upstream supercritical flow can be calculated which the adjusted Froude number is ($F'_{r1(\text{adjusted})}$):

$$F'_{r1(\text{adjusted})} = \sqrt{\frac{\left(\frac{2Y_2}{Y_1}+1\right)^2 - 1}{8}} \tag{13}$$

The efficiency of the jump was calculated by taking the ratio of the specific energy before and after the jump (Chow, 1959):

$$\frac{E_2}{E_1} = \frac{\left(8F_{r1}{}^2 + 1\right)^{3/2} - 4F_{r1}{}^2 + 1}{8Fr_1{}^2\left(2 + F_{r1}{}^2\right)} \tag{14}$$

The efficiency of the jump in the incomplete jump can be calculated by using the adjusted Froude number ($F'_{r1(\text{adjusted})}$):

$$\left(\frac{E_2}{E_1}\right)' = \frac{\left(8F'^2_{r1(adjusted)} + 1\right)^{3/2} - 4F'^2_{r1(adjusted)} + 1}{8F'^2_{r1(adjusted)}\left(2 + F'^2_{r1(adjusted)}\right)} \tag{15}$$

where E_1 is the energy head before the jump, inches, E_2 is the energy head after the jump, inches, and $F'_{r1(\text{adjusted})}$ is the Froude number before the jump.

The total head loss between upstream and downstream of the structure was calculated by applying the Bernoulli equation:

$$THL = \left(H + \frac{V_{u/s}^2}{2g} + Z\right) - \left(Y_{d/s} + \frac{V_{d/s}^2}{2g}\right) \tag{16}$$

where THL is total head loss, inches, H is water depth upstream of the culvert, inches, and Z is the drop between upstream and downstream which in the model was 18 inches, representing a 30-foot drop in the prototype.

The loss of energy or energy dissipation in the jump was calculated by taking the difference between the specific energy before the jump and after the jump:

$$\Delta E = E_1 - E_2 = \frac{(Y_2 - Y_1)^3}{4Y_1Y_2} \quad (17)$$

where E_1 is energy head before the jump, inches and E_2 is energy head after the jump, inches.

Experiment 11 was run without any energy dissipation devices or sill in order to evaluate the hydraulic characteristics of the model, including the Froude number and supercritical flow conditions. This experiment is also an example of the current field practice to allow the kinetic energy of fluid to be transferred downstream without energy reduction. This experiment did not produce a hydraulic jump. The results can be found in Table 13, below. The flow regime is classified as supercritical flow, which means the Froude number is greater than 1. A hydraulic jump occurs when the flow has a sudden change from supercritical flow to subcritical flow. At the start of the jump the flow depth will begin to increase and the velocity will slow creating an area of turbulence.

Table 13. Hydraulic parameters for Experiment 11

Scenario	11A	11B	11C
CASE	(0.8d)	(1.0d)	(1.2d)
Q (cfs)	0.90	1.21	1.50
$V_{u/s}$ (fps)	2.24	2.43	2.50
Y_1 (in)	1.50	1.75	1.75
$Y_{d/s}$ (in)	1.50	1.65	1.85
F_{r1}	**5.23**	**4.90**	**4.90**
V_1 (fps)	10.49	10.62	10.62
$V_{d/s}$ (fps)	9.83	10.23	10.36
THL (in)	3.23	4.10	5.02

Experiment 12 was run with one sill: a 2.5-inch sill at the end of the culvert. This experiment demonstrated the use of one sill to control the hydraulic jump under pressure flow conditions. Pressure flow condition is defined by the fluid excreting pressure against the top of the model. A hydraulic jump was observed in all three flow conditions. The results showed that the Froude number values ranged from 4.53 to 5.48. Cases are indicative of a steady jump. The total head loss for the whole culvert ranges from 10.26 inches to 11.44 inches. We calculated this table according to equations 1 to 3, and for Y_2, Equation 15 was used to calculate the E_2/E_1 under pressure flow conditions. All results can be seen in Table 14.

Table 14. Hydraulic parameters for Experiment 12

Scenario	12A	12B	12C
CASE	(0.8d)	(1.0d)	(1.2d)
Q (cfs)	0.92	1.22	1.50
$V_{u/s}$ (fps)	2.30	2.43	2.50
Y_1 (in)	1.20	1.65	2.00
Y_2 (in)	8.88	10.60	12.00
$Y_{d/s}$ (in)	2.50	3.00	3.50
F_{r1}	**5.48**	**4.74**	**4.53**
V_1 (fps)	9.83	9.96	10.49
V_2 (fps)	4.91	4.63	5.18
$V_{d/s}$ (fps)	3.66	4.01	6.95
ΔE (in)	10.63	10.26	11.42
THL (in)	18.78	19.10	13.87
E_2/E_1	**0.46**	**0.52**	**0.53**

Experiment 13 was run with one sill: a 2.5-inch sill located 19 inches from the end of the culvert. This experiment demonstrated the use of one sill to control the hydraulic jump under pressure flow conditions. Pressure flow condition is defined by the fluid excreting pressure against the top of the model. A hydraulic jump was observed in all three flow conditions. The results showed that the Froude number values ranged from 4.56 to 5.09. Cases are indicative of a steady jump. The total head loss for the whole culvert ranges from 16.74 inches to 20.01 inches. We calculated this table according to equations 1 to 3. All results can be seen in Table 15.

Table 15. Hydraulic parameters for Experiment 13

Scenario	13A	13B	13C
CASE	(0.8d)	(1.0d)	(1.2d)
Q (cfs)	0.91	1.21	1.41
$V_{u/s}$ (fps)	2.27	2.41	2.36
Y_1 (in)	1.35	1.65	1.85
Y_2 (in)	9.26	10.80	11.50
$Y_{d/s}$ (in)	2.50	2.85	3.00
F_{r1}	**5.09**	**4.80**	**4.56**
V_1 (fps)	9.69	10.10	10.16
V_2 (fps)	2.84	1.64	4.01
$V_{d/s}$ (fps)	2.59	5.43	5.67
ΔE (in)	9.88	10.76	10.55
THL (in)	20.01	16.74	17.23
E_2/E_1	**0.49**	**0.51**	**0.53**

Experiment 14 was run with a 2.5-inch sill located 19 inches from the end of the culvert and 15 flat-faced friction blocks (FFFBs) at 11 inches from the toe. This experiment demonstrates the use of one sill to control the hydraulic jump under pressure flow conditions. A hydraulic jump was observed in all three flow conditions. The results show that the Froude number values ranged from 4.53 to 4.89. This range of Froude number values are indicates an oscillating hydraulic jump. The total head loss for the whole culvert ranged from 16.93 inches to 17.23 inches. Additional results can be seen in Table 16.

Table 16. Hydraulic parameters for Experiment 14

Scenario	14A	14B	14C
CASE	(0.8d)	(1.0d)	(1.2d)
Q (cfs)	0.91	1.22	1.41
$V_{u/s}$ (fps)	2.18	2.43	2.36
Y_1 (in)	1.65	1.75	2.00
Y_2 (in)	11.10	11.52	12.44
$Y_{d/s}$ (in)	2.25	2.75	3.00
F_{r1}	**4.89**	**4.78**	**4.53**
V_1 (fps)	10.30	10.36	10.49
V_2 (fps)	2.84	4.49	4.63
$V_{d/s}$ (fps)	4.91	5.31	5.67
ΔE (in)	11.53	11.56	11.44
THL (in)	16.93	17.10	17.23
E_2/E_1	**0.51**	**0.51**	**0.53**

Experiment 15 was run with a 2.5-inch sill located 19 inches from the end of the culvert and 30 FFFBs at 11 inches from the toe. This experiment demonstrates the use of one sill to control the hydraulic jump under pressure flow conditions. A hydraulic jump was observed in all three flow conditions. The results show that the Froude number values ranged from 5.16 for case 15A, to 4.53 for case 15B, which both indicate a steady jump, but the F_{r1} = 4.22 for case 15C is indicative of an oscillating jump. The total head loss for the whole culvert ranged from 15.50 inches to 16.44 inches. Additional results can be seen in Table 17.

Table 17. Hydraulic parameters for Experiment 15

Scenario	15A	15B	15C
CASE	(0.8d)	(1.0d)	(1.2d)
Q (cfs)	0.87	1.25	1.51
$V_{u/s}$ (fps)	2.18	2.50	2.52
Y_1 (in)	1.50	2.00	2.25
Y_2 (in)	10.69	12.00	12.00
$Y_{d/s}$ (in)	2.25	3.00	3.13
F_{r1}	**5.16**	**4.53**	**4.22**
V_1 (fps)	10.36	10.49	10.36
V_2 (fps)	1.16	4.24	5.18
$V_{d/s}$ (fps)	5.18	5.67	6.45
ΔE (in)	12.09	10.42	8.58
THL (in)	16.44	16.16	15.50
E_2/E_1	**0.48**	**0.55**	**0.60**

Experiment 17 was run with a 1.5-inch sill located 19 inches from the end of the culvert and 6 FFFBs 2 × 2 inches at 14 inches from the toe. A hydraulic jump was observed in all three flow conditions. The results show that the Froude number values ranged from 2.83 to 3.29, which both indicate a oscillating jump. The total head loss for the whole culvert ranged from 17.09 inches to 18.26 inches. Additional results can be seen in Table 18.

Table 18. Hydraulic parameters for Experiment 17

Scenario	17A	17B	17C
CASE	(0.8d)	(1.0d)	(1.2d)
Q (cfs)	0.87	1.20	1.52
$V_{u/s}$ (fps)	2.18	2.40	2.53
Y_1 (in)	2.00	2.50	3.00
Y_2 (in)	6.89	10.08	11.38
$Y_{d/s}$ (in)	2.25	3.25	3.13
F_{r1}	**2.83**	**3.29**	**3.19**
V_1 (fps)	6.55	8.51	9.05
V_2 (fps)	3.28	2.32	2.46
$V_{d/s}$ (fps)	4.83	4.91	5.18
ΔE (in)	2.12	4.32	4.30
THL (in)	17.09	17.32	18.26
E_2/E_1	**0.77**	**0.70**	**0.71**

6.2.1 PRESSURE FLOW CONDITIONS USING FRICTION BLOCKS

Experiment 18 was run with a 6 FFFBs 2 × 2 inches located 19 inches from the end of the culvert. A hydraulic jump was observed in all three flow conditions. The results show that the Froude number values ranged from 4.36 to 5.62, which both indicate an oscillating to steady jump. The total head loss for the whole culvert ranged from 17.26 inches to 20.10 inches. Additional results can be seen in Table 19.

Table 19. Hydraulic parameters for Experiment 18

Scenario	18A	18B	18C
CASE	(0.8d)	(1.0d)	(1.2d)
Q (cfs)	0.91	1.20	1.52
$V_{u/s}$ (fps)	2.27	2.41	2.53
Y_1 (in)	1.25	1.75	2.13
Y_2 (in)	9.64	11.46	12.00
$Y_{d/s}$ (in)	3.00	2.65	2.75
F_{r1}	**5.62**	**4.76**	**4.36**
V_1 (fps)	10.30	10.32	10.43
V_2 (fps)	5.91	7.68	6.95
$V_{d/s}$ (fps)	4.33	4.01	4.33
ΔE (in)	12.53	10.79	9.40
THL (in)	17.26	19.43	20.10
E_2/E_1	**0.45**	**0.51**	**0.57**

Experiment 19 was run with a 2 FFFBs 3 × 3 inches located at the end of the culvert. A hydraulic jump was observed in all three flow conditions. The results show that the Froude number values ranged from 3.33 to 4.72, which both indicate a oscillating jump. The total head loss for the whole culvert ranged from 17.57 inches to 19.03 inches. Additional results can be seen in Table 20.

Table 20. Hydraulic parameters for Experiment 19

Scenario	19A	19B	19C
CASE	(0.8d)	(1.0d)	(1.2d)
Q (cfs)	0.92	1.20	1.50
$V_{u/s}$ (fps)	2.30	2.40	2.49
Y_1 (in)	1.25	1.65	2.25
Y_2 (in)	9.07	10.54	12.00
$Y_{d/s}$ (in)	3.25	3.50	4.50
F_{r1}	**5.37**	**4.71**	**4.05**
V_1 (fps)	9.83	9.92	9.96
V_2 (fps)	1.16	1.37	3.84
$V_{d/s}$ (fps)	2.84	4.63	4.01
ΔE (in)	10.54	10.11	8.58
THL (in)	19.03	17.57	18.86
E_2/E_1	**0.47**	**0.52**	**0.60**

6.3 OPEN CHANNEL FLOW WITH SLOTTED SILLS

Experiment 23 was run with a 3.50-inch slotted sill located 20 inches from the end of the culvert. This experiment demonstrates the use of one slotted sill to control the hydraulic jump under open channel flow conditions. Experiment 23 was chosen for two reasons: (1) a hydraulic jump formed inside the horizontal section of the model for all three flow conditions, and (2) it is an example of the field being under open channel flow due to the confines of the model. A hydraulic jump was observed in all experiments using three flow conditions. The results show that the Froude number values ranged from 4.53 to 4.83 which indicated an oscillating jump. The total head loss for the whole culvert ranged from 17.36 inches to 17.82 inches. Additional results can be seen in Table 21.

Table 21. Hydraulic parameters for Experiment 23

Scenario	23A	23B	23C
CASE	(0.8d)	(1.0d)	(1.2d)
Q (cfs)	0.88	1.20	1.50
$V_{u/s}$ (fps)	2.21	2.40	2.50
Y_1 (in)	1.65	1.85	2.00
Y_2 (in)	8.00	9.25	10.50
$Y_{d/s}$ (in)	2.85	3.25	4.00
F_{r1}	**4.83**	**4.59**	**4.53**
V_1 (fps)	10.16	10.23	10.49
V_2 (fps)	2.01	4.33	5.43
$V_{d/s}$ (fps)	4.33	4.63	5.18
ΔE (in)	4.85	5.92	7.31
THL (in)	17.36	17.82	17.36
E_2/E_1	**0.52**	**0.55**	**0.55**

Experiment 24 was run with a 3.5-inch slotted sill 20 inches from the end of the culvert and 6 FFFBs 2 × 2 inches at 18 inches from the toe, utilizing the increased culvert height of 12 inches. A hydraulic jump was observed in all three flow conditions. The results show that the Froude number values ranged from 4.54 for case 24A. This indicated a steady jump. For both cases 24B and 24C the Froude numbers were 4.44 and 4.28 respectfully. This indicated that both were oscillating jumps. The energy loss due to hydraulic jump ranged from 5.72 inches to 6.55 inches and the total head loss for the whole culvert ranged from 15.10 inches to 16.28 inches. All results can be seen in Table 22.

Table 22. Hydraulic parameters for Experiment 24

Scenario	24A	24B	24C
CASE	0.8d	1.0d	1.2d
Q (cfs)	0.92	1.19	1.49
$V_{u/s}$ (fps)	2.30	2.39	2.48
Y_s (in)	2.00	2.65	3.50
Y_t (in)	1.65	1.75	2.00
Y_1 (in)	1.65	1.75	2.13
Y_2 (in)	8.50	9.25	10.50
$Y_{d/s}$ (in)	2.50	2.75	3.50
F_{r1}	**4.54**	**4.44**	**4.28**
V_1 (fps)	9.55	9.62	10.23
V_2 (fps)	4.01	5.56	5.18
$V_{d/s}$ (fps)	5.18	5.67	6.45
L (in)	16.00	16.00	15.00
X (in)	33.00	33.00	29.50
ΔE (in)	5.72	6.52	6.55
THL (in)	16.28	16.31	15.10
E_2/E_1	**0.55**	**0.56**	**0.58**

Experiment 25 was run with a 4.5-inch slotted sill at the end of the culvert. A hydraulic jump was observed in all three flow conditions. The results show that the Froude number values ranged from 5.37 for case 25A to 4.86 for case 25B, which indicated a steady jump. For case 25C the Froude number was 4.33, which indicated an oscillating jump. The energy loss due to hydraulic jump ranged from 6.99 inches to 8.97 inches and the total head loss for the whole culvert ranged from 19.29 inches to 19.72 inches. The energy dissipation ranges from 0.48 to 0.57. Additional results can be seen in Table 23.

Table 23. Hydraulic parameters for Experiment 25

Scenario	25A	25B	25C
CASE	0.8d	1.0d	1.2d
Q (cfs)	0.89	1.18	1.49
$V_{u/s}$ (fps)	2.22	2.37	2.48
Y_s (in)	2.00	2.50	3.50
Y_t (in)	1.50	1.75	2.00
Y_1 (in)	1.25	1.65	2.13
Y_2 (in)	8.50	9.25	10.75
$Y_{d/s}$ (in)	1.75	2.50	3.00
F_{r1}	**5.37**	**4.86**	**4.33**
V_1 (fps)	9.83	10.23	10.36
V_2 (fps)	1.16	1.64	2.01
$V_{d/s}$ (fps)	3.47	4.18	4.49
L (in)	16.00	16.00	18.00
X (in)	31.00	31.00	29.00
ΔE (in)	8.97	7.19	6.99
THL (in)	19.72	19.29	19.59
E_2/E_1	**0.48**	**0.52**	**0.57**

Experiment 26 was run with a 4.5-inch slotted sill located at the end of the culvert. In addition, 6 FFFBs 2 × 2 inches were placed in the horizontal portion of the channel in the pattern at 31 inches from the toe. A hydraulic jump was observed in all three flow conditions. The results show that the Froude number values ranged from 4.42 to 4.97. The F_{r1} Case 26A and case 26B indicate a steady type of hydraulic jump, but case 26C indicates an oscillating jump. The total head loss due to hydraulic jump ranged from 19.97 inches to 21.59 inches and the energy loss for the whole culvert ranged from 6.21 inches to 7.31 inches. The efficiency of the hydraulic jump in these experiments ranged from 0.51 to 0.56. Additional results can be seen in Table 24.

Table 24. Hydraulic parameters for Experiment 26

Scenario	26A	26B	26C
CASE	0.8d	1.0d	1.2d
Q (cfs)	0.90	1.20	1.48
$V_{u/s}$ (fps)	2.24	2.40	2.47
Y_s (in)	2.00	2.75	3.35
Y_t (in)	1.50	1.75	2.00
Y_1 (in)	1.50	1.75	2.00
Y_2 (in)	8.25	9.50	10.50
$Y_{d/s}$ (in)	1.50	1.75	2.25
F_{r1}	**4.97**	**4.70**	**4.42**
V_1 (fps)	9.96	10.19	10.23
V_2 (fps)	2.32	2.84	4.01
$V_{d/s}$ (fps)	3.06	3.28	3.66
L (in)	16.00	18.00	19.00
X (in)	47.00	49.00	50.00
ΔE (in)	6.21	7.00	7.31
THL (in)	20.49	21.32	21.59
E_2/E_1	**0.51**	**0.54**	**0.56**

6.4 PRESSURE FLOW WITH SLOTTED SILLS

Experiment 27 was run with a 2.50-inch slotted sill located at the end of the culvert. This experiment demonstrates the use of one slotted sill to control the hydraulic jump under pressure flow conditions. A hydraulic jump was observed in all three flow conditions. The results show that the Froude number values ranged from 4.16 to 4.78. Case 27A and 27B indicate a steady type of hydraulic jump, but case 27C indicates an oscillating jump. The total head loss for the whole culvert ranged from 13.36 inches to 19.38 inches. All the results can be seen in Table 25.

Table 25. Hydraulic parameters for Experiment 27

Scenario	27A	27B	27C
CASE	0.8d	1.0d	1.2d
Q (cfs)	0.89	1.20	1.50
$V_{u/s}$ (fps)	2.23	2.41	2.49
Y_s (in)	2.00	2.75	3.25
Y_t (in)	1.50	1.75	2.13
Y_1 (in)	1.50	1.75	2.25
Y_2 (in)	9.56	11.52	12.00
$Y_{d/s}$ (in)	2.50	3.50	4.00
F_{r1}	**4.76**	**4.78**	**4.16**
V_1 (fps)	9.55	10.36	10.23
V_2 (fps)	3.84	3.47	3.28
$V_{d/s}$ (fps)	3.15	3.66	6.95
L (in)	11.00	11.00	13.00
X (in)	13.00	16.00	20.00
ΔE (in)	9.13	11.56	8.58
THL (in)	19.38	19.08	13.36
E_2/E_1	**0.52**	**0.51**	**0.60**

Experiment 28 was run with a 2.50-inch slotted sill located at the end of the culvert and 6 FFFBs 2 × 2 inches placed in the horizontal portion of the channel in the pattern at 28 inches from the toe. A hydraulic jump was observed in all three flow conditions. The results show that the Froude number values ranged from 4.32 to 4.97. Case 28A and 28B indicated a steady type of hydraulic jump, but case 28C indicated an oscillating jump. The total head loss for the whole culvert ranged from 18.36 inches to 20.33 inches. All results can be seen in Table 26.

Table 26. Hydraulic parameters for Experiment 28

Scenario	28A	28B	28C
CASE	0.8d	1.0d	1.2d
Q (cfs)	0.94	1.20	1.50
$V_{u/s}$ (fps)	1.57	2.00	2.50
Y_s (in)	2.13	2.50	3.50
Y_t (in)	1.65	2.00	2.13
Y_1 (in)	1.50	1.85	2.25
Y_2 (in)	10.13	11.82	12.00
$Y_{d/s}$ (in)	1.75	2.00	2.50
F_{r1}	**4.97**	**4.65**	**4.32**
V_1 (fps)	9.96	10.36	10.62
V_2 (fps)	3.06	7.68	8.11
$V_{d/s}$ (fps)	3.06	3.84	5.43
L (in)	12.00	12.00	16.00
X (in)	40.00	41.00	44.00
ΔE (in)	10.56	11.32	8.58
THL (in)	19.76	20.00	18.36
E_2/E_1	**0.50**	**0.52**	**0.60**

Experiment 29 was run with a 3-inch slotted sill located 25 inches from the end of the culvert. This experiment demonstrated the use of one slotted sill to control the hydraulic jump under pressure flow conditions. A hydraulic jump was observed in all three flow conditions. The results show that the Froude number values ranged from 4.47 to 4.91. All Froude number values are indicative of a steady jump. The total head loss for the whole culvert ranges from 18.30 inches to 21.11 inches. Additional results can be seen in Table 27.

Table 27. Hydraulic parameters for Experiment 29

Scenario	29A	29B	29C
CASE	0.8d	1.0d	1.2d
Q (cfs)	0.93	1.18	1.50
$V_{u/s}$ (fps)	2.32	2.37	2.50
Y_s (in)	2.00	2.50	3.50
Y_t (in)	1.50	1.85	2.00
Y_1 (in)	1.60	1.75	2.00
Y_2 (in)	10.74	11.83	12.00
$Y_{d/s}$ (in)	3.00	3.00	3.50
F_{r1}	**4.91**	**4.87**	**4.47**
V_1 (fps)	10.16	10.55	10.36
V_2 (fps)	5.67	4.63	6.13
$V_{d/s}$ (fps)	3.66	3.84	3.06
L (in)	12.00	12.00	18.00
X (in)	14.50	16.00	26.00
ΔE (in)	11.11	12.37	10.42
THL (in)	18.30	19.29	21.11
E_2/E_1	**0.50**	**0.50**	**0.55**

Experiment 30 was run with a 3-inch slotted sill located 25 inches from the end of the culvert and 6 FFFBs 2 × 2 inches placed in the horizontal portion of the channel in the pattern at 18 inches from the toe. This experiment demonstrated the use of one slotted sill to control the hydraulic jump under pressure flow conditions. This experiment produced a hydraulic jump for all three conditions. A hydraulic jump was observed in all three flow conditions. The results show that the Froude number values ranged from 4.11 to 4.53. Case 30A is indicative of a steady type of hydraulic jump, but cases 30B and 30C are indicative of oscillating jump. The total head loss for the whole culvert ranged from 16.48 inches to 19.35 inches. All the results can be seen in Table 28.

Table 28. Hydraulic parameters for Experiment 30

Scenario	30A	30B	30C
CASE	0.8d	1.0d	1.2d
Q (cfs)	0.90	1.22	1.49
$V_{u/s}$ (fps)	2.24	2.43	2.48
Y_s (in)	2.00	2.50	3.50
Y_t (in)	1.85	2.00	2.25
Y_1 (in)	1.85	2.00	2.25
Y_2 (in)	11.39	11.11	12.00
$Y_{d/s}$ (in)	2.75	3.00	3.50
F_{r1}	**4.53**	**4.18**	**4.11**
V_1 (fps)	10.10	9.69	10.10
V_2 (fps)	5.91	5.31	4.33
$V_{d/s}$ (fps)	4.91	5.31	4.33
L (in)	14.00	15.00	17.00
X (in)	27.00	29.00	29.00
ΔE (in)	10.30	8.51	9.23
THL (in)	16.48	16.85	19.35
E_2/E_1	**0.54**	**0.58**	**0.58**

Experiment 31 was run with a 6 FFFBs 2 × 2 inches placed in the horizontal portion of the channel in the pattern located 18 inches from the toe of the culvert. This experiment demonstrated the use of six FFFBs to control the hydraulic jump under pressure flow conditions. A hydraulic jump was observed in all three flow conditions. The results show that the Froude number values ranged from 4.47 to 5.66. All Froude number values are indicative of a steady jump. The total head loss for the whole culvert ranges from 16.99 inches to 17.11 inches. Additional results can be seen in Table 29.

Table 29. Hydraulic parameters for Experiment 31

Scenario	31A	31B	31C
CASE	0.8d	1.0d	1.2d
Q (cfs)	0.90	1.23	1.50
$V_{u/s}$ (fps)	2.24	2.45	2.49
Y_s (in)	1.75	2.50	2.50
Y_t (in)	1.25	1.75	2.13
Y_1 (in)	1.25	1.75	2.13
Y_2 (in)	9.73	11.83	12.00
$Y_{d/s}$ (in)	2.75	3.25	2.00
F_{r1}	**5.66**	**4.87**	**4.47**
V_1 (fps)	10.36	10.55	10.68
V_2 (fps)	4.91	4.63	2.59
$V_{d/s}$ (fps)	4.63	5.08	5.67
L (in)	10.00	9.00	13.00
X (in)	12.00	12.00	14.00
ΔE (in)	12.53	12.37	9.40
THL (in)	16.99	17.07	16.86
E_2/E_1	**0.45**	**0.50**	**0.57**

Experiment 32 was run with a 2 FFFBs 3 × 3 inches located at the end of the culvert. This experiment demonstrated the use of two FFFBs to control the hydraulic jump under pressure flow conditions. This experiment produced a hydraulic jump for all three conditions. A hydraulic jump was observed in all three flow conditions. The results show that the Froude number values ranged from 4.53 to 5.09. The Froude number is indicative of a steady type of hydraulic jump. The total head loss for the whole culvert ranged from 17.86 inches to 20.34 inches. All the results can be seen in Table 30.

Table 30. Hydraulic parameters for Experiment 32

Scenario	32A	32B	32C
CASE	0.8d	1.0d	1.2d
Q (cfs)	0.90	1.23	1.50
$V_{u/s}$ (fps)	2.24	2.47	2.49
Y_s (in)	2.00	2.50	3.50
Y_t (in)	1.50	1.75	2.25
Y_1 (in)	1.35	1.75	2.00
Y_2 (in)	9.26	11.66	12.00
$Y_{d/s}$ (in)	1.75	2.25	2.50
F_{r1}	**5.09**	**4.82**	**4.53**
V_1 (fps)	9.69	10.45	10.49
V_2 (fps)	2.32	3.06	4.33
$V_{d/s}$ (fps)	3.06	4.18	5.67
L (in)	9.00	11.00	14.00
X (in)	9.00	13.00	22.00
ΔE (in)	9.88	11.93	10.42
THL (in)	20.34	19.63	17.86
E_2/E_1	**0.49**	**0.51**	**0.55**

7 Results

The main purpose of this report is to find optimum energy dissipation in open channel and pressure flow conditions for middle and end sill with regular and slotted sill and combined sill with FFFBs. In these experiments, the optimum end sill height was determined first. Second, the sill moved to the middle to get the optimum sill location. Finally the effectiveness of friction blocks in combination with the optimum regular and slotted sill parameters were determined. For all experiments the determining factor for effectiveness is the energy dissipation E_2/E_1. Experiments 4 and 14 with 15 FFFBs were chosen instead of experiments 10 and 15 with 30 FFFBs because there was no significant difference in energy by adding an additional 15 FFFB. It would also not be economically feasible to build the extra friction blocks for the design cost. Ultimately the friction blocks do minimal energy dissipation and the experiments using just the sill would be more cost effective. Also, 2 × 2 inches, 3 × 3 inches, and 4 × 4 inches were tested regular and slotted sill.

7.1 OPEN CHANNEL FLOW CONDITIONS FOR REGULAR SILLS

After careful evaluation, Experiment 3 was selected from the data analysis portion for open channel flow conditions. This experiment used a middle sill and was selected by analyzing several factors, including the relatively low downstream velocities, high total hydraulic head losses, acceptable hydraulic jump efficiency, and possible reduction in channel length. This experiment consisted of a 3.5-inch sill located 20 inches from the end of the culvert. It was found that this experiment yielded results most applicable to the new construction of culverts due to the increased ceiling height of the culvert. The culvert barrel could be reduced by reducing a section at the end of the channel where the water surface profile is more uniform. The reduction of culvert length could be 30 feet for the three cases of the experiment. Figure 22 shows characteristics of the hydraulic jump for Experiment 3A. Figure 23 shows the characteristics of Experiment 3B, and Figure 24 shows Experiment 3C characteristics. The results are shown in Table 31.

Table 31. Selected factors for Experiment 3

Scenario	3A	3B	3C
CASE	0.8d	1.0d	1.2d
Q (cfs)	0.91	1.22	1.50
$V_{u/s}$ (fps)	2.26	2.43	2.49
Y_1 (in)	1.35	1.75	2.25
Y_2 (in)	8.50	9.75	10.75
F_{r1}	**5.09**	**4.60**	**3.77**
V_1 (fps)	9.69	9.96	9.27
V_2 (fps)	2.83	3.06	6.13
ΔE (in)	7.96	7.50	6.35
THL (in)	15.57	15.60	16.51
E_2/E_1	**0.50**	**0.55**	**0.64**

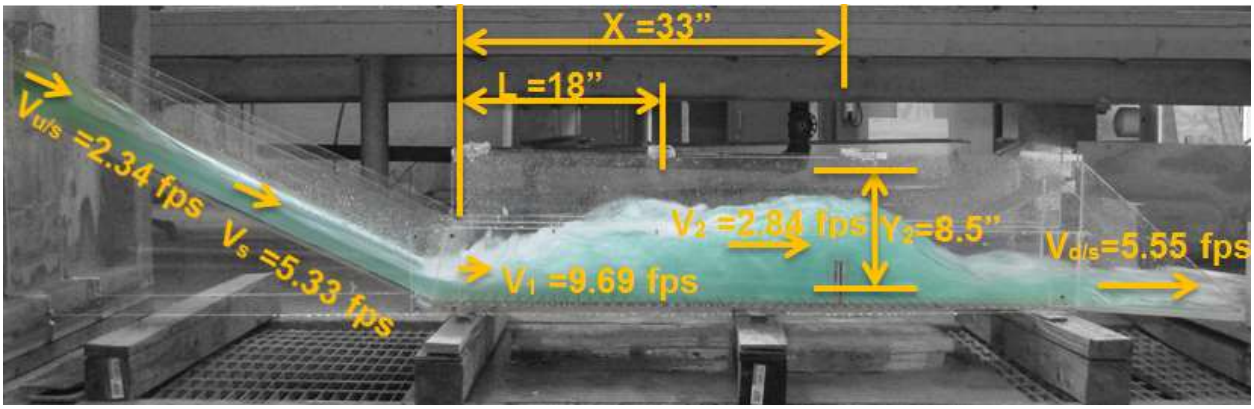

Figure 22. Hydraulic jump characteristics for Experiment 3A

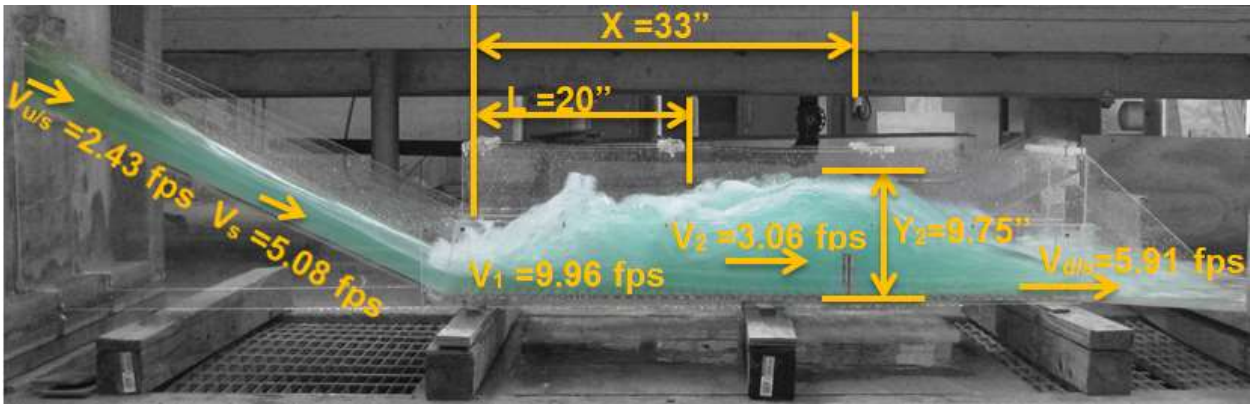

Figure 23. Hydraulic jump characteristics for Experiment 3B

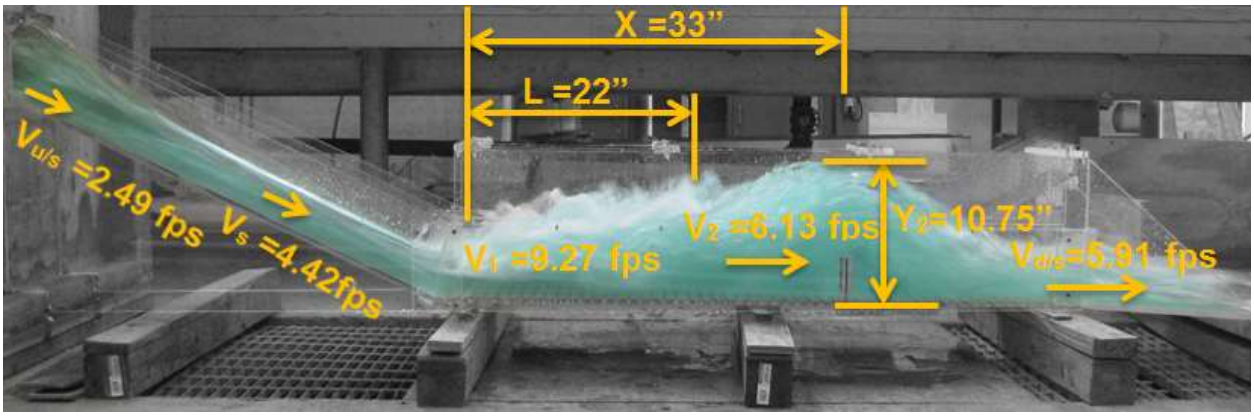

Figure 24. Hydraulic jump characteristics for Experiment 3C

Experiment 4 was selected from the data analysis portion for an open channel flow conditions. This experiment was selected by examining many factors, including the relatively low downstream velocities, high total hydraulic head losses, acceptable hydraulic jump efficiency, and possible reduction in channel length. This experiment consisted of a 3.5-inch sill 20 inches from the end of the culvert with 15 flat faced-friction blocks. Experiment 4 was chosen using 15 FFFBs over the 30 or 45 FFFBs because the increase to 30 FFFBs had drawn hydraulic jump. With this experiment, it was not found that the friction blocks represented increase in the energy dissipation; therefore, they are not economically or practically adequate to the culvert. The culvert barrel could be reduced by reducing a section at the end of the channel where the water surface profile is more uniform. Selected factors for the experiments are included in Table 32.

Table 32. Selected factors for Experiment 4

Scenario	4A	4B	4C
CASE	0.8d	1.0d	1.2d
Q (cfs)	0.91	1.23	1.50
$V_{u/s}$ (fps)	2.26	2.45	2.50
Y_1 (in)	1.50	1.75	2.00
Y_2 (in)	8.75	9.00	9.00
$Y_{d/s}$ (in)	2.50	3.25	3.50
F_{r1}	**4.83**	**4.72**	**4.53**
V_1 (fps)	9.69	10.23	10.49
V_2 (fps)	3.66	4.17	5.18
ΔE (in)	7.26	6.05	4.76
THL (in)	15.75	12.87	14.62
E_2/E_1	**0.52**	**0.53**	**0.55**

Experiment 8 was selected from the data analysis portion for an open channel flow conditions. This experiment was selected by examining many factors, including the relatively low downstream velocities, high total hydraulic head losses, acceptable hydraulic jump efficiency, and possible reduction in channel length. This experiment consisted of a 4-inch sill at the end of the culvert. Experiment 8 was chosen instead of Experiment 10 because the increase to 30 FFFBs had no increase in energy dissipation. It was found that Experiment 8 yielded results most applicable to the existing construction of culverts due to the increased ceiling height of the culvert. Selected factors for the experiments are included in Table 33.

Table 33. Selected factors for Experiment 8

Scenario	8A	8B	8C
CASE	0.8d	1.0d	1.2d
Q (cfs)	0.87	1.20	1.43
$V_{u/s}$ (fps)	2.18	2.41	2.39
Y_1 (in)	1.50	1.75	1.85
Y_2 (in)	8.50	9.65	10.35
F_{r1}	**4.90**	**4.29**	**4.30**
V_1 (fps)	9.83	9.55	9.96
V_2 (fps)	2.32	2.59	2.84
ΔE (in)	6.73	6.65	7.03
THL (in)	18.94	18.58	20.26
E_2/E_1	**0.52**	**0.58**	**0.58**

Experiment 9 was selected from the data analysis portion for an open channel flow conditions. This experiment consisted of a 4-inch sill at the end of the culvert with 15 FFFBs at 25 inched from the toe. Experiment 9 was chosen instead of Experiment 10 because the increase to 30 FFFBs had no increase in energy dissipation. With this experiment, it was not found that the friction blocks represented increase in the energy dissipation; therefore, they are not economically or practically adequate to the culvert. Selected factors for the experiments are included in Table 34.

Table 34. Selected factors for Experiment 9

Scenario	9A	9B	9C
CASE	0.8d	1.0d	1.2d
Q (cfs)	0.94	1.21	1.68
$V_{u/s}$ (fps)	2.34	2.41	2.79
Y_t (in)	1.75	1.75	2.25
Y_1 (in)	1.75	1.85	2.13
Y_2 (in)	8.25	9.50	10.25
F_{r1}	**4.34**	**4.50**	**4.28**
V_1 (fps)	9.41	10.03	10.23
V_2 (fps)	3.06	4.33	2.84
ΔE (in)	4.76	6.37	6.13
THL (in)	18.82	18.84	18.66
E_2/E_1	**0.57**	**0.55**	**0.58**

7.2 PRESSURE FLOW CONDITIONS FOR REGULAR SILLS

After careful evaluation, Experiment 13 was selected from the data analysis portion for pressure flow conditions. This experiment was selected by examining many factors, including the relatively low downstream velocities, high total hydraulic head losses, and possible reduction in channel length. This experiment consisted of a 2.50-inch sill 19 inches from the end of the culvert. It was found that this experiment yielded results most applicable to modifying existing culverts with the addition of sills and/or friction blocks. The culvert barrel could be reduced by reducing a section at the end of the channel where the water surface profile is more uniform which is 30 feet. Figure 25 shows characteristics of the hydraulic jump for Experiment 13A, Figure 26 shows Experiment 13B, and Figure 27 shows Experiment 13C; all are included in Table 35.

Table 35. Selected factors for Experiment 13

Scenario	13A	13B	13C
CASE	(0.8d)	(1.0d)	(1.2d)
Q (cfs)	0.91	1.21	1.41
$V_{u/s}$ (fps)	2.27	2.41	2.36
Y_1 (in)	1.35	1.65	1.85
Y_2 (in)	9.26	10.80	11.50
F_{r1}	**5.09**	**4.80**	**4.56**
V_1 (fps)	9.83	10.10	10.16
V_2 (fps)	2.84	1.64	4.01
ΔE (in)	9.88	10.76	10.55
THL (in)	20.01	16.74	17.23
E_2/E_1	**0.49**	**0.51**	**0.53**

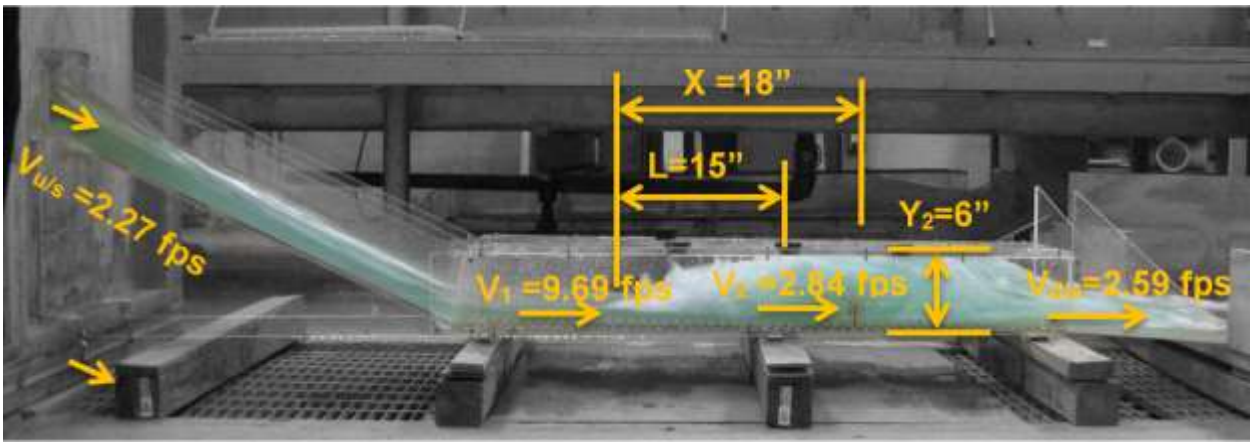

Figure 25. Hydraulic jump characteristics for Experiment 13A

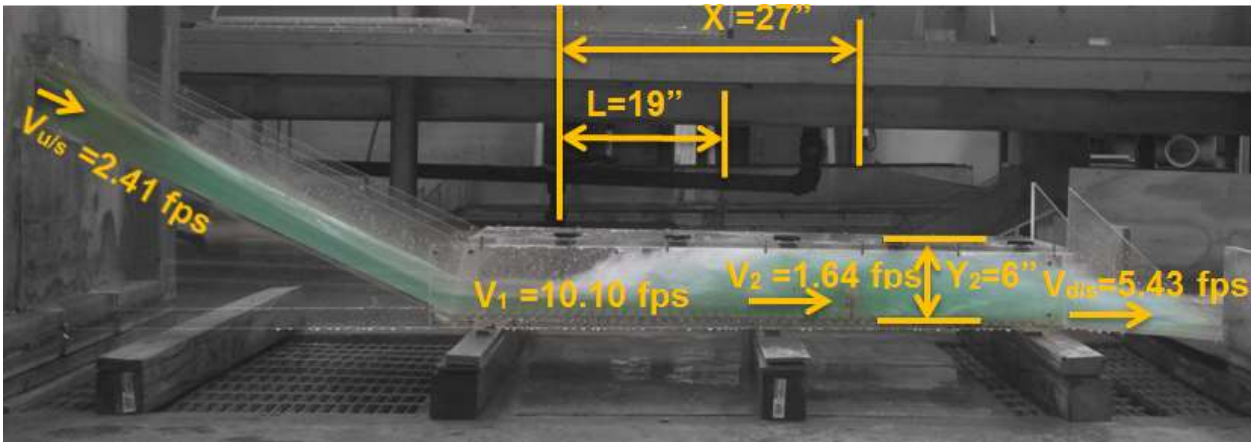

Figure 26. Hydraulic jump characteristics for Experiment 13B

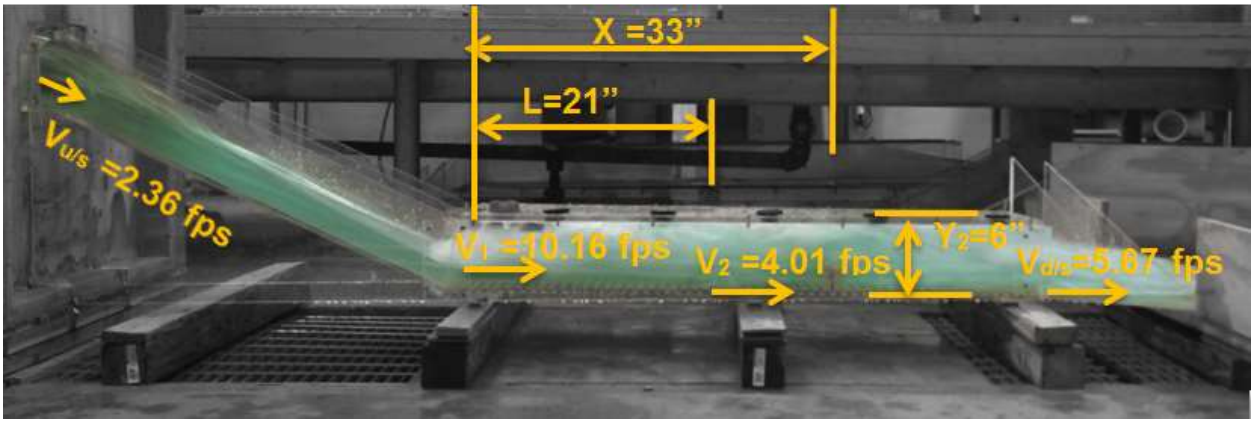

Figure 27. Hydraulic jump characteristics for Experiment 13C

Experiment 14 was selected from the data analysis portion for pressure flow conditions. This experiment was selected by examining many factors; including the relatively low downstream velocities, high total hydraulic head losses, and possible reductions in channel length. This experiment consisted of a 2.50-inch sill 19 inches from the end of the culvert with 15 FFFBs at 11 inches from the toe. It was found that these experiment yielded results most applicable to modifying existing culverts with the addition of sills and/or friction blocks. The culvert barrel could be reduced by reducing a section at the end of the channel where the water surface profile is more uniform which is 30 feet. The characteristics of the hydraulic jump for Experiment 14 are in Table 36.

Table 36. Selected factors for Experiment 14

Scenario	14A	14B	14C
CASE	(0.8d)	(1.0d)	(1.2d)
Q (cfs)	0.91	1.22	1.41
$V_{u/s}$ (fps)	2.18	2.43	2.36
Y_1 (in)	1.65	1.75	2.00
Y_2 (in)	11.10	11.52	12.00
F_{r1}	**4.89**	**4.78**	**4.53**
V_1 (fps)	10.30	10.36	10.49
V_2 (fps)	2.84	4.49	4.63
ΔE (in)	11.53	11.56	11.44
THL (in)	16.94	17.10	17.23
E_2/E_1	**0.50**	**0.51**	**0.53**

Experiment 12 was selected from the data analysis portion for pressure flow conditions. This experiment was selected by examining many factors; including the relatively low downstream velocities, high total hydraulic head losses, and possible reductions in channel length. This experiment consisted of a 2.50-inch sill located at the end of the culvert. It was found that these experiment yielded results most applicable to modifying existing culverts with the addition of sills and/or friction blocks. Experiment 12 was chosen instead of adding 30 or 45 FFFBs because the increase to 30 or 45 friction blocks had a drawn hydraulic jump, which mean the jump formatted in the slant part. The characteristics of the hydraulic jump for Experiment 12 are in Table 37.

Table 37. Selected factors for Experiment 12

Scenario	12A	12B	12C
CASE	(0.8d)	(1.0d)	(1.2d)
Q (cfs)	0.92	1.22	1.50
$V_{u/s}$ (fps)	2.30	2.43	2.50
Y_1 (in)	1.20	1.65	2.00
Y_2 (in)	8.88	10.60	12.00
$Y_{d/s}$ (in)	2.50	3.00	3.50
F_{r1}	**5.47**	**4.74**	**4.53**
V_1 (fps)	9.83	9.96	10.49
V_2 (fps)	4.91	4.63	5.18
$V_{d/s}$ (fps)	3.50	4.01	6.95
ΔE (in)	10.63	10.26	10.42
THL (in)	21.28	19.10	13.87
E_2/E_1	**0.46**	**0.52**	**0.55**

Experiment 17 was selected from the data analysis portion for pressure flow conditions. This experiment was selected by examining many factors; including the relatively low downstream velocities, high total hydraulic head losses, and possible reductions in channel length. This experiment consisted of a 1.50-inch sill 19 inches from the end of the culvert with 6 FFFBs 2 × 2 inches at 14 inches from the toe. It was found that these experiments with big FFFBs increased the energy dissipation around 15%. The culvert barrel could be reduced by reducing a section at the end of the channel where the water surface profile is more uniform which is 30 feet. The characteristics of the hydraulic jump for Experiment 17 are in Table 38.

Table 38. Selected factors for Experiment 17

Scenario	17A	17B	17C
CASE	(0.8d)	(1.0d)	(1.2d)
Q (cfs)	0.87	1.20	1.52
$V_{u/s}$ (fps)	2.18	2.40	2.53
Y_1 (in)	2.00	2.50	3.00
Y_2 (in)	6.89	10.08	11.38
F_{r1}	**2.83**	**3.29**	**3.19**
V_1 (fps)	6.55	8.51	9.05
V_2 (fps)	3.28	2.32	2.46
ΔE (in)	2.12	4.32	4.30
THL (in)	17.09	17.32	18.26
E_2/E_1	**0.78**	**0.72**	**0.74**

7.3 OPEN CHANNEL FLOW CONDITIONS FOR SLOTTED SILLS

After careful evaluation, Experiment 21 was not selected for analysis because six large friction blocks are not practical or economical. Experiment 23 was selected from the data analysis portion for open channel flow conditions. This experiments was selected by examining many factors, including the relatively low downstream velocities, high total hydraulic head losses, acceptable hydraulic jump efficiency, and possible reduction in channel length. This experiment consisted of a 3.50-inch slotted sill 20 inches from the end of the culvert. It was found that this experiment yielded results most applicable to the new construction of culverts due to the increased ceiling height of the culvert. The culvert barrel could be reduced by reducing a section at the end of the channel where the water surface profile is more uniform. Figures 28, 29, and 30 show the hydraulic jump characteristics for Experiment 23; all are included in Table 39.

Table 39. Selected factors for Experiment 23

Scenario	23A	23B	23C
CASE	(0.8d)	(1.0d)	(1.2d)
Q (cfs)	0.88	1.20	1.50
$V_{u/s}$ (fps)	2.21	2.40	2.50
Y_1 (in)	1.65	1.85	2.00
Y_2 (in)	8.00	9.25	10.50
F_{r1}	**4.83**	**4.59**	**4.53**
V_1 (fps)	10.16	10.23	10.49
V_2 (fps)	2.01	4.33	5.43
ΔE (in)	4.85	5.92	7.31
THL (in)	17.36	17.82	17.36
E_2/E_1	**0.52**	**0.55**	**0.55**

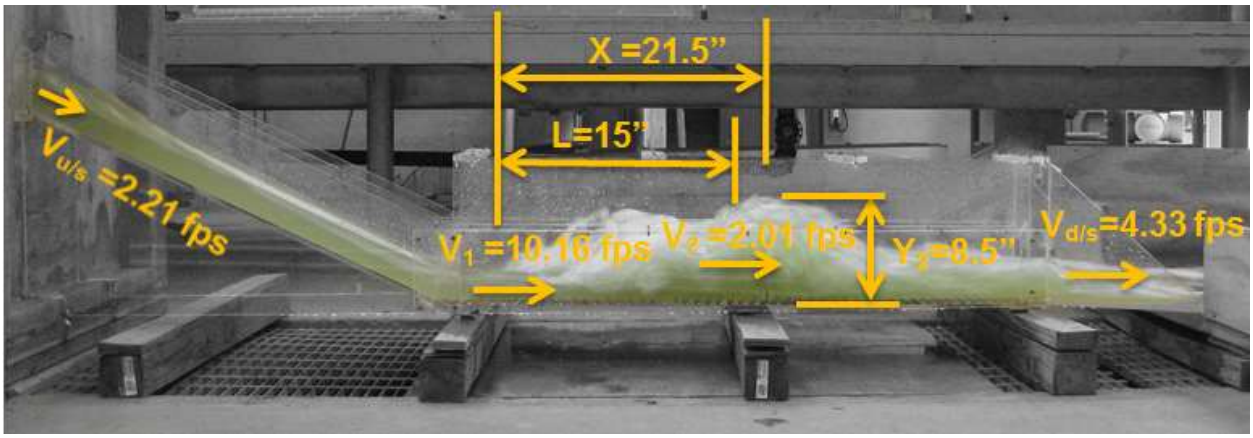

Figure 28. Hydraulic jump characteristics for Experiment 23A

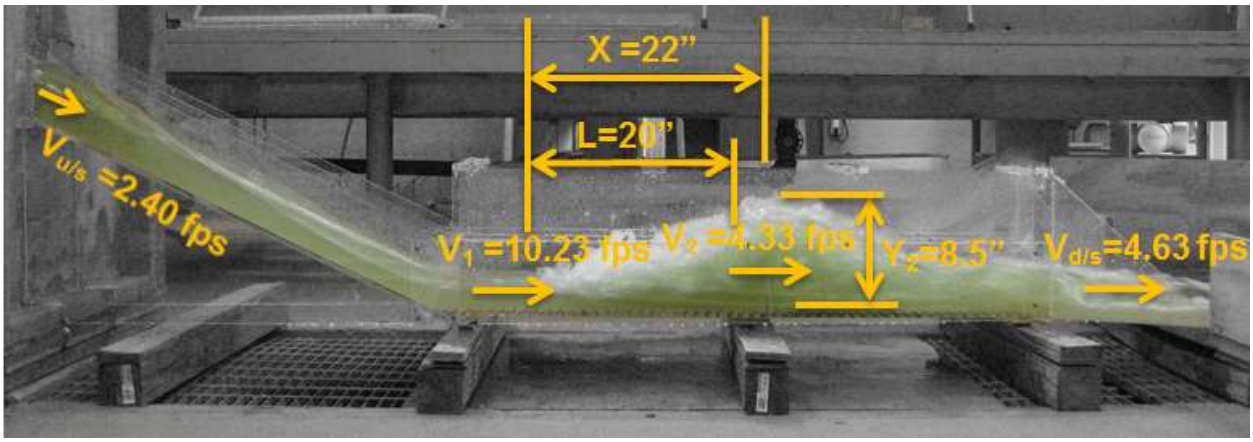

Figure 29. Hydraulic jump characteristics for Experiment 23B

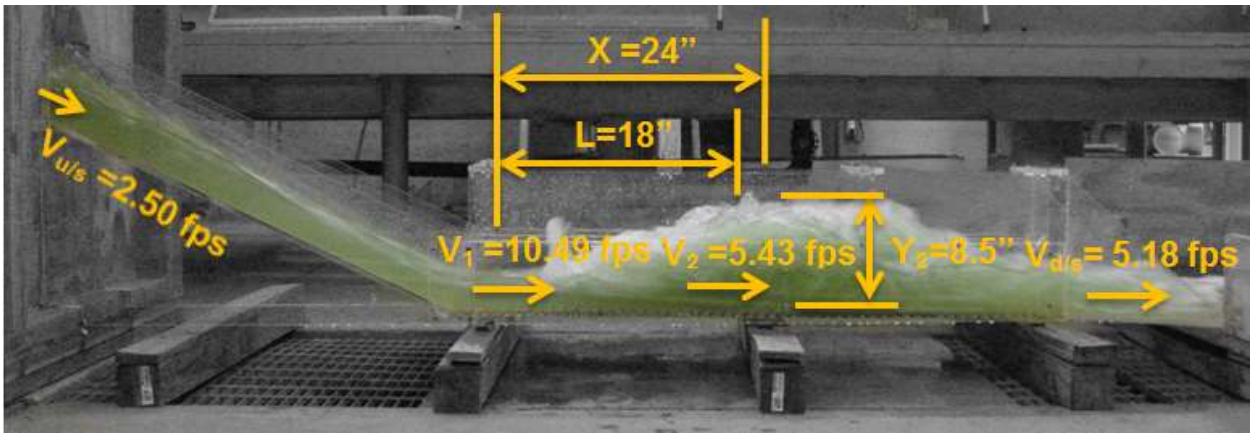

Figure 30. Hydraulic jump characteristics for Experiment 23C

Experiment 24 was selected from the data analysis portion for open channel flow conditions. This experiment was selected by examining many factors, including the relatively low downstream velocities, high total hydraulic head losses, acceptable hydraulic jump efficiency, and possible reduction in channel length. This experiment consisted of a 3.50-inch slotted sill 20 inches from the end of the culvert with 6 FFFBs 2 × 2 inches at 18 inches from the toe. With this experiment, it was found that the friction blocks represented only a 2% increase in the energy dissipation; therefore they are not economically or practically adequate to the culvert. The culvert barrel could be reduced by reducing a section at the end of the channel where the water surface profile is more uniform. Selected factors for the experiments are included in Table 40.

Table 40. Selected factors for Experiment 24

Scenario	24A	24B	24C
CASE	0.8d	1.0d	1.2d
Q (cfs)	0.92	1.19	1.49
$V_{u/s}$ (fps)	2.30	2.39	2.48
Y_1 (in)	1.65	1.75	2.13
Y_2 (in)	8.50	9.25	10.50
F_{r1}	**4.54**	**4.44**	**4.28**
V_1 (fps)	9.55	9.62	10.23
V_2 (fps)	4.01	5.56	5.18
ΔE (in)	5.73	6.52	6.55
THL (in)	16.28	16.31	15.10
E_2/E_1	**0.55**	**0.56**	**0.58**

Experiment 25 was selected from the data analysis portion for open channel flow conditions. This experiment consisted of a 4.50-inch slotted sill at the end of the culvert. The culvert barrel could not be reduced by reducing a section at the end of the channel. It was found that this experiment yielded results most applicable to the new and existing construction of culverts due to the increased ceiling height of the culvert. Selected factors for the experiments are included in Table 41. Figures 31, 32, and 33 show the hydraulic jump characteristics for Experiment 23

Table 41. Selected factors for Experiment 25

Scenario	25A	25B	25C
CASE	0.8d	1.0d	1.2d
Q (cfs)	0.89	1.18	1.49
$V_{u/s}$ (fps)	2.22	2.37	2.48
Y_1 (in)	1.25	1.65	2.13
Y_2 (in)	8.50	9.25	10.75
F_{r1}	**5.37**	**4.86**	**4.33**
V_1 (fps)	9.83	10.23	10.36
V_2 (fps)	1.16	1.64	2.01
ΔE (in)	8.97	7.19	6.99
THL (in)	19.72	19.29	19.59
E_2/E_1	**0.48**	**0.52**	**0.57**

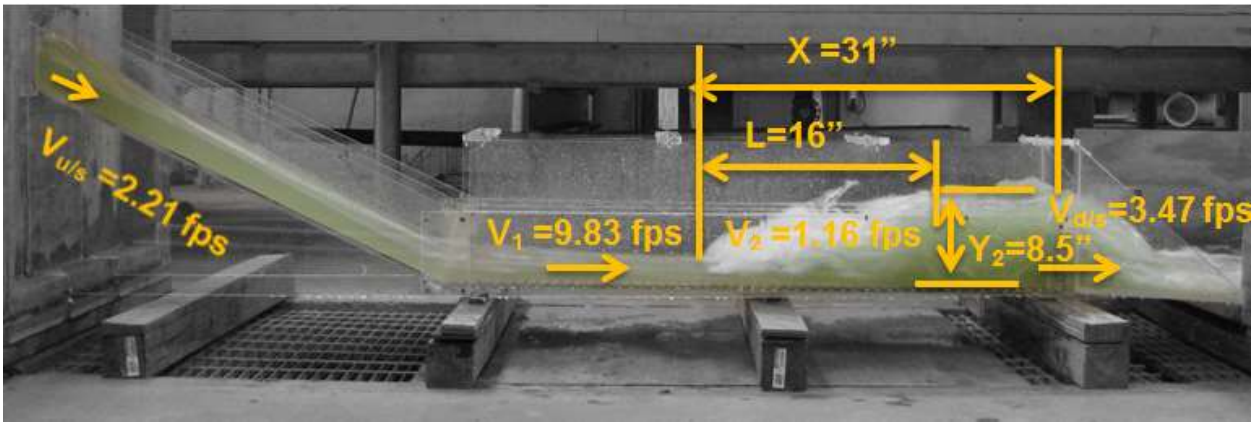

Figure 31. Hydraulic jump characteristics for Experiment 25A

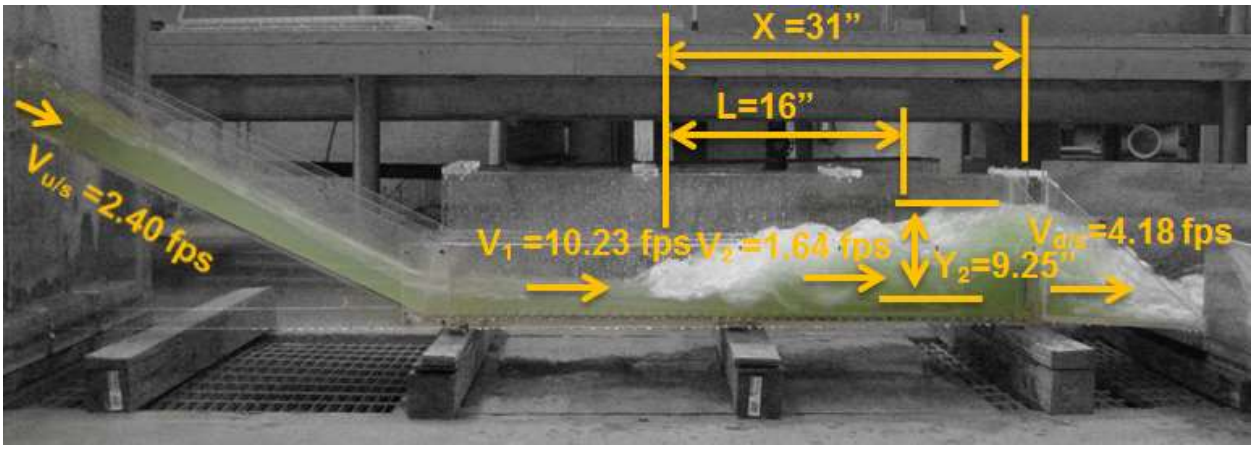

Figure 32. Hydraulic jump characteristics for Experiment 25B

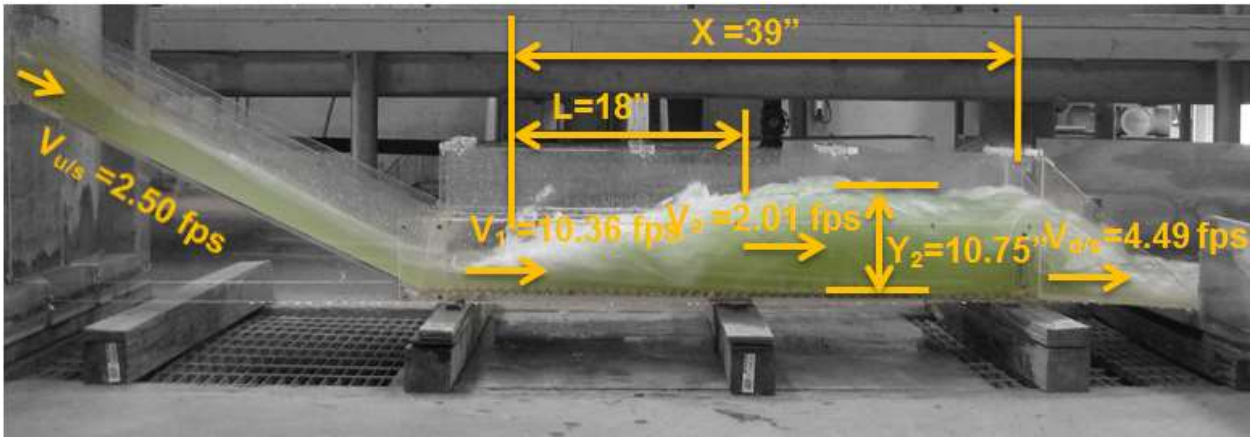

Figure 33. Hydraulic jump characteristics for Experiment 25C

7.4 PRESSURE FLOW CONDITIONS FOR SLOTTED SILL

After careful evaluation, Experiment 27 was selected from the data analysis portion for pressure flow conditions. This experiment was selected by examining many factors, including the relatively low downstream velocities, high total hydraulic head losses, and possible reduction in channel length. This experiment consists of a 2.50-inch slotted sill at the end of the culvert. It was found that this experiment yielded results most applicable to modifying existing culverts with the addition of sills and/or friction blocks. The culvert barrel could not be reduced by shortening a section at the end of the channel. Figure 34, 35, and 36 show the hydraulic jump characteristics for Experiment 27; selected factors for the experiments are included in Table 42.

Table 42. Selected factors for Experiment 27

Scenario	27A	27B	27C
CASE	0.8d	1.0d	1.2d
Q (cfs)	0.89	1.20	1.50
$V_{u/s}$ (fps)	2.23	2.41	2.49
Y_1 (in)	1.50	1.75	2.25
Y_2 (in)	9.56	11.52	12.00
F_{r1}	**4.76**	**4.78**	**4.16**
V_1 (fps)	9.55	10.36	10.23
V_2 (fps)	3.84	3.47	3.28
ΔE (in)	9.13	11.56	8.58
THL (in)	19.38	19.08	13.36
E_2/E_1	**0.52**	**0.51**	**0.60**

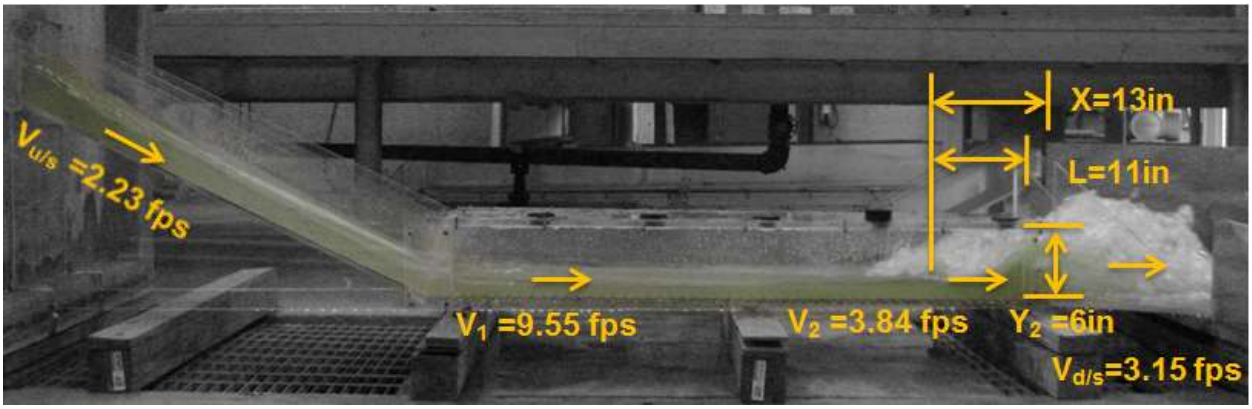

Figure 34. Hydraulic characteristics of Experiment 27A

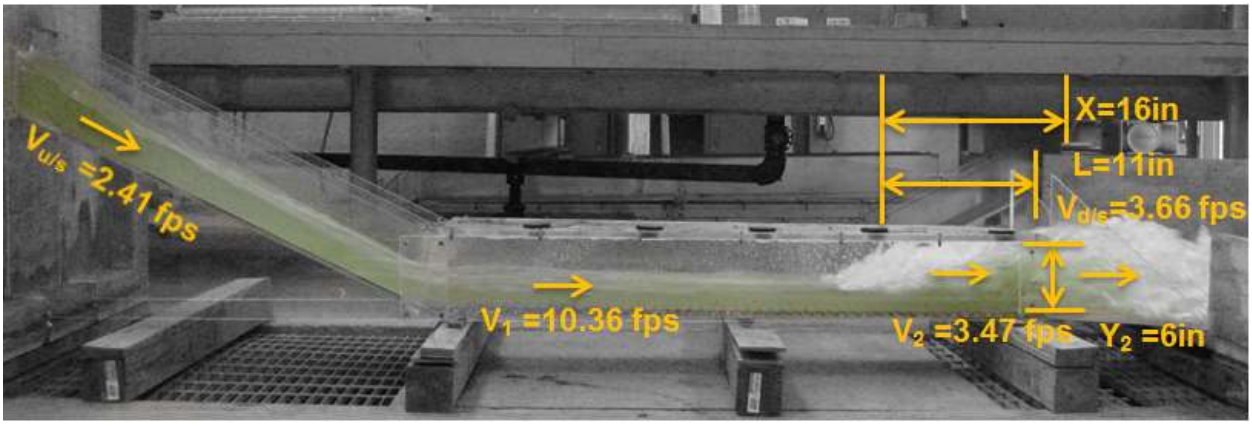

Figure 35. Hydraulic characteristics of Experiment 27B

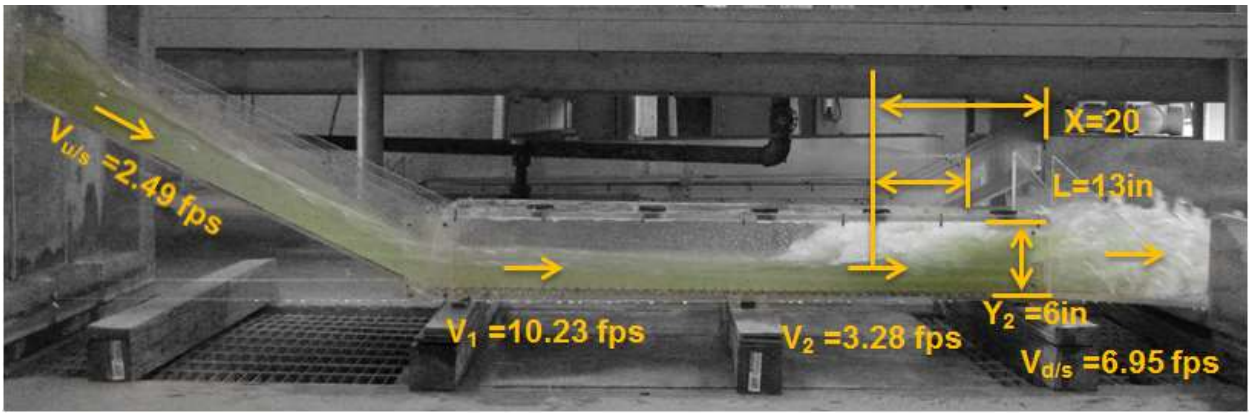

Figure 36. Hydraulic characteristics of Experiment 27C

Experiment 28 was selected from the data analysis portion for pressure flow conditions. This experiment consisted of a 2.50-inch slotted sill at the end of the culvert with 6 FFFBs 2 × 2 inches at 28 inches from the toe of the culvert. It was found that these experiments yielded results most applicable to modifying existing culverts with the addition of sills and/or friction blocks. The culvert barrel could not be reduced by shortening a section at the end of the channel. The characteristics of the hydraulic jump for Experiment 28 are shown in Table 43.

Table 43. Selected factors for Experiment 28

Scenario	28A	28B	28C
CASE	0.8d	1.0d	1.2d
Q (cfs)	0.94	1.20	1.50
$V_{u/s}$ (fps)	1.57	2.00	2.50
Y_1 (in)	1.50	1.85	2.00
Y_2 (in)	10.13	11.82	12.00
F_{r1}	**4.97**	**4.65**	**4.32**
V_1 (fps)	9.96	10.36	10.62
V_2 (fps)	3.06	7.68	8.11
ΔE (in)	10.56	11.32	10.42
THL (in)	20.33	20.32	18.36
E_2/E_1	**0.50**	**0.52**	**0.60**

Experiment 29 was selected from the data analysis portion for pressure flow conditions. This experiment was selected by examining many factors, including the relatively low downstream velocities, high total hydraulic head losses, and possible reduction in channel length. This experiment consists of a 3-inch slotted sill located 25 inches from the end of the culvert. It was found that this experiment yielded results most applicable to modifying existing culverts with the addition of sills and/or friction blocks. The culvert barrel could be reduced by shortening a section at the end of the channel which is between 35 to 40 feet. Figure 37, 38, and 39 show the hydraulic jump characteristics for Experiment 29; selected factors for the experiments are included in Table 44.

Table 44. Selected factors for Experiment 29

Scenario	29A	29B	29C
CASE	0.8d	1.0d	1.2d
Q (cfs)	0.93	1.18	1.50
$V_{u/s}$ (fps)	2.32	2.37	2.50
Y_1 (in)	1.60	1.75	2.00
Y_2 (in)	10.74	11.82	12.00
F_{r1}	**4.91**	**4.87**	**4.47**
V_1 (fps)	10.16	10.55	10.36
V_2 (fps)	5.67	4.63	6.13
ΔE (in)	11.11	12.36	10.42
THL (in)	18.30	19.29	21.11
E_2/E_1	**0.50**	**0.50**	**0.55**

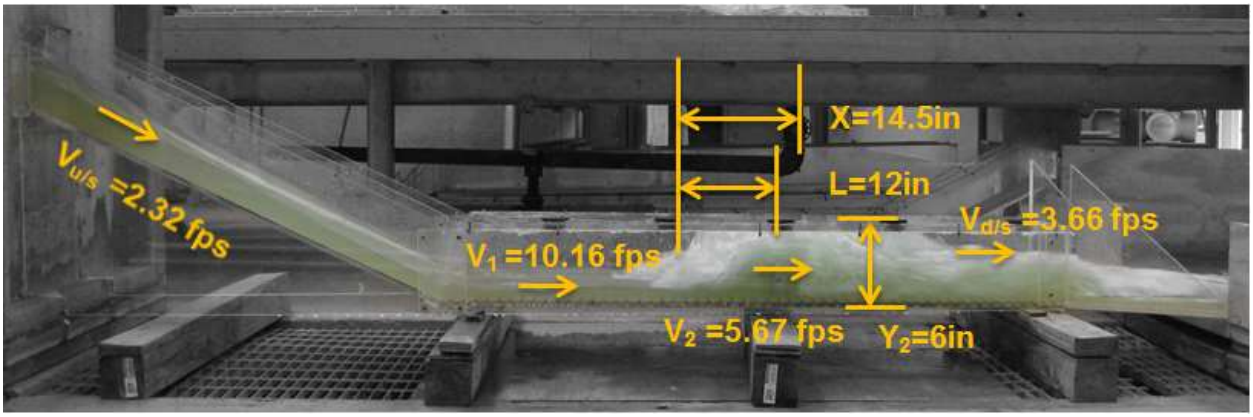

Figure 37. Hydraulic jump characteristics for Experiment 29A

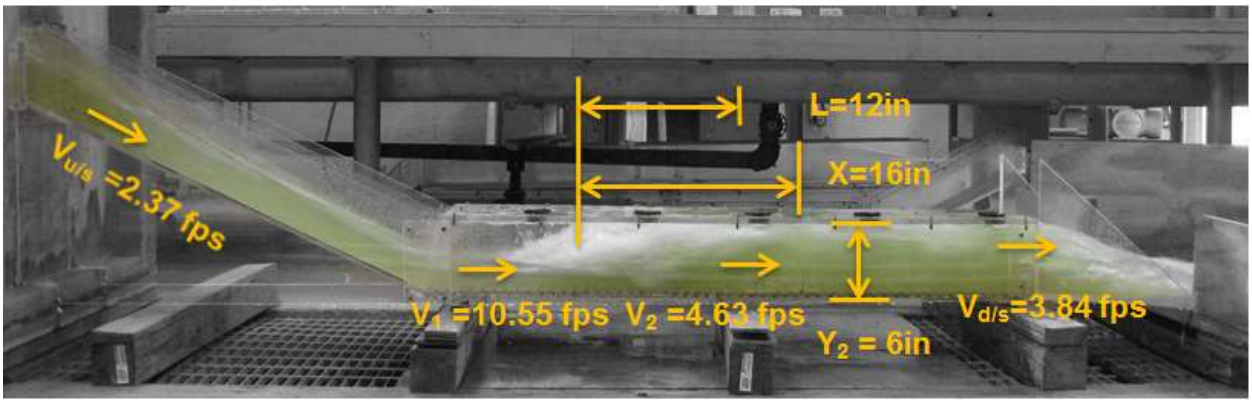

Figure 38. Hydraulic jump characteristics for Experiment 29B

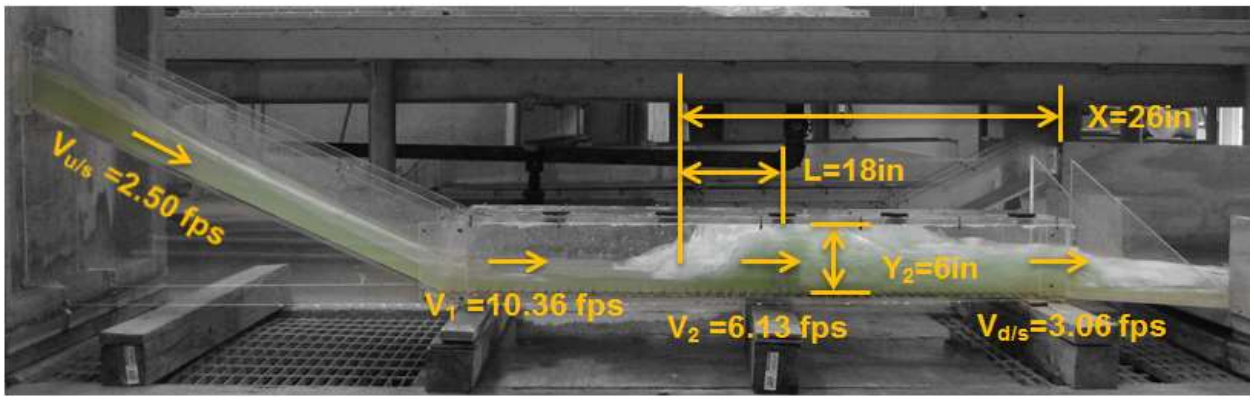

Figure 39. Hydraulic jump characteristics for Experiment 29C

Experiment 30 was selected from the data analysis portion for pressure flow conditions. This experiment consisted of a 3-inch slotted sill at the end of the culvert with 6 FFFBs 2 × 2 inches at 18 inches from the toe of the culvert. It was found that these experiments yielded results most applicable to modifying existing culverts with the addition of sills and/or friction blocks. The culvert barrel could be reduced by shortening a section at the end of the channel which is 35 to 40 feet. The characteristics of the hydraulic jump for Experiment 30 are shown in Table 45.

Table 45. Hydraulic parameters for Experiment 30

Scenario	30A	30B	30C
CASE	0.8d	1.0d	1.2d
Q (cfs)	0.90	1.22	1.49
$V_{u/s}$ (fps)	1.49	2.03	2.48
Y_1 (in)	1.85	2.00	2.25
Y_2 (in)	11.39	11.11	12.00
F_{r1}	**4.53**	**4.18**	**4.11**
V_1 (fps)	10.10	9.69	10.10
V_2 (fps)	5.91	5.31	4.33
ΔE (in)	10.30	8.51	9.23
THL (in)	16.49	16.85	19.35
E_2/E_1	**0.54**	**0.58**	**0.58**

7.5 OBSERVATIONS OF REGULAR AND SLOTTED SILLS

Two sill types were used in this experiment. One was the regular sill and the other was the slotted sill. The regular sill is a rectangular shape with two small orifices on the bottom of the sill seen in Figure 40. The slotted sill is made of two identical shapes that are rectangular and have one small orifice on the bottom of each piece. The slotted sill is similar to the regular sill other than there is a gap in the middle of the slotted sill allowing water and debris to pass through as seen in Figure 41.

The slotted sill was designed to do everything the regular sill does, but allow some additional water, sediments, and debris to pass through so there would be less build up behind the sill. It was believed that the slotted sill could be adjusted to provide energy dissipation similar to that of the regular sill. After experimentation it was found that a model height increase of one half inch of the slotted sill vs. the regular sill gave nearly identical energy dissipation results. The one half inch increase in the model size translates to 0.833 feet in full scale.

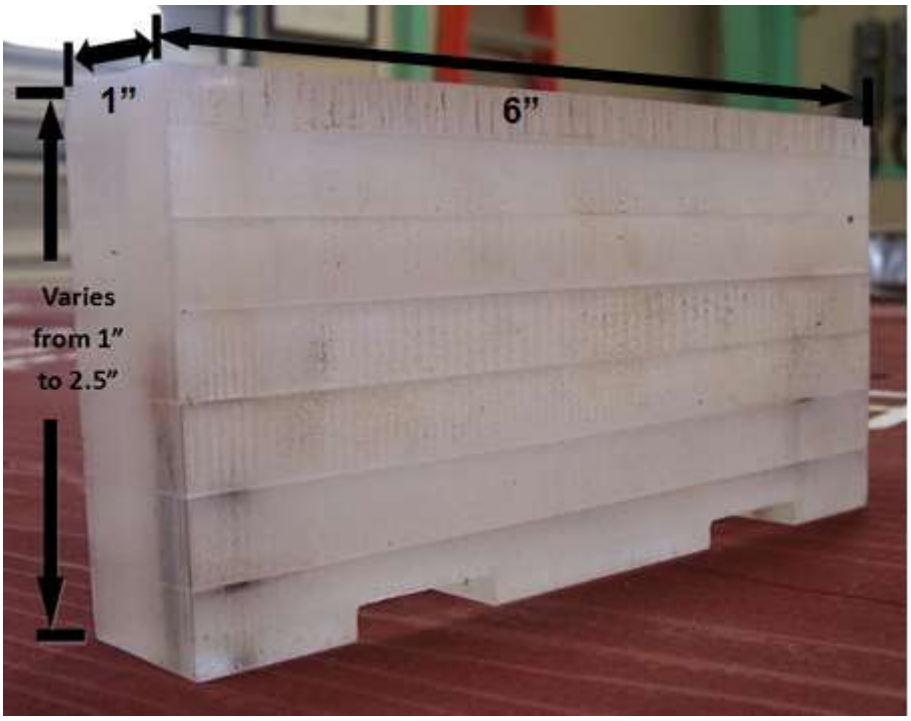

Figure 40. Regular Sill

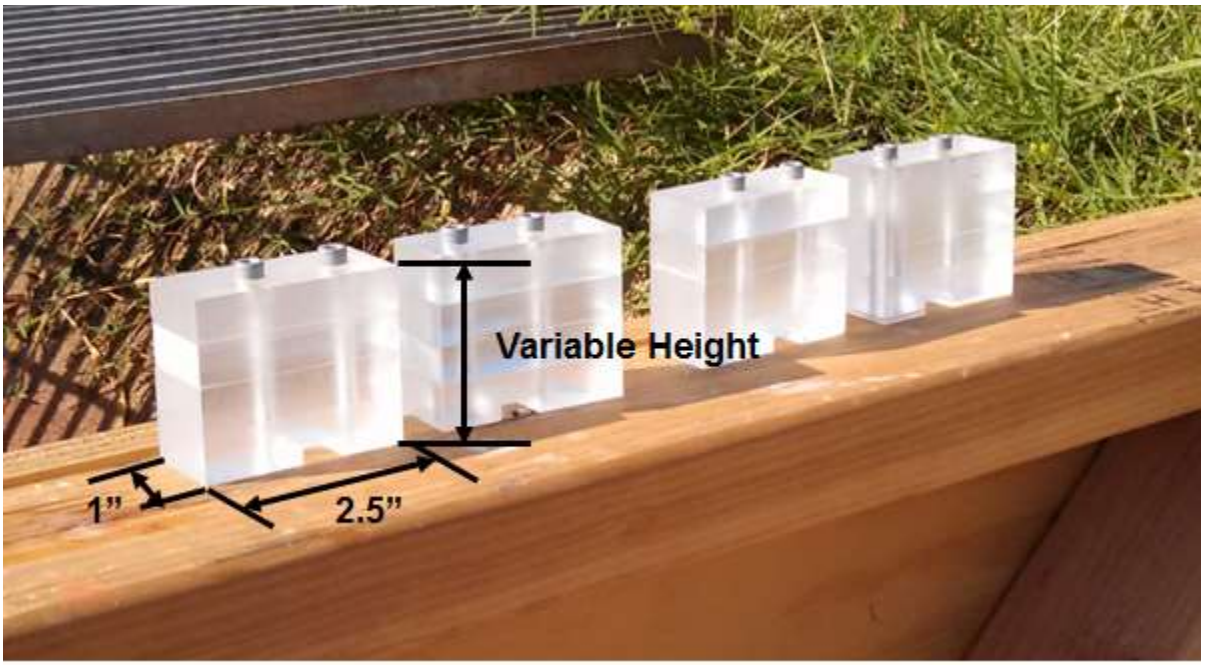

Figure 41. Slotted Sill

8 Conclusions

8.1 REGULAR SILL

A laboratory model was constructed to represent a broken-back culvert. The idealized prototype contains a 1 (vertical) to 2 (horizontal) slope, a 60-foot horizontal length steep section of culvert continuing down to a 90-foot mild section of the culvert. The mild section is built with a slope of 1 percent. The model was made to 1:20 scale. The following dimensions are in terms of the prototype culvert. It was noted that the current practice of not using any energy dissipaters (as in Experiment 1) allowed all the energy to flow through the culvert instead of reducing or dissipating it. The following conclusions can be drawn based on the laboratory experiments for open channel flow conditions.

8.1.1 OPEN CHANNEL FLOW CONDITIONS

1) For new culvert construction, Experiment 3 is the best option for open channel flow conditions. This option includes one 5.83-foot sill with two small orifices at the bottom for draining the culvert completely located 33.33 feet from the end of the culvert. The height of the culvert should be at least 17.92 feet to allow open channel condition in the culvert.

2) If one sill 5.83 feet high is placed in the flat part of the culvert, it results in 64 percent energy dissipation as seen in Experiment 3C in Figure 23 and Table 25.

3) If one sill 5.83 feet high with 15 flat-faced friction blocks is placed in the flat part of the culvert starting at the initiation of the hydraulic jump, energy dissipation of 55 percent occurs as seen in Experiment 4C.

4) The reduction of energy due to friction blocks is marginal. The optimal 5.83-foot sill is the most economical option.

5) Experiment 3 shows an opportunity to reduce the culvert length at the end in the range of 30 to 33 feet. The 30-foot reduction was determined by eliminating the

downstream segment of the culvert where the water surface is no longer uniform after the jump. The 43-foot reduction results from removing a portion of the downstream culvert from the sill to the beginning of the downstream wing-wall section. This option is important if there are problems with the right-of-way.

6) The difference of efficiency when flat-faced friction blocks were used varied by only 1%. The energy loss ranged between 6.35 feet to 7.96 feet.

7) For existing and new culvert construction, Experiment 8 is the best option for end sill. This option includes one 6.67-foot end sill. The height of the culvert should be at least 17.25 feet to allow open channel condition in the culvert.

8) If one end sill 6.67 feet high is placed in the end the culvert, it results in 58 percent energy dissipation as seen in Experiment 8C.

9) If one end sill 6.67 feet high with 15 flat-faced friction blocks is placed in the flat part of the culvert, energy dissipation of 58 percent occurs, so that friction block affect marginal on energy dissipation.

10) The optimal friction block height for 30-foot drop is a 3.33 feet (2 inch) friction block. The 1.67 feet (1 inch) friction block most often created a sky jump, and the friction blocks of larger sizes acted like a sill.

8.1.2 PRESSURE FLOW CONDITIONS

Formation of a hydraulic jump is used in reducing downstream degradation of broken-back culverts. A broken-back culvert is used in areas of high relief and steep topography as it has one or more breaks in the profile slope. The advantage of a culvert is to safely pass water underneath the roadways constructed in hilly topography or on the side of a relatively steep hill. A laboratory model was constructed to represent a 150-foot broken-back culvert. The drop between upstream and downstream was 30 feet. The idealized prototype contains a 1 (vertical) to 2 (horizontal) slope, a 60-foot horizontal length of the slanted part of the culvert continuing down to a 90-foot flat culvert with a 1 percent slope. The prototype for these experiments was a two-barrel, 10-foot by 10-foot reinforced concrete culvert. The model was made to 1:20 scale. The following dimensions are in terms of the prototype culvert. The following conclusions can be drawn based on the laboratory experiments for pressure flow conditions:

1) For retrofitting an existing culvert, Experiment 13 is the best option using a regular sill, a 4.17-foot sill 31.67 feet from the end of the culvert.

2) Optimal placement of the sill, 4.17 feet high, resulted in 28.72 feet THL and energy dissipation of 53 percent as shown in Experiment 13C.

3) For Experiment 13, reductions in culvert length can be made between 25 feet to 30 feet, as seen in Table 15 and 35.

4) If one 4.17-foot sill at 31.67 feet from the end of the culvert and 15 flat-faced friction blocks are placed in the flat section of the culvert starting at the formation of the hydraulic jump, the THL is 28.72 feet and energy dissipation is 53 percent as seen in Experiment 35C.

5) The reduction of energy due to the region of friction blocks is marginal.

6) For existing and new construction of culvert, the best end sill option is Experiment 12, which consisted of 4.17-foot sill at the end of culvert, resulted in 28.72 feet THL and energy dissipation of 55 percent as shown in Experiment 12C, as seen in Table 37.

8.2 SLOTTED SILL

The slotted sill has one cut in the middle and contains two small orifices at the bottom of the other parts to allow the culvert to completely drain and to use the middle cut to clean up the sediment behind the slotted sill. Slotted sills were used in the middle and the end of the culvert. Also, the impact of friction blocks was found to be minimal. No friction blocks were used to further dissipate the energy. The following conclusions can be drawn based on the laboratory experiments for open channel and pressure flow conditions:

8.2.1 OPEN CHANNEL FLOW CONDITIONS

1) The slotted sill is easier to access and clean due to the opening.

2) Slotted sills can dissipate energy levels similar to a traditional (regular) sill if the slotted sill is raised 0.5 inches in the model or 0.8333 feet in full scale.

3) Experiment 23 is the best option for the middle slotted sill. This option includes one 5.83-foot slotted sill located 33.33 feet from the end of the culvert. It results in 55 percent of energy dissipation in case 23C.

4) Experiment 24 is Experiment 23 with 6 flat-face friction blocks 3.33 × 3.33 feet (2 × 2 inches). It results in 58 percent of energy dissipation in case 24C. The energy dissipation due to friction block is 3%

5) Experiment 25 is the best option for the end sill. Experiment 25 includes one 7.5 feet slotted end sill. It results in 57 percent of energy dissipation in case 25C.

6) Experiment 26 is Experiment 25 with 6 flat-face friction blocks 3.33 × 3.33 feet (2 × 2 inches). It results in 56 percent of energy dissipation in case 26C. The energy dissipation due to friction block is the same without friction blocks

8.2.2 PRESSURE FLOW CONDITIONS

1) Experiment 27 is the best option for the end slotted sill. This option includes one 4.17-foot slotted sill located at the end of the culvert. It was resulted in 60 percent of energy dissipation in case 27C.

2) Experiment 28 is Experiment 27 with an added 6 flat-face friction blocks 3.33 × 3.33 feet (2 × 2 inches). It results in 60 percent of energy dissipation in case 28C. The energy dissipation due to friction blocks is negligible.

3) Experiment 29 is the best option for the end sill. Experiment 29 includes one 5.00 feet slotted end sill. It results in 56 percent of energy dissipation in case 29C, as shown in Table 44.

4) Experiment 30 is Experiment 29 with 6 flat-face friction blocks 3.33× 3.33 (2× 2 inches). It results in 60 percent of energy dissipation in case 30C. The energy dissipation due to friction block is 4%, as shown in Table 45.

8.4 FRICTION BLOCKS ONLY

Several numbers and sizes of friction flat-faced friction blocks have been tested experimentally. It was found that friction blocks could not give sufficient energy dissipation by themselves, unless several larger friction blocks such as 5 × 5 feet (3 × 3 inches), 6.67 × 6.67 feet (4 × 4 inches). These large friction blocks worked like a sill if more than 2 friction blocks were placed. Following are the best experiment options:

1) For open channel flow conditions, Experiment 20 is the best option with 4, 5 feet flat-faced friction blocks (FFFBs) height at the end of culvert, it results in 55 percent of energy dissipation in case 20C.

2) For open channel flow conditions, Experiment 22 with 4, 6.67 x 6.67 feet flat-faced friction blocks height at the end of culvert; it results in 61 percent of energy dissipation in case 22C, which increased the energy dissipation by 6%. Therefore, the optimal FFFBs height would be 5-foot FFFBs, and the increase in energy dissipation could be worth the extra cost.

3) For pressure flow conditions, Experiment 31 is the best option with 6, 3.33 feet FFFBs height at 18 inches from the end of culvert, it results in 57 percent of energy dissipation in case 31C.

4) For pressure flow conditions, the best option is Experiment 32 with 2, 5 feet flat-faced friction blocks height at the end of culvert; it results in 55 percent of energy dissipation in case 32C, which is almost the energy dissipation as Experiment 31. Therefore, the optimal FFFBs height can be 3.33-foot FFFBs, and could be the most economical option.

9 Recommendations

The following are the recommendations based on the results of the experiments:

1) The slotted sill is recommended for use because of ease of cleaning drains faster and higher energy dissipation.
2) Numerical model explores possibility flow of energy dissipation for any size of drop. Once the numerical modeling methodology is perfected, it can be used for any drop of broken-back culvert. Then it does not have to be for fixed 6, 12, 18, 24, and 30 feet.

References

Alikhani, A., Behroz-Rad, R., and Fathi-Moghadam, M. (2010). Hydraulic Jump in Stilling Basin with Vertical End Sill. International Journal of Physical Sciences. 5(1), 25-29.

Bhutto, H., Mirani, S. and Chandio, S. (1989). "Characteristics of Free Hydraulic Jump in Rectangular Channel." *Mehran University Research Journal of Engineering and Technology, 8(2)*, 34 – 44.

Baylar, A., Unsal, M., and Ozkan, F. (2011). "The Effect of Flow Patterns and Energy Dissipation over Stepped Chutes on Aeration Efficiency." *KSCE Journal of Civil Engineering.* 15(8), PP. 1329-1334

Bessaih, N., and Rezak, A. (2002). "Effect of Baffle Blocks with Sloping Front Face on the Length of the Jump*." Journal of Civil Engineering*, 30(2), PP. 101-108.

Caterpillar Performance Handbook, (2008). Edition 38. Cat® publication by Caterpillar Inc., Peoria, Illinois, U.S.A..

CAT website. (2013). <http://www.cat.com/cda/layout?m=361746&x=7>.

Chanson, H. (2008). "Acoustic Doppler velocimetery (ADV) in the field and in laboratory: practical experiences." *International Meeting on Measurements and Hydraulics of Sewers*, 49-66.

Chanson, H. (2009). "Current knowledge in hydraulic jumps and related phenomena." *European Journal of Mechanics B/Fluid*. 29(2009), 191-210.

Chow, V.T. (1959). Open-channel Hydraulics. McGraw-Hill, New York, NY, 680 pages.

Debabeche, M., and Achour, B. (2007). "Effect of sill in the hydraulic jump in a triangular channel." *Journal of Hydraulic Research.* 45(1), PP. 135-139

Eloubaidy, A., Al-baidbani, J., and Ghazali, A. (1999). "Dissipation of Hydraulic Energy by Curved Baffle Blocks." *Pertanika Journal Science Technology*. 7 (1), 69-77 (1999).

Federal Highway Administration (2006). The Hydraulic Design of Energy Dissipaters for Culverts and Channels.

Finnemore, J. E., and Franzini, B. J., (2002) *Fluid Mechanics with Engineering Applications.* McGraw-Hill, New York, NY, 790.

Gharanglk, A. and Chaudhry, M. (1991). "Numerical simulation of hydraulic jump." *Journal of Hydraulic Engineering. 117(9),* 1195 – 1211.

Goring, D., Nikora, V. (2002). "Despiking Ascoustic doppler Velocimeter Data." *Journal of Hydraulic Engineering,* 128(1), 117-128.

Goodridge W. (2009). Sediment Transport Impacts Upon Culvert Hydraulics. Ph.D. Dissertation. Utah State University, Logan, Uath.

Hotchkiss, R. and Donahoo, K. (2001). "Hydraulic design of broken-back culvert." *Urban Drainage Modeling, American Society of Civil Engineers*, 51 – 60.

Hotchkiss, R., Flanagan, P. and Donahoo, K. (2003). "Hydraulic Jumps in Broken-Back Culvert." *Transportation Research Record* (1851), 35 – 44.

Hotchkiss, R. and Larson, E. (2005). Simple Methods for Energy Dissipation at Culvert Outlets. *Impact of Global Climate Change*. World Water and Environmental Resources Congress.

Hotchkiss, R., Thiele, E., Nelson, J., and Thompson, P. (2008). "Culvert Hydraulics: Comparison of Current Computer Models and Recommended Improvements." *Journal of the Transportation Research Board*, No. 2060, Transportation Research Board of the National Academies, Washington, D.C, 2008, pp. 141-149.

Habibzadeh, A., and Loewen, M. R., Rajaratnam, N. (2011). "Performance of Baffle Blocks in Submerged Hydraulic Jumps." *Journal of Hydraulic Engineering.*

Habibzadeh, A., Wu, S., Ade, F., Rajaratnam, N., and Loewen, M. R. (2011). "Exploratory study of submerged hydraulic jumps with blocks." *Journal of Hydraulic Engineering,* PP.706-710

Larson, E. (2004). *Energy dissipation in culverts by forcing a hydraulic jump at the outlet.* Master's Thesis, Washington State University.

Lewis, P., Personal Communication, (2012). Civil and Environmental Engineering, Oklahoma State University.

Jamshidnia, J., Takeda, Y., and Firoozabadi, B. (2010). "Effect of standing baffle on the flow structure in a rectangular open channel." *Journal of Hydraulic Research*. 48(3) PP. 400-404

Mignot, E. and Cienfuegos, R. (2010). "Energy dissipation and turbulent production in weak hydraulic jumps." *Journal of Hydraulic Engineering*, ASCE, 136 (2), 116-121.

Mori, N. Suzuki, T., and Kakuno, S. (2007). "Noise of acoustic doppler velocimeter data in bubbly flows." *Journal of Engineering Mechanics*, *133(1),* 122-125.

Meselhe, E. and Hebert, K., (2007). "Laboratory Measurements of Flow through Culverts." *Journal of Hydraulic Engineering.* 133(8), PP. 973-976

Noshi, H., (1999). *Energy dissipation near the bed downstream end-sill.* 28th IAHR Congress, Hydraulic Research Institute, National Water Research Center.

Ohtsu I., Yasuda, Y., and Hashiba, H. (1996). "Incipient jump conditions for flows over a vertical sill." *Journal of Hydraulic Engineering*, *ASCE*. 122(8) 465-469. doi: 10.1061/(ASCE)0733-29(1996)122:8(465).

Ohtsu, I et al. (2001). "Hydraulic condition for undular jump formation." *Journal of Hydraulic Research*. 39(2), 203-209. http://cat.inist.fr/?aModele=ffficheN&cpsidt=1054107.

Oosterholt, G.A. (1947). "An Investigation of the Energy Dissipated in a Surface Roller." *Applying Science Resource*. A1, 107-130

Pagliara, S., Lotti, I., and Palermo, M. (2008). "Hydraulic jump on rough bed of stream rehabilitation structures." *Journal of Hydro-environment Research* 2(1), 29-38.

Rusch, R. (2008) Personal communication, Oklahoma Department of Transportation.

SonTek/YSI, Inc. *ADVField/Hydra System Manual* (2001).

Singley, B. and Hotchkiss, R. (2010). Differences between Open-Channel and Culvert Hydraulics: Implications for Design. World Environmental and Water Resources Congress 2010: Challenges of Change. 2010 ASCE, PP 1278-1287

Tyagi, A. K. and Schwarz, B. (2002). A Prioritizing Methodology for Scour-critical Culverts in Oklahoma. Oklahoma Transportation Center. Oklahoma, 13 pp.

Tyagi, A.K. and Albert, J. (2008). "Review of Laboratory Experiments and Computer Models for Broken-box Culverts" Oklahoma Department of Transportation, ODOT Item Number: 2193, Oklahoma, 43 pp.

Tyagi, A.K., et al., (2009). "Laboratory Modeling of Energy Dissipation in Broken-back Culverts – Phase I," Oklahoma Transportation Center, Oklahoma, 82 pp.

Tyagi, A. K., Brown, J., A. Al-Madhhachi, and Ali, A. (2009). Energy Dissipation in Broken-Back Culverts. ASCE Annual Conference, August 2009, ATRC Building, OSU Campus, Stillwater, OK.

Tyagi, A. K., Brown, J., Al-Madhhachi, A., and Ali, A. (2010a). Energy dissipation in Broken-Back culverts under open channel flow conditions. American Society of Civil Engineering, International Perspective on current and future state of Water Resources and the Environment, January 6-10, 2010, Chennai, India. 10 pp.

Tyagi, A. K., Al-Madhhachi, A., Brown, J., and Ali, A. (2011b). Energy dissipation in Broken-Back culverts under pressure flow conditions. 4th ASCE-EWRI International Perspective on Water Resources & the Environment, January 4-6, 2011, National University of Singapore, Singapore. 10 pp.

Tyagi, A. K., Johnson, N. and Ali, A. (2011). Energy Dissipation in 24-foot Drop Broken Back Culverts under Open Channel Conditions. ASCE, *Journal Hydraulic Engineering.* (Submitted or peer review)

Tyagi, A.K., Ali, A., Johnson, N. and Ali, A. Brown, J. (2011). "Laboratory Modeling of Energy Dissipation in Broken-back Culverts–Phase II," Oklahoma Transportation Center, Oklahoma, 80 pp.

Tyagi, A. K., Johnson, N. Ali, A. and Brown, J. (2012). Energy Dissipation in Six-Foot Drop Broken Back Culverts under Open Channel Conditions. *5th International Perspective on Water Resources and the Environment Conference, Marrakech, Morocco.*

Tyagi, A. K., Johnson, N. and Ali, A. (2012). Energy Dissipation in Six-Foot Drop Broken Back Culverts under Open Channel Conditions. *Journal Hydraulic Engineering. ASCE*. (Submitted or peer review)

Tyagi, A. K., Ali, A., Johnson, N., Motte, M., and Davis, T. (2012). Energy Dissipation in Eighteen-Foot Broken-back Culverts Laboratory Models – Phase III, Oklahoma Department of Transportation, Oklahoma, 119 pp.

Tyagi, A. K., Ali, A., Johnson, N., Motte, M., and Davis, T. (2013). Energy Dissipation in Twelve-Foot Broken-back Culverts Laboratory Models – Phase IV, Oklahoma Department of Transportation, Oklahoma, 146 pp.

Tyagi, A. K., Ali, A., and. Johnson, N. (2013). Energy Dissipation in Eighteen-foot Drop Broken-Back Culverts under Open Channel Conditions. *Environmental and Water Resources Institute of ASCE 2013*, 19 – 23 May, 2013 Cincinnati, Ohio.

Utah Department of Transportation (2004.) *Manual of Instruction – Roadway Drainage and Culverts*.

Varol, F., Cevik, E., and Yuksel, Y. (2009). The effect of water jet on the hydraulic jump. Thirteenth International Water Technology Conference, IWTC. 13 (2009), 895-910, Hurghada, Egypt.

Wahl, T. (2000). Analyzing ADV data using WinADV. *2000 joint water resources engineering and water resources planning and management,* July 30- August 2, 2000- Minneapolis, Minnesota.

Wahl, T. (2003). Discussion of “Despiking acoustic Doppler velocimeter data” by Goring, D. and Nikora, V. *Journal of Hydraulic Engineering,129(6),* 484-487.

Appendix A - Laboratory Experiments for Hydraulic Jump

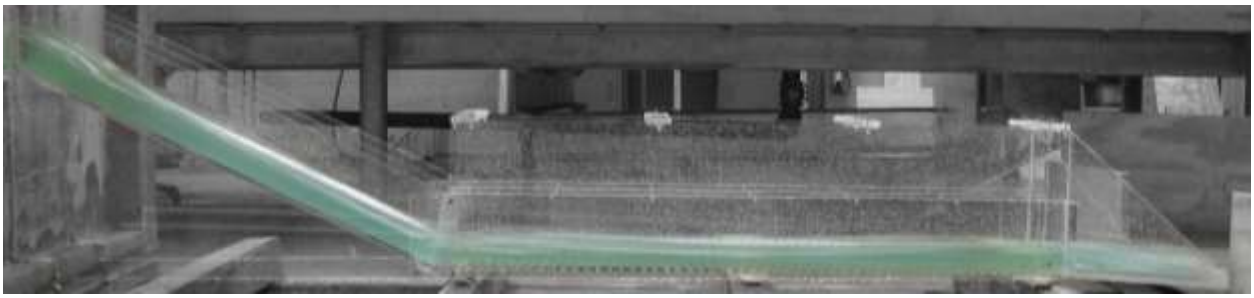

Figure A1. Experiment 1A

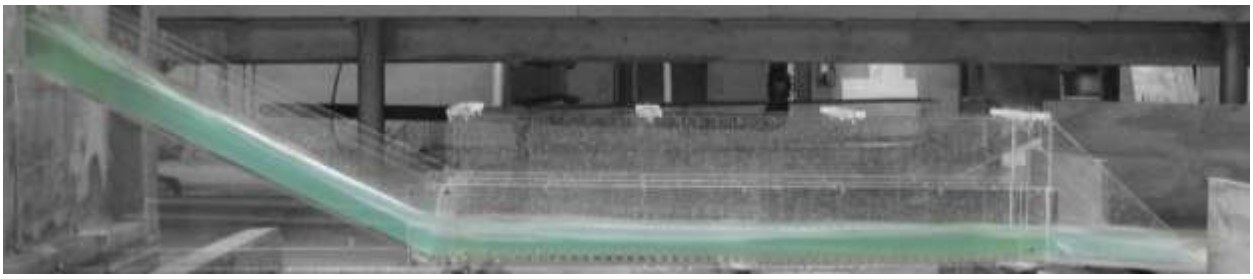

Figure A2. Experiment 1B

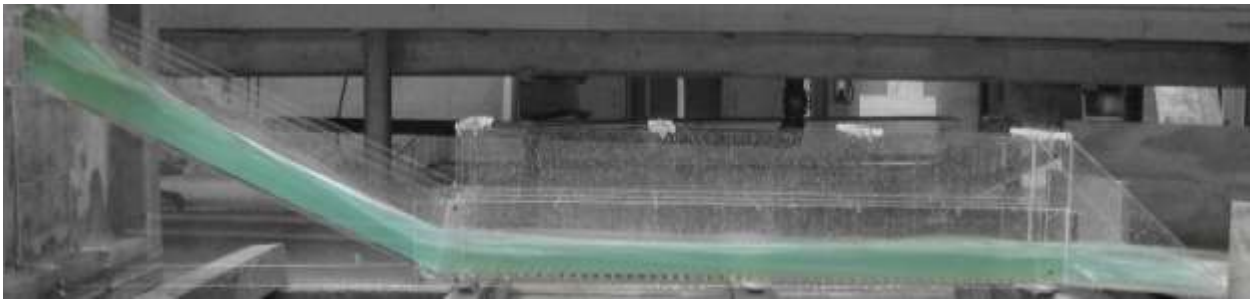

Figure A3. Experiment 1C

Table A1. Experiment 1 using open channel flow conditions with 6" horizontal channel without any friction blocks

H.J.	Run	H	Q	$V_{u/s}$	Y_s	Y_{toe}	Y_1	Y_2	$Y_{d/s}$	F_{r1}	V_1	V_2	$V_{d/s}$	L	X	ΔE	THL	E_2/E_1
N	1A	0.8d	1.16	2.91	2.00	1.25	1.25	1.13	1.25	5.37	9.8285 P-tube	-	9.6911 P-tube	-	-	-	5.6263	-
N	1B	1.0d	1.23	2.45	2.75	1.75	1.75	1.60	1.65	4.72	10.2299 P-tube	-	9.8285 P-tube	-	-	-	7.1187	-
N	1C	1.2d	1.49	2.49	3.25	2.00	2.00	1.85	1.85	4.42	10.2299 P-tube	-	10.0312 P-tube	-	-	-	5.7457	-

Figure A4. Experiment 2A

Figure A5. Experiment 2B

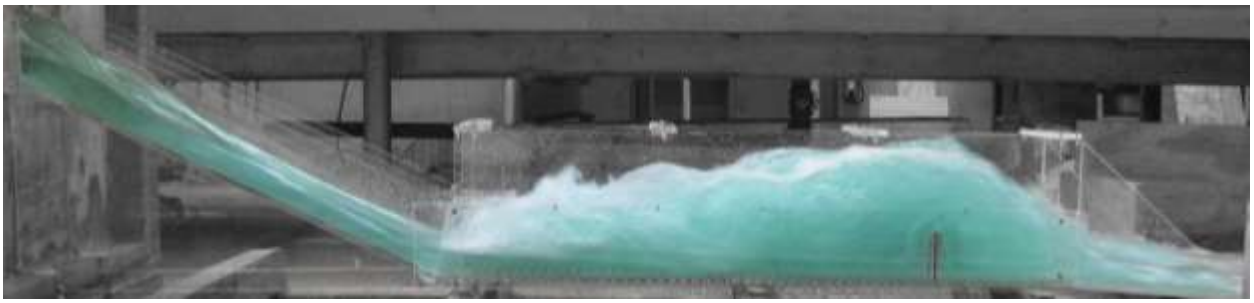

Figure A6. Experiment 2C

Table A2. Experiment 2 using open channel flow conditions with 4" regular sill at 12" from the end with extended channel height of 12"

H.J.	Run	H	Q	$V_{u/s}$	Y_s	Y_{toe}	Y_1	Y_2	$Y_{d/s}$	F_{r1}	V_1	V_2	$V_{d/s}$	L	X	ΔE	THL	E_2/E_1
Y	2A	0.8d	0.9225	2.3063	2.13	1.75	1.75	8.50	2.80	4.07	8.8214 P-tube	2.0720 P-tube	4.3340 P-tube	23.00	41.00	5.1689	17.4911	0.6005
Y	2B	1.0d	1.2252	2.4502	2.50	2.00	2.00	9.50	3.00	4.06	9.4101 P-tube	2.3166 P-tube	3.4749 P-tube	28.00	41.00	5.5510	19.8687	0.6015
Y	2C	1.2d	1.4825	2.4708	3.35	2.13	2.13	9.75	4.00	4.11	9.8285 P-tube	3.2762 P-tube	2.8373 P-tube	13.30	41.00	5.3262	20.8376	0.5960

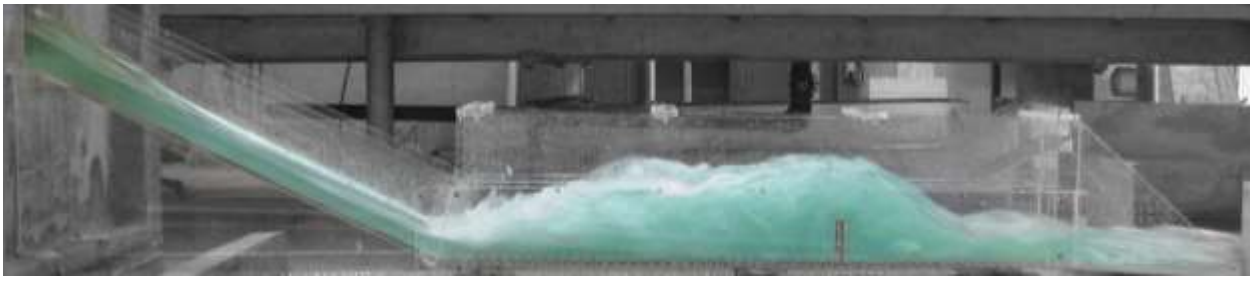

Figure A7. Experiment 3A

Figure A8. Experiment 3B

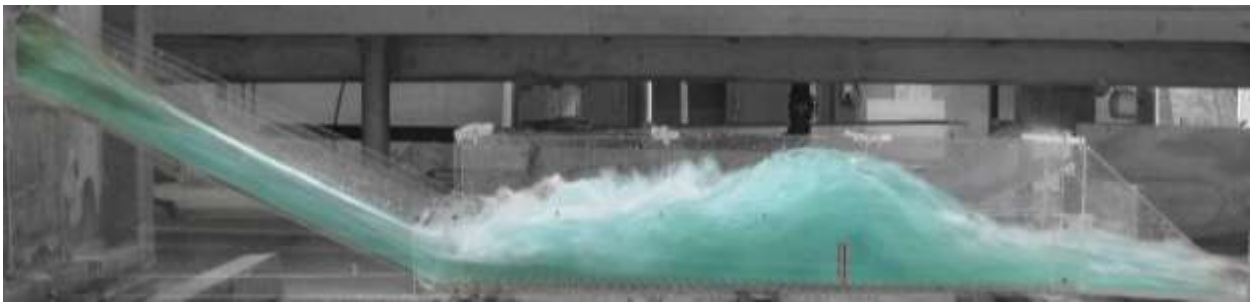

Figure A9. Experiment 3C

Table A3. Experiment 3 using open channel flow conditions with 3.5" regular sill at 20" from the end with extended channel height of 12"

H.J.	Run	H	Q	$V_{u/s}$	Y_s	Y_{toe}	Y_1	Y_2	$Y_{d/s}$	F_{r1}	V_1	V_2	$V_{d/s}$	L	X	ΔE	THL	E_2/E_1
Y	3A	0.8d	0.9354	2.3385	2.00	1.35	1.35	8.50	2.50	5.0918	9.6911 P-tube	2.8373 P-tube	5.5550 P-tube	18.00	33.00	7.9635	15.5690	0.5017
Y	3B	1.0d	1.2169	2.4338	2.85	1.75	1.75	9.75	3.00	4.5981	9.9641 P-tube	3.0646 P-tube	5.9062 P-tube	20.00	33.00	7.5018	15.6037	0.5456
Y	3C	1.2d	1.4958	2.4930	3.50	2.25	2.25	10.75	3.35	3.7712	9.2664 P-tube	6.1292 P-tube	5.9062 P-tube	22.00	33.00	6.3475	16.5081	0.6359

Figure A10. Experiment 4A

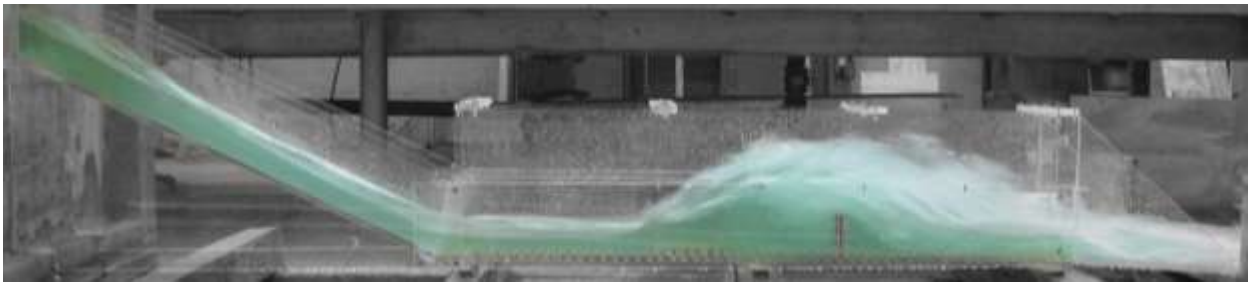

Figure A11. Experiment 4B

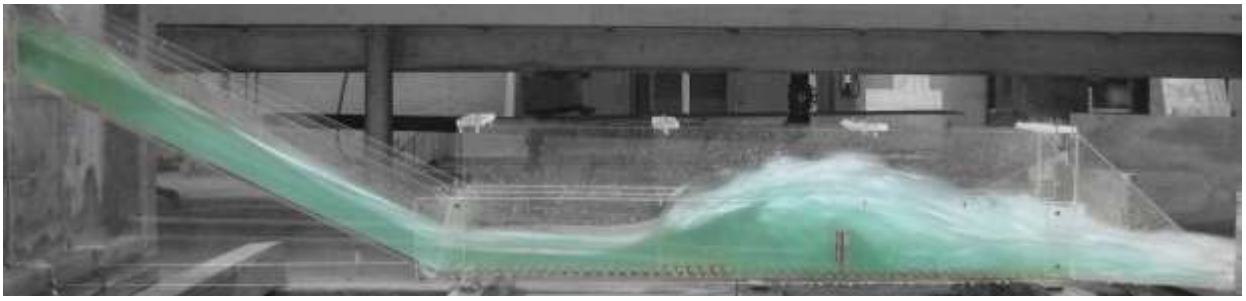

Figure A12. Experiment 4C

Table A4. Experiment 4 using open channel flow conditions with 3.5” regular sill at 20” from end with extended channel height of 12” with 15 FFFBs 19” from the toe

H.J.	Run	H	Q	$V_{u/s}$	Y_s	Y_{toe}	Y_1	Y_2	$Y_{d/s}$	F_{r1}	V_1	V_2	$V_{d/s}$	L	X	ΔE	THL	E_2/E_1
Y	4A	0.8d	0.9050	2.2625	2.25	1.50	1.50	8.75	2.50	4.8305	9.6911 P-tube	3.6629 P-tube	5.4329 P-tube	17.00	33.00	7.2586	15.7538	0.5241
Y	4B	1.0d	1.2251	2.4502	2.75	1.50	1.75	9.00	3.25	4.7208	10.2299 P-tube	4.1763 P-tube	6.9498 P-tube	16.00	33.00	6.0489	12.8687	0.5341
Y	4C	1.2d	1.5011	2.5018	3.50	1.85	2.00	9.00	3.50	4.5277	10.4889 P-tube	5.1801 P-tube	6.6539 P-tube	16.00	33.00	4.7639	14.6163	0.5524

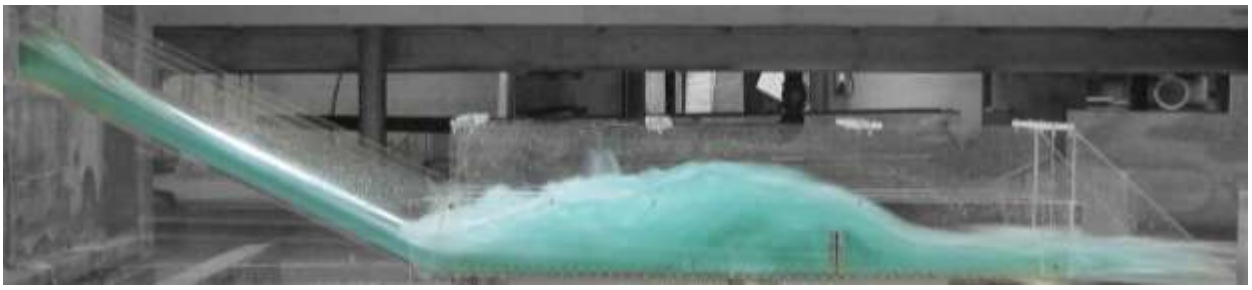

Figure A13. Experiment 5A

Figure A14. Experiment 5B

Figure A15. Experiment 5C

Table A5. Experiment 5 using open channel flow conditions with 3.5” regular sill 20” from end with 6 FFFB 2” × 2” at 18” from the toe

H.J.	Run	H	Q	$V_{u/s}$	Y_s	Y_{toe}	Y_1	Y_2	$Y_{d/s}$	F_{r1}	V_1	V_2	$V_{d/s}$	L	X	ΔE	THL	E_2/E_1
Y	5A	0.8d	0.8644	2.1610	2.00	2.50	2.50	8.25	2.00	3.4641	8.9722 P-tube	2.3166 P-tube	5.4329 P-tube	17.00	33.00	2.3044	16.1702	0.6758
Y	5B	1.0d	1.1837	2.3674	2.75	2.00	2.00	9.25	2.50	3.9370	9.1205 P-tube	5.0498 P-tube	5.7915 P-tube	19.00	33.00	5.1497	16.2943	0.6159
Y	5C	1.2d	1.4361	2.3935	3.00	2.13	2.13	9.75	3.25	4.2790	10.2299 P-tube	5.6745 P-tube	6.0187 P-tube	22.00	33.00	5.3262	16.2675	0.5777

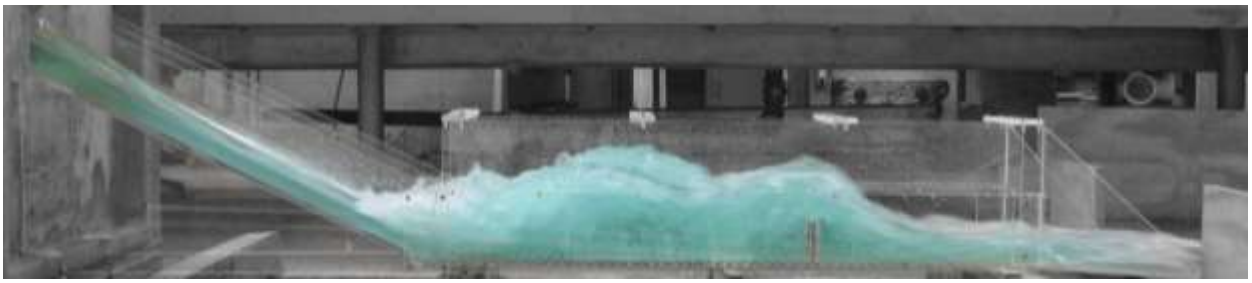

Figure A16. Experiment 6A

Figure A17. Experiment 6B

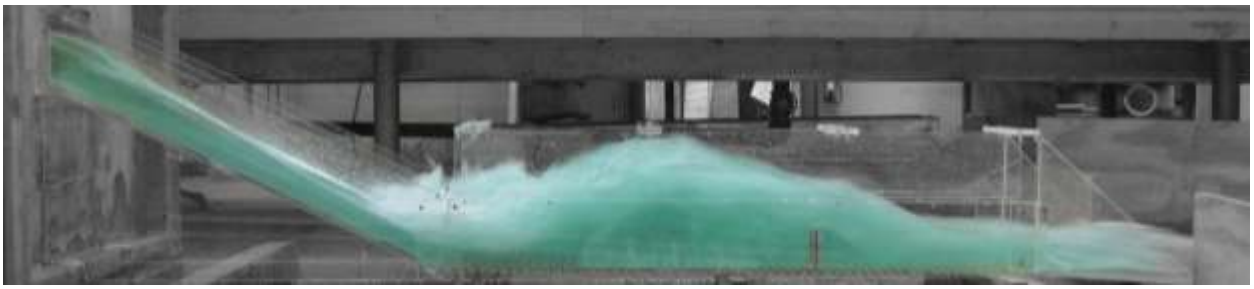

Figure A18. Experiment 6C

Table A6. Experiment 6 using open channel flow conditions with 3.5” regular sill 20” from end with 12 FFFB 2” × 2” at 18” from the toe

H.J.	Run	H	Q	$V_{u/s}$	Y_s	Y_{toe}	Y_1	Y_2	$Y_{d/s}$	F_{r1}	V_1	V_2	$V_{d/s}$	L	X	ΔE	THL	E_2/E_1
Y	6A	0.8d	2.9340	2.2293	2.00	3.99	2.75	8.75	2.25	2.6968	7.3258 P-tube	4.0125 P-tube	5.4329 P-tube	17.00	33.00	2.2442	15.9760	0.7918
Y	6B	1.0d	2.9108	2.3674	2.50	4.00	3.75	10.00	2.85	2.5298	8.0250 P-tube	4.6332 P-tube	5.7915 P-tube	18.00	33.00	1.6276	15.9443	0.8197
Y	6C	1.2d	1.4690	2.4483	3.50	4.50	4.00	11.25	3.50	2.5495	8.3526 P-tube	5.4329 P-tube	6.1292 P-tube	20.00	33.00	2.1171	15.8170	0.8164

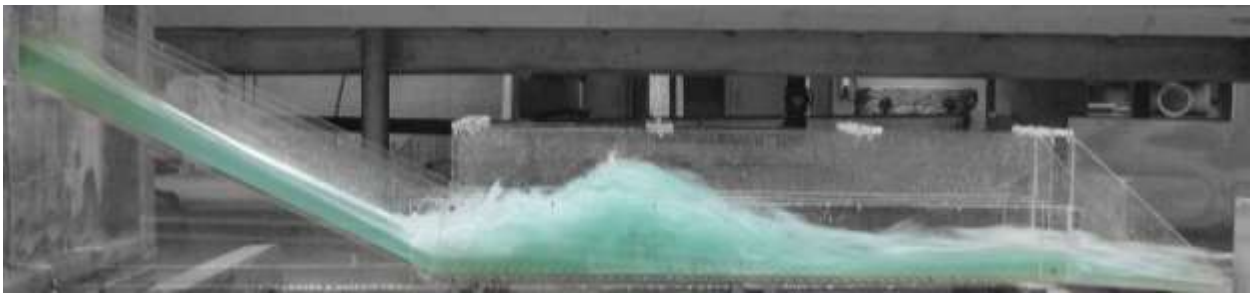

Figure A19. Experiment 7A

Figure A20. Experiment 7B

Figure A21. Experiment 7C

Table A7. Experiment 7 using open channel flow conditions with 12 FFFB 2” × 2” at 26” from the toe

H.J.	Run	H	Q	$V_{u/s}$	Y_s	Y_{toe}	Y_1	Y_2	$Y_{d/s}$	F_{r1}	V_1	V_2	$V_{d/s}$	L	X	ΔE	THL	E_2/E_1
N	7A	0.8d	0.8962	2.2405	2.00	2.50	2.50	8.85	2.50	2.8636	7.4168 P-tube	1.6381 P-tube	4.9143 P-tube	16.00	26.00	2.8932	16.7354	0.7618
N	7B	1.0d	1.2038	2.4076	2.65	2.35	2.35	9.50	3.25	3.8037	9.5516 P-tube	6.1292 P-tube	5.4329 P-tube	18.00	26.00	4.0932	16.3301	0.6309
N	7C	1.2d	1.4554	2.4257	3.00	3.13	3.13	10.00	3.50	3.3200	9.6216 P-tube	4.6332 P-tube	5.6745 P-tube	18.00	26.00	2.5898	16.7964	0.6941

Figure A22. Experiment 8A

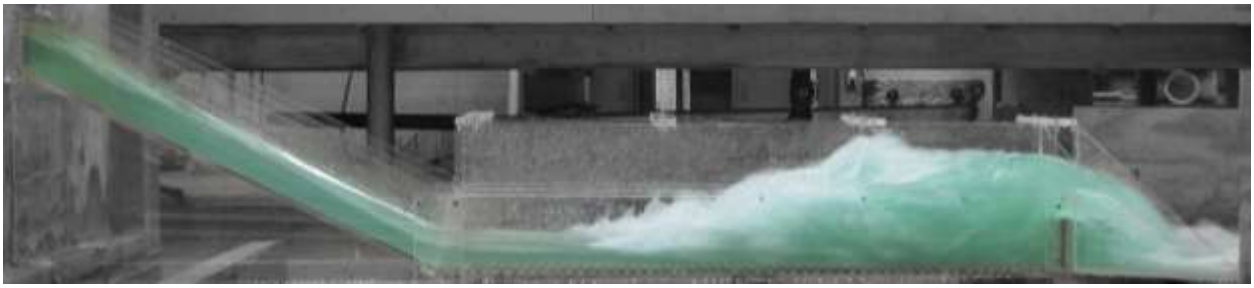

Figure A23. Experiment 8B

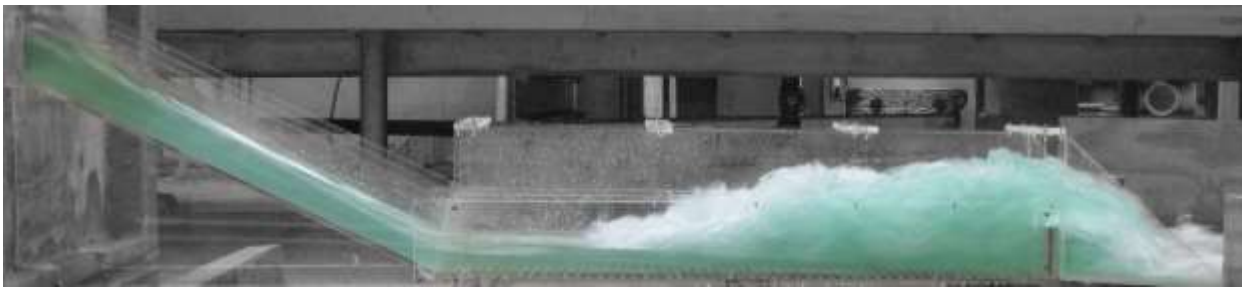

Figure A24. Experiment 8C

Table A8. Experiment 8 using open channel flow conditions with 4" regular sill at the end of culvert

H.J.	Run	H	Q	$V_{u/s}$	Y_s	Y_{toe}	Y_1	Y_2	$Y_{d/s}$	F_{r1}	V_1	V_2	$V_{d/s}$	L	X	ΔE	THL	E_2/E_1
Y	8A	0.8d	0.8736	2.1840	1.85	1.50	1.50	8.50	1.75	4.8990	9.8285 P-tube	2.3166 P-tube	4.0125 P-tube	18.00	50.00	6.7255	18.9388	0.5181
Y	8B	1.0d	1.2038	2.4076	2.75	1.75	1.85	9.65	2.50	4.2870	9.5516 Tube	2.5900 P-tube	4.6332 P-tube	19.00	35.00	6.6455	18.5801	0.5769
Y	8C	1.2d	1.4333	2.3888	3.00	1.85	2.00	10.35	2.25	4.3012	9.9641 P-tube	2.8373 P-tube	4.4861 P-tube	22.00	36.00	7.0312	20.2633	0.5754

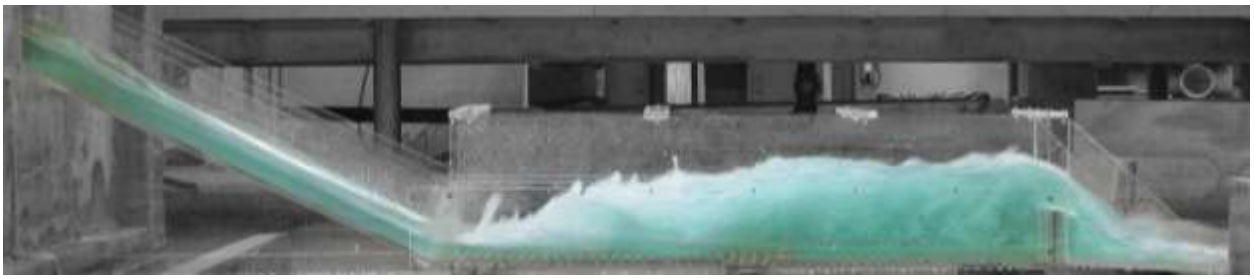

Figure A25. Experiment 9A

Figure A26. Experiment 9B

Figure A27. Experiment 9C

Table A9. Experiment 9 using open channel flow conditions with 4" regular sill at the end with 15 FFFBs at 25" from the toe

H.J.	Run	H	Q	$V_{u/s}$	Y_s	Y_{toe}	Y_1	Y_2	$Y_{d/s}$	F_{r1}	V_1	V_2	$V_{d/s}$	L	X	ΔE	THL	E_2/E_1
Y	9A	0.8d	0.9354	2.3385	2.13	1.75	1.75	8.25	1.50	4.3425	9.4101 P-tube	3.0646 P-tube	4.3340 P-tube	18.00	47.00	4.7554	18.8190	0.5711
Y	9B	1.0d	1.2071	2.4142	2.75	1.75	1.85	9.50	2.00	4.5023	10.0312 P-tube	4.3340 P-tube	4.7758 P-tube	21.00	41.00	6.3684	18.8360	0.5549
Y	9C	1.2d	1.6765	2.7942	2.25	1.25	2.13	10.25	2.50	4.2790	10.2299 P-tube	2.8373 P-tube	5.4329 P-tube	22.00	44.00	6.1306	18.6548	0.5777

Figure A28. Experiment 10A

Figure A29. Experiment 10B

Figure A30. Experiment 10C

Table A10. Experiment 10 using open channel flow conditions with 4” regular sill at the end with 30 FFFBs at 25” from the toe

H.J.	Run	H	Q	$V_{u/s}$	Y_s	Y_{toe}	Y_1	Y_2	$Y_{d/s}$	Fr_1	V_1	V_2	$V_{d/s}$	L	X	ΔE	THL	E_2/E_1
Y	10A	0.8d	0.9006	2.2515	2.00	1.50	1.50	8.50	1.50	4.5461	9.1205 P-tube	2.0062 P-tube	4.0125 P-tube	18.00	52.00	6.7255	19.2446	0.5506
Y	10B	1.0d	1.2396	2.4792	2.65	1.75	2.00	9.75	1.75	4.4159	10.2299 P-tube	2.0062 P-tube	3.0646 P-tube	19.00	40.00	5.9677	21.6453	0.5636
Y	10C	1.2d	1.4958	2.4930	3.00	2.13	2.00	10.25	2.00	4.3012	9.9641 P-tube	3.0646 P-tube	5.1801 P-tube	21.00	43.00	6.8478	19.3581	0.5754

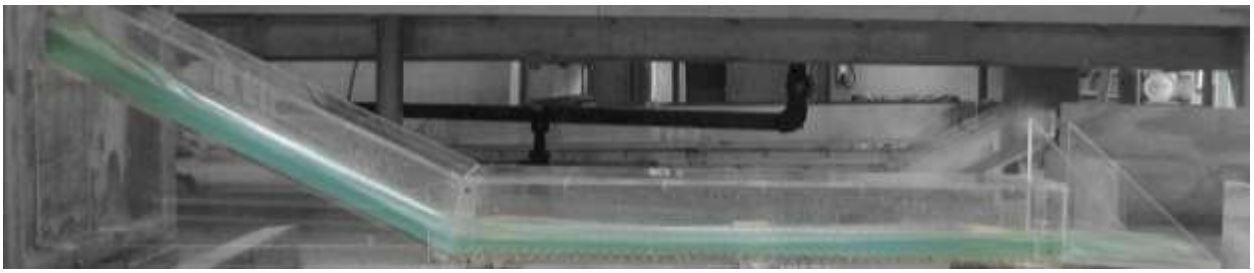

Figure A31. Experiment 11A

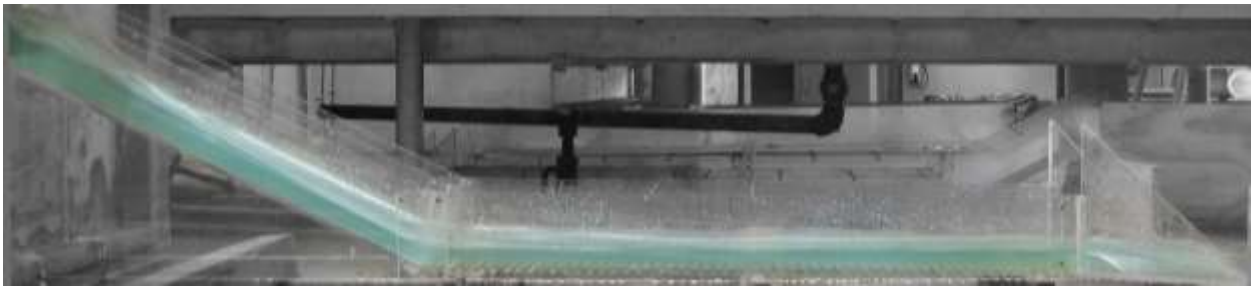

Figure A32. Experiment 11B

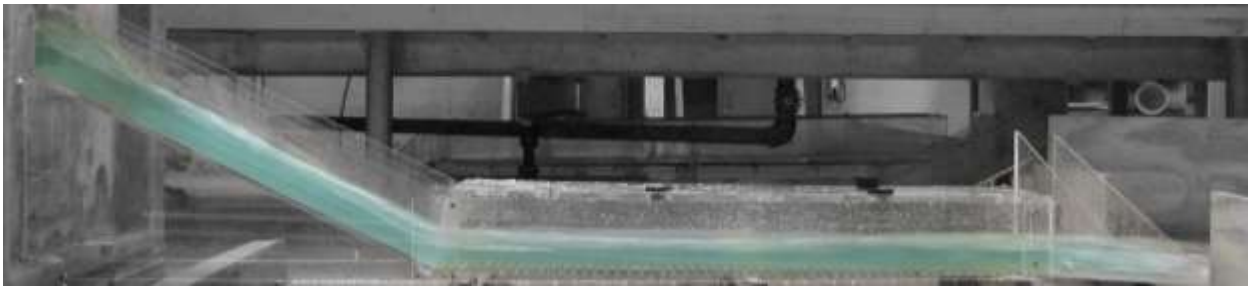

Figure A33. Experiment 11C

Table A11. Experiment 11 using pressure flow conditions without sill or FFFBs

H.J.	Run	H	Q	$V_{u/s}$	Y_s	Y_{toe}	Y_1	Y_2	$Y_{d/s}$	F_{r1}	V_1	V_2	$V_{d/s}$	L	X	ΔE	THL	E_2/E_1
Y	11A	0.8d	0.8962	2.2405	2.00	1.50	1.50	1.25	1.50	5.2281	10.4889 P-tube	10.0979 P-tube	9.8285 P-tube	-	-	-	3.2354	-
Y	11B	1.0d	1.2137	2.4274	2.50	1.75	1.75	1.65	1.65	4.8990	10.6160 P-tube	10.1904 P-tube	10.2299 P-tube	-	-	-	4.0979	-
Y	11C	1.2d	1.5011	2.5018	3.35	1.65	1.75	1.75	1.85	4.8990	10.6160 P-tube	10.2299 P-tube	10.3602 P-tube	-	-	-	5.0163	-

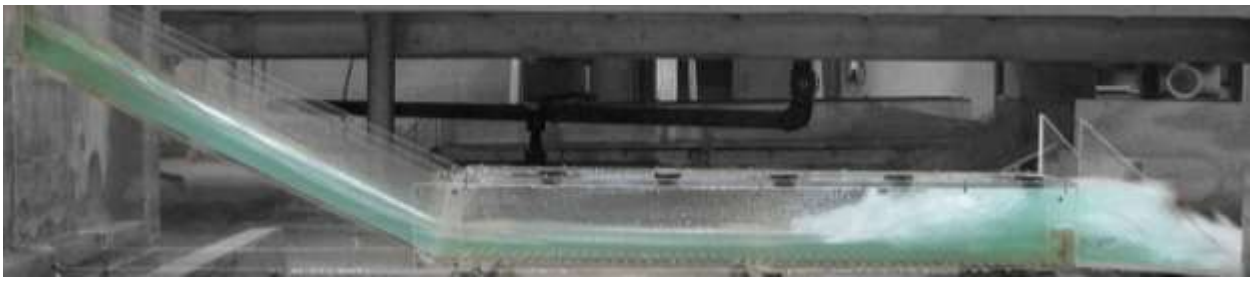

Figure A34. Experiment 12A

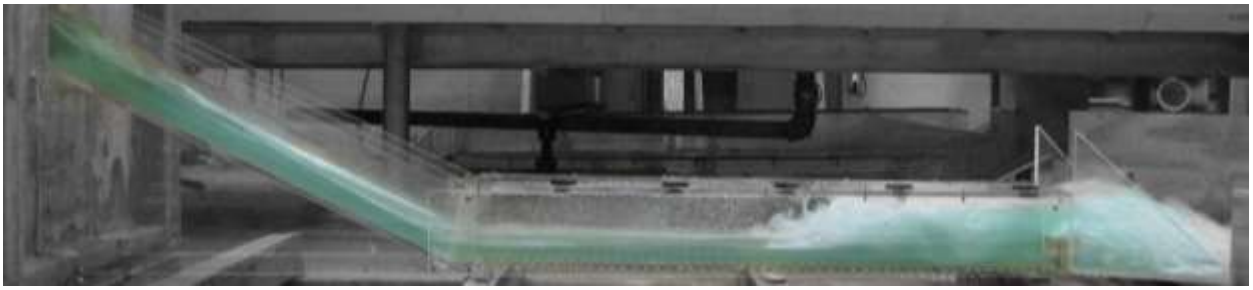

Figure A35. Experiment 12B

Figure A36. Experiment 12C

Table A12. Experiment 12 using pressure flow conditions with 2.5” at the end

H.J.	Run	H	Q	$V_{u/s}$	Y_s	Y_{toe}	Y_1	Y_2	$Y_{d/s}$	F_{r1}	V_1	V_2	$V_{d/s}$	L	X	ΔE	THL	E_2/E_1
Y	12A	0.8d	0.9182	2.2955	2.13	1.35	1.20	8.88	2.50	5.4772	9.8285 P-tube	4.9143 P-tube	- P-tube	14.00	19.00	10.6275	21.2819	0.4646
Y	12B	1.0d	1.2169	2.4338	2.75	1.75	1.65	10.60	3.00	4.7354	9.9641 P-tube	4.6332 P-tube	4.0125 P-tube	19.00	26.00	10.2568	19.1037	0.5193
Y	12C	1.2d	1.5011	2.5081	3.13	1.75	2.00	12.00	3.50	4.5277	10.4889 P-tube	5.1801 P-tube	6.9498 P-tube	19.00	35.00	10.4167	13.8663	0.5323

Figure A37. Experiment 13A

Figure A38. Experiment 13B

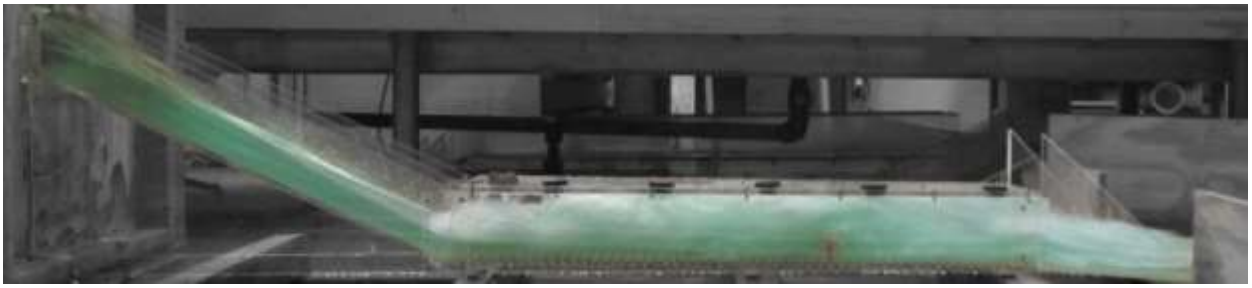

Figure A39. Experiment 13C

Table A13. Experiment 13 using pressure flow conditions with 2.5” sill 19” from the end

H.J.	Run	H	Q	$V_{u/s}$	Y_s	Y_{toe}	Y_1	Y_2	$Y_{d/s}$	F_{r1}	V_1	V_2	$V_{d/s}$	L	X	ΔE	THL	E_2/E_1
Y	13A	0.8d	0.9094	2.2735	2.00	1.50	1.35	9.26	2.50	5.0918	9.6911 P-tube	2.8373 P-tube	2.5900 P-tube	15.00	18.00	9.8841	20.0131	0.4938
Y	13B	1.0d	1.2071	2.4142	2.75	1.65	1.65	10.80	2.85	4.7990	10.0979 P-tube	1.6381 P-tube	5.4329 P-tube	19.00	27.00	10.7551	16.70	0.5119
Y	13C	1.2d	1.4137	2.3562	3.25	1.85	1.85	11.50	3.00	4.5619	10.1641 P-tube	4.0125 P-tube	5.6745 P-tube	21.00	33.00	10.5500	17.2344	0.5328

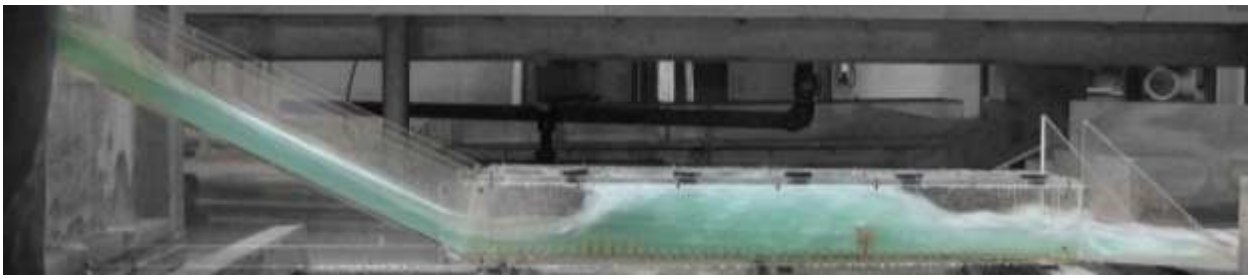

Figure A40. Experiment 14A

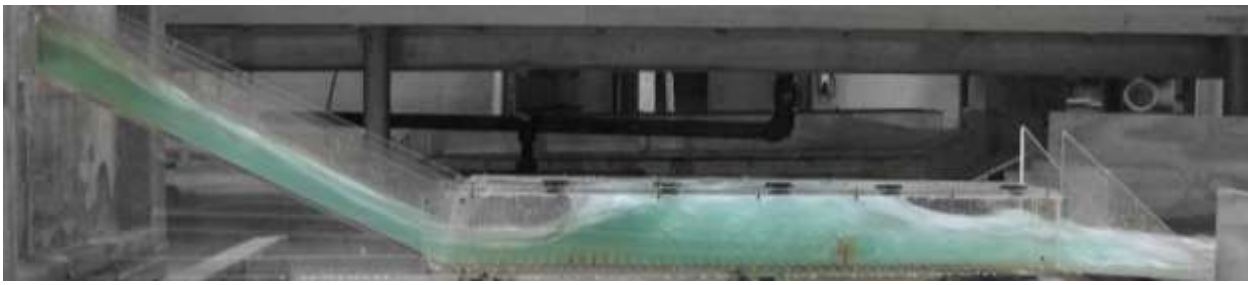

Figure A41. Experiment 14B

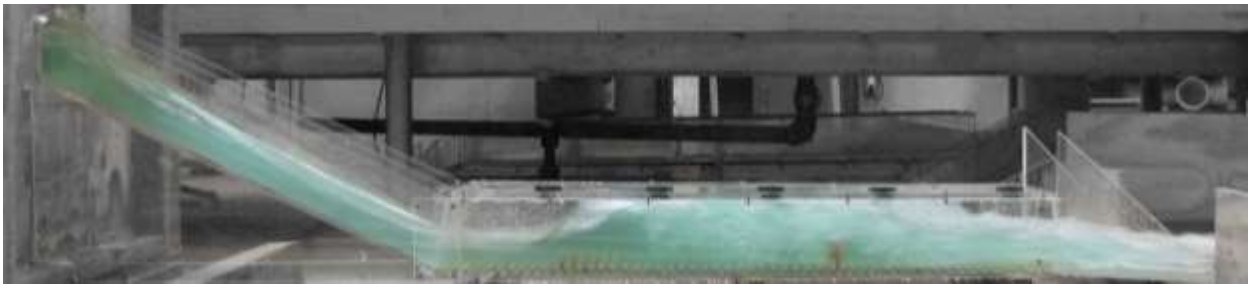

Figure A42. Experiment 14C

Table A14. Experiment 14 using pressure flow conditions with 2.5” sill 19” from the end with 15 FFFBs at 11” from the toe

H.J.	Run	H	Q	$V_{u/s}$	Y_s	Y_{toe}	Y_1	Y_2	$Y_{d/s}$	F_{r1}	V_1	V_2	$V_{d/s}$	L	X	ΔE	THL	E_2/E_1
Y	14A	0.8d	0.8736	2.1840	1.13	1.50	1.65	11.10	2.25	4.8928	10.2952 P-tube	2.8373 P-tube	4.9143 P-tube	12.00	25.00	11.5251	16.9388	0.5011
Y	14B	1.0d	1.2169	2.4338	2.50	1.75	1.75	11.52	2.75	4.7809	10.3602 P-tube	4.4861 P-tube	5.3080 P-tube	12.00	25.00	11.5624	17.1037	0.5098
Y	14C	1.2d	1.4137	2.3562	3.13	2.00	2.00	12.00	3.00	4.5277	10.4889 P-tube	4.6332 P-tube	5.6743 P-tube	16.00	25.00	11.4443	17.2344	0.5323

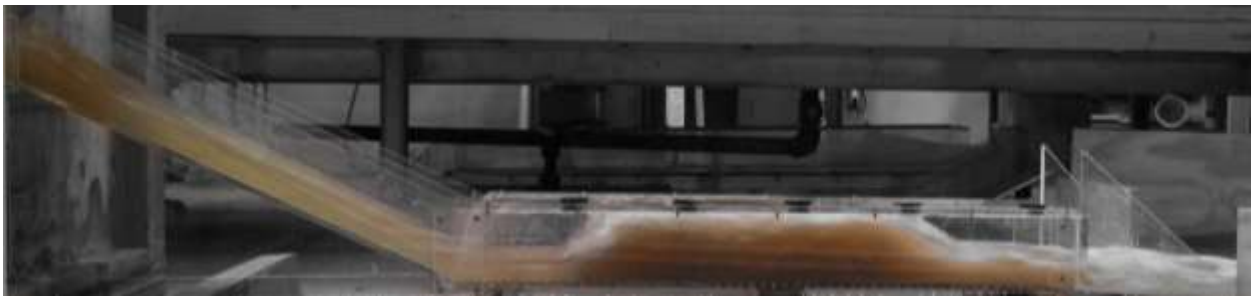

Figure A43. Experiment 15A

Figure A44. Experiment 15B

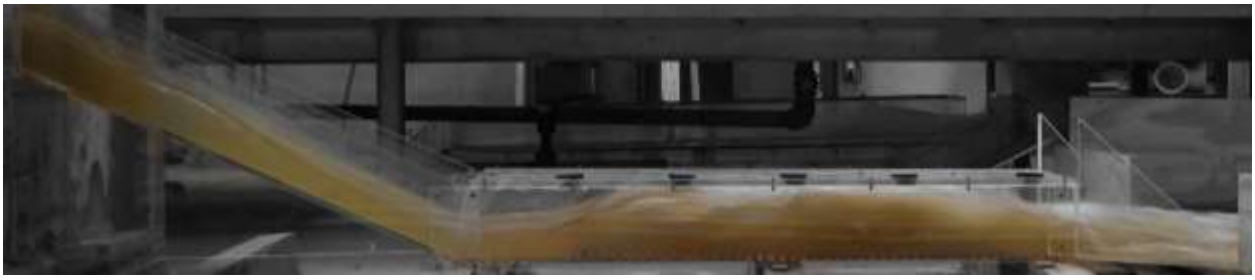

Figure A45. Experiment 15C

Table A15. Experiment 15 using pressure flow conditions with 2.5" sill 19" from the end with 30 FFFBs at 11" from the toe

H.J.	Run	H	Q	$V_{u/s}$	Y_s	Y_{toe}	Y_1	Y_2	$Y_{d/s}$	F_{r1}	V_1	V_2	$V_{d/s}$	L	X	ΔE	THL	E_2/E_1
Y	15A	0.8d	0.8736	2.1480	2.00	1.50	1.50	10.69	2.25	5.1640	10.3602 P-tube	1.1583 P-tube	5.1801 P-tube	14.00	26.00	12.0939	16.4388	0.4789
Y	15B	1.0d	1.2492	2.4984	2.50	1.75	2.00	12.00	3.00	4.5277	10.4889 P-tube	4.2401 P-tube	5.6745 P-tube	12.00	25.50	10.4167	16.1631	0.5471
Y	15C	1.2d	1.5117	2.5195	3.50	2.13	2.25	12.00	3.13	4.2164	10.3602 P-tube	5.1801 P-tube	6.4492 P-tube	12.00	26.00	8.5820	15.5028	0.5961

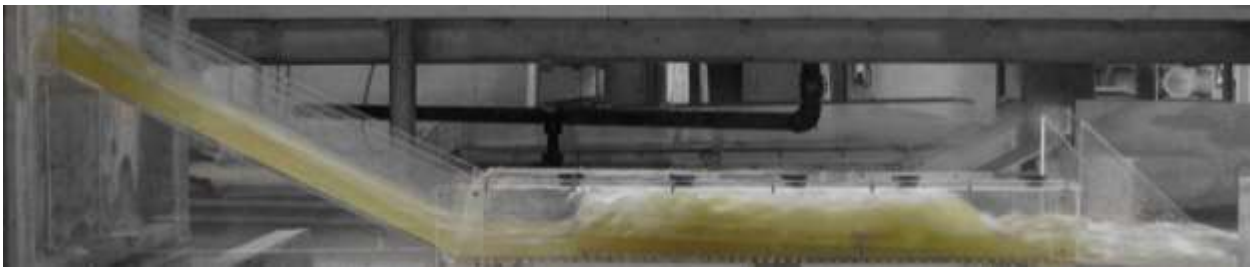

Figure A46. Experiment 16A

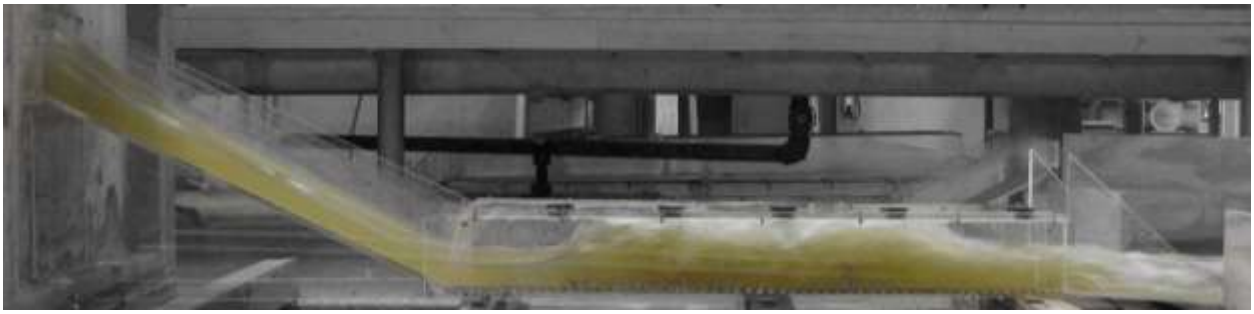

Figure A47. Experiment 16B

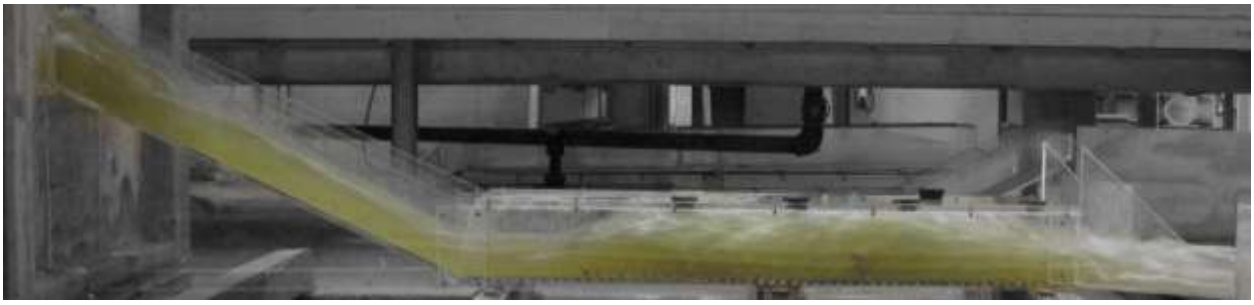

Figure A48. Experiment 16C

Table A16. Experiment 16 using pressure flow conditions with 1.5” sill 19” from the end and 2” sill at 27” from the end

H.J.	Run	H	Q	$V_{u/s}$	Y_s	Y_{toe}	Y_1	Y_2	$Y_{d/s}$	F_{r1}	V_1	V_2	$V_{d/s}$	L	X	ΔE	THL	E_2/E_1
Y	16A	0.8d	0.8962	2.2405	2.00	1.50	1.50	5.75	2.50	5.1446	10.3213 P-tube	1.6381 P-tube	4.6322 P-tube	16.00	25.00	2.2251	17.2354	0.4974
Y	16B	1.0d	1.2440	2.4008	2.50	1.85	1.85	5.75	2.65	4.6399	10.2602 P-tube	3.6629 P-tube	5.3080 P-tube	12.00	25.00	1.3941	17.1740	0.5407
Y	16C	1.2d	1.5091	2.5152	3.25	2.35	2.25	5.75	3.50	4.2426	10.4247 P-tube	8.1412 P-tube	5.4329 P-tube	12.00	26.00	0.8285	17.3788	05816

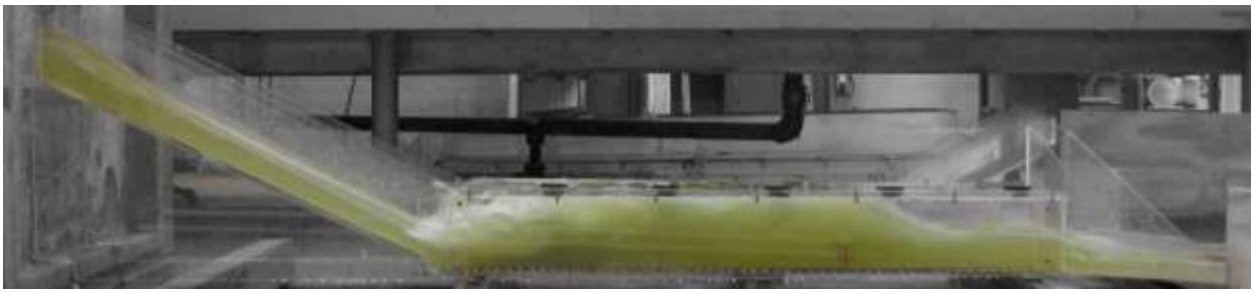

Figure A49. Experiment 17A

Figure A50. Experiment 17B

Figure A51. Experiment 17C

Table A17. Experiment 17 using pressure flow conditions with 1.5” sill 19” from the end with 6 FFFBs 2” × 2” at 14” from the toe

H.J.	Run	H	Q	$V_{u/s}$	Y_s	Y_{toe}	Y_1	Y_2	$Y_{d/s}$	F_{r1}	V_1	V_2	$V_{d/s}$	L	X	ΔE	THL	E_2/E_1
Y	17A	0.8d	0.8736	2.1840	2.00	2.00	2.00	6.89	2.25	2.8284	6.5524 P-tube	3.2762 P-tube	4.8317 P-tube	11.00	36.00	2.1203	17.0888	0.7804
Y	17B	1.0d	1.2004	2.4008	2.75	2.50	2.50	10.08	3.25	3.2863	8.5188 P-tube	2.3166 P-tube	4.9143 P-tube	10.00	36.00	4.3249	17.3240	0.7152
Y	17C	1.2d	1.5170	2.5283	3.50	3.00	3.00	11.38	3.13	3.1885	9.0466 P-tube	2.4626 P-tube	5.1801 P-tube	10.00	36.00	4.3035	18.2611	0.7412

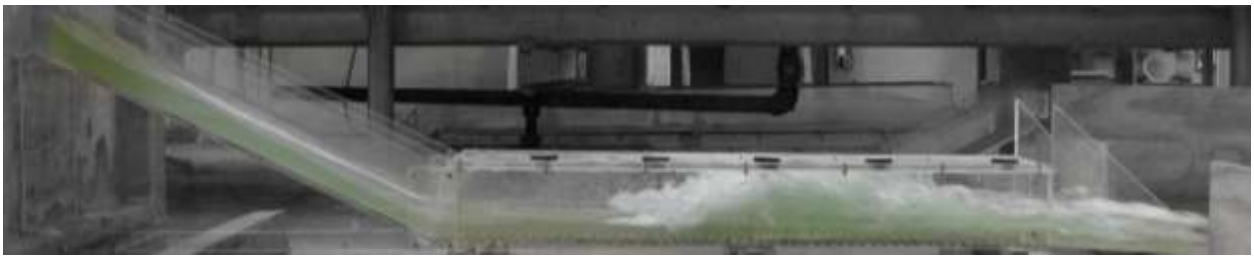

Figure A52. Experiment 18A

Figure A53. Experiment 18B

Figure A54. Experiment 18C

Table A18. Experiment 18 using pressure flow conditions with 6 FFFBs 2" × 2" at 19" from the end

H.J.	Run	H	Q	$V_{u/s}$	Y_s	Y_{toe}	Y_1	Y_2	$Y_{d/s}$	F_{r1}	V_1	V_2	$V_{d/s}$	L	X	ΔE	THL	E_2/E_1
Y	18A	0.8d	0.9094	2.2735	2.13	1.65	1.25	9.64	3.00	5.6214	10.2952 P-tube	5.9062 P-tube	4.3340 P-tube	10.00	12.00	12.2683	17.2631	0.4490
Y	18B	1.0d	1.2038	2.4076	2.65	2.00	1.75	11.46	2.65	4.7630	10.3213 P-tube	7.6833 P-tube	4.0125 P-tube	10.00	12.00	11.4052	19.4301	0.5119
Y	18C	1.2d	1.4878	2.4797	3.13	2.13	2.13	12.00	2.75	4.3605	10.4247 P-tube	6.9498 P-tube	4.3340 P-tube	10.00	12.00	9.4044	20.0957	0.5731

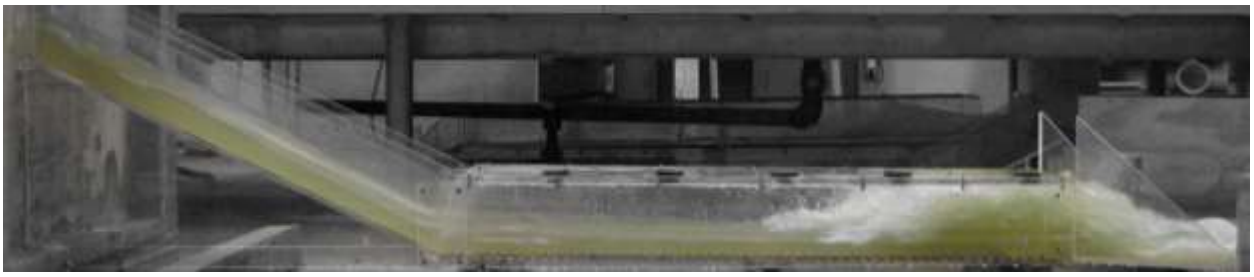

Figure A55. Experiment 19A

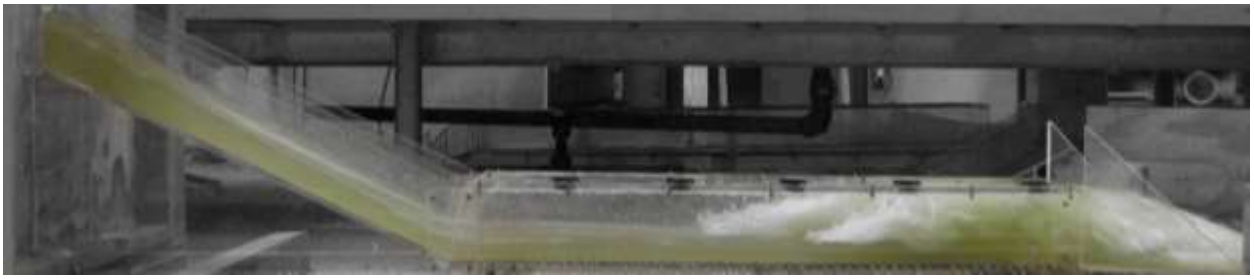

Figure A56. Experiment 19B

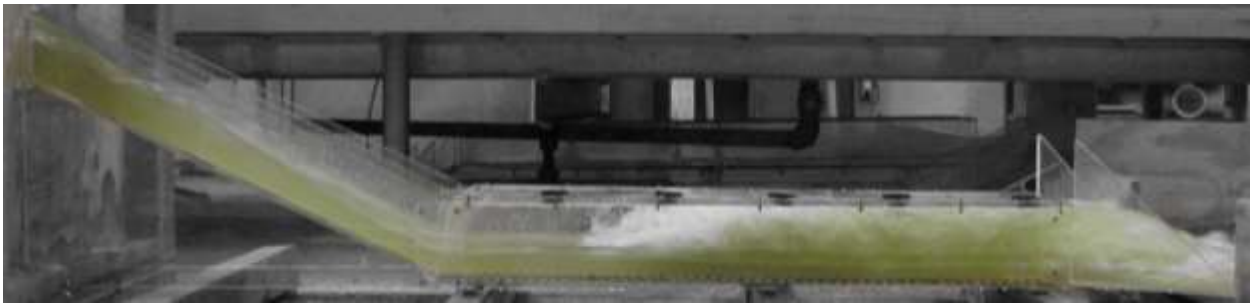

Figure A57. Experiment 19C

Table A19. Experiment 19 using pressure flow conditions with 2 FFFBs 3" × 3" at the end of the culvert

H.J.	Run	H	Q	$V_{u/s}$	Y_s	Y_{toe}	Y_1	Y_2	$Y_{d/s}$	Fr1	V_1	V_2	$V_{d/s}$	L	X	ΔE	THL	E_2/E_1
Y	19A	0.8d	0.9182	2.2955	1.75	1.65	1.25	9.07	3.25	5.3666	9.8285 P-tube	1.1583 P-tube	2.8373 P-tube	14.00	20.00	10.5383	19.0319	0.4721
Y	19B	1.0d	1.2004	2.4008	2.50	1.75	1.65	10.54	3.50	4.7162	9.9236 P-tube	1.3705 P-tube	4.6332 P-tube	14.00	20.00	10.1096	17.5740	0.5216
Y	19C	1.2d	1.4958	2.4930	3.50	2.13	2.25	12.00	4.50	4.0552	9.9641 P-tube	3.8417 P-tube	4.0125 P-tube	16.00-	37.00	8.5820	18.8581	0.5961

Figure A58. Experiment 20A

Figure A59. Experiment 20B

Figure A60. Experiment 20C

Table A20. Experiment 20 using open channel flow conditions with 4 FFFBs 3" × 3" at 20" from the end of culvert

H.J.	Run	H	Q	$V_{u/s}$	Y_s	Y_{toe}	Y_1	Y_2	$Y_{d/s}$	F_{r1}	V_1	V_2	$V_{d/s}$	L	X	ΔE	THL	E_2/E_1
Y	20A	0.8d	0.9396	2.3490	2.00	1.75	1.75	8.50	2.75	4.4078	9.5516 P-tube	3.8417 P-tube	5.4329 P-tube	20.00	24.00	5.1689	15.5782	0.5644
Y	20B	1.0d	1.2004	2.4008	2.50	2.00	2.00	9.50	3.00	4.4159	10.2299 P-tube	2.1366 P-tube	5.7915 P-tube	21.00	25.00	5.5510	15.8240	0.5636
Y	20C	1.2d	1.5117	2.5195	3.50	2.00	2.00	10.50	4.00	4.5277	10.4889 P-tube	6.3443 P-tube	6.1292 P-tube	21.00	24.00	7.3110	15.3828	0.5524

Figure A61. Experiment 21A

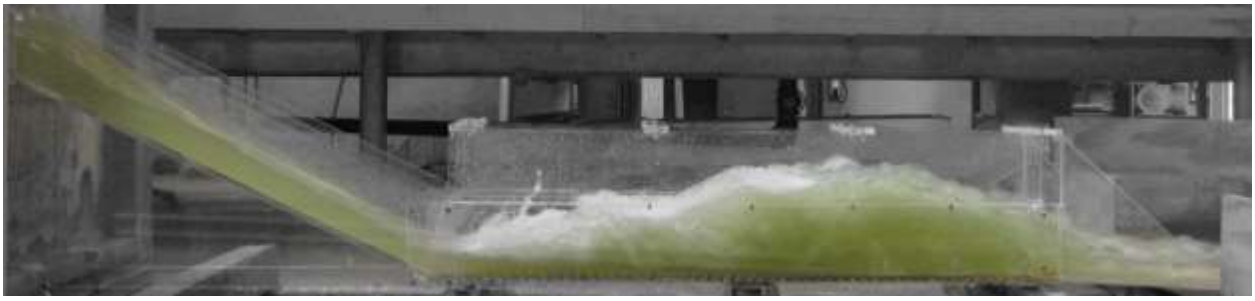

Figure A62. Experiment 21B

Figure A63. Experiment 21C

Table A21. Experiment 21 using open channel flow conditions with 6 FFFBs 3” × 3” at 8” from the end of culvert

H.J.	Run	H	Q	$V_{u/s}$	Y_s	Y_{toe}	Y_1	Y_2	$Y_{d/s}$	F_{r1}	V_1	V_2	$V_{d/s}$	L	X	ΔE	THL	E_2/E_1
Y	21A	0.8d	0.8827	2.2068	2.00	1.75	1.75	8.75	3.25	4.2426	9.1937 P-tube	2.5900 P-tube	1.1583 P-tube	21.00	27.00	5.6000	20.2074	0.5816
Y	21B	1.0d	1.2169	2.4338	2.50	1.85	1.85	9.50	3.25	4.5914	10.2299 P-tube	3.2762 P-tube	2.0062 P-tube	22.00	34.00	6.3684	21.1037	0.4563
Y	21C	1.2d	1.4824	2.4707	3.35	2.13	2.13	10.75	4.75	4.0246	9.6216 P-tube	5.9062 P-tube	4.7758 P-tube	23.00	28.00	6.9932	17.3374	0.6058

Figure A64. Experiment 22A

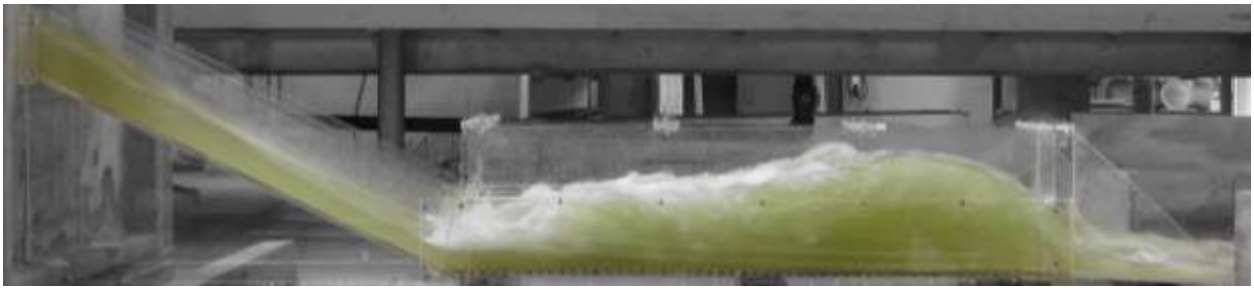

Figure A65. Experiment 22B

Figure A66. Experiment 22C

Table A22. Experiment 22 using open channel flow conditions with 3 FFFBs 4” x 4” at the end of culvert

H.J.	Run	H	Q	$V_{u/s}$	Y_s	Y_{toe}	Y_1	Y_2	$Y_{d/s}$	F_{r1}	V_1	V_2	$V_{d/s}$	L	X	ΔE	THL	E_2/E_1
Y	22A	0.8d	0.9050	2.2625	2.00	2.25	2.25	9.00	2.50	3.6515	8.9722 P-tube	1.1583 P-tube	2.3166 P-tube	20.00	40.00	3.7969	20.2538	0.6511
Y	22B	1.0d	1.2169	2.4338	2.50	2.00	2.00	10.50	3.50	4.0620	9.4101 P-tube	2.3166 P-tube	3.2762 P-tube	18.00	41.00	7.3110	19.6037	0.6015
Y	22C	1.2d	1.4416	2..4027	3.50	2.50	2.50	11.00	4.00	3.9497	10.2299 P-tube	2.3166 P-tube	3.2762 P-tube	20.00	39.00	5.5830	20.2757	0.6144

Figure A67. Experiment 23A

Figure A68. Experiment 23B

Figure A69. Experiment 23C

Table A23. Experiment 23 using open channel flow conditions with 3.5" slotted sill 20" from the end of culvert

H.J.	Run	H	Q	$V_{u/s}$	Y_s	Y_{toe}	Y_1	Y_2	$Y_{d/s}$	F_{r1}	V_1	V_2	$V_{d/s}$	L	X	ΔE	THL	E_2/E_1
Y	23A	0.8d	0.8827	2.2068	2.00	1.50	1.65	8.00	2.85	4.8305	10.1641 P-tube	2.0062 P-tube	4.3340 P-tube	15.00	21.50	4.8494	17.3574	0.5241
Y	23B	1.0d	1.2004	2.4008	2.65	1.85	1.85	9,25	3.25	4.5914	10.2299 P-tube	4.3340 P-tube	4.6332 P-tube	20.00	22.00	5.9200	17.8240	0.5463
Y	23C	1.2d	1.4985	2.4975	3.25	2.00	2.00	10.50	4.00	4.5277	10.4889 P-tube	5.4329 P-tube	5.1801 P-tube	18.00	24.00	7.3110	17.3623	0.5524

Figure A70. Experiment 24A

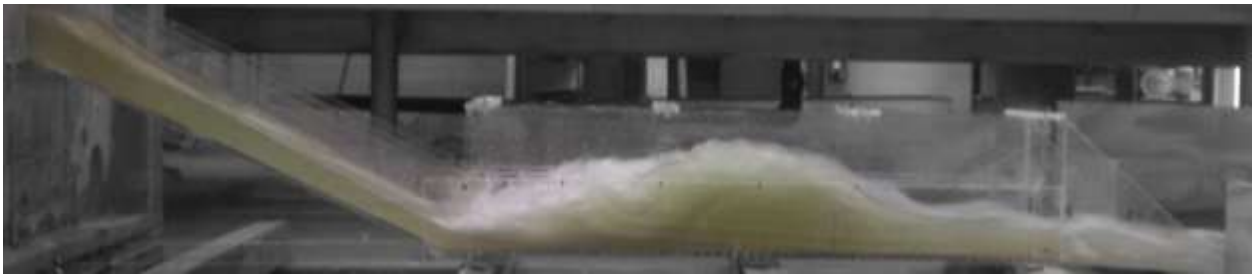

Figure A71. Experiment 24B

Figure A72. Experiment 24C

Table A24. Experiment 24 using open channel flow conditions with 3.5” slotted sill 20” from the end with 6 FFFBs 2” × 2” at 18” from the toe

H.J.	Run	H	Q	$V_{u/s}$	Y_s	Y_{toe}	Y_1	Y_2	$Y_{d/s}$	F_{r1}	V_1	V_2	$V_{d/s}$	L	X	ΔE	THL	E_2/E_1
Y	24A	0.8d	0.9182	2.2955	2.00	1.65	1.65	8.50	2.50	4.5394	9.5516 P-tube	4.0125 P-tube	5.1801 P-tube	16.00	33.00	5.7294	16.2819	0.5513
Y	24B	1.0d	1.1938	2.3876	2.65	1.75	1.75	9.25	2.75	4.4401	9.6216 P-tube	5.5550 P-tube	5.6745 P-tube	16.00	33.00	6.5154	16.3122	0.5611
Y	24C	1.2d	1.4878	2.4797	3.50	2.00	2.13	10.50	3.50	4.2790	10.2299 P-tube	5.1801 P-tube	6.4492 P-tube	15.00	29.50	6.5546	15.0957	0.5777

Figure A73. Experiment 25A

Figure A74. Experiment 25B

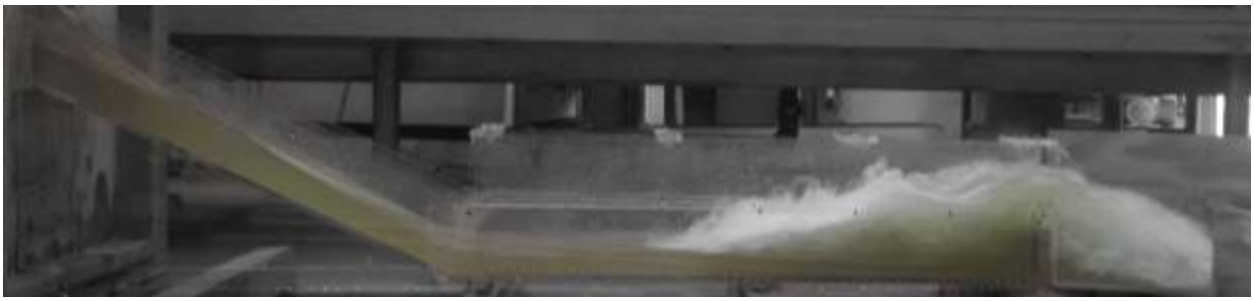

Figure A75. Experiment 25C

Table A25. Experiment 25 using open channel flow conditions with 4.5" slotted sill at the end of culvert

H.J.	Run	H	Q	$V_{u/s}$	Y_s	Y_{toe}	Y_1	Y_2	$Y_{d/s}$	F_{r1}	V_1	V_2	$V_{d/s}$	L	X	ΔE	THL	E_2/E_1
Y	25A	0.8d	o.8872	2.2180	2.00	1.50	1.25	8.50	1.75	5.3666	9.8285 P-tube	1.1583 P-tube	3.4749 P-tube	16.00	31.00	8.9665	19.7167	0.4799
Y	25B	1.0d	1.1837	2.3674	2.50	1.75	1.65	9.25	2.50	4.8617	10.2299 P-tube	1.6381 P-tube	4.1763 P-tube	16.00	31.00	7.1904	19.2943	0.5214
Y	25C	1.2d	1.4852	2.4753	3.50	2.00	2.13	10.75	3.00	4.3335	10.3602 P-tube	2.0062 P-tube	4.4861 P-tube	18.00	39.00	6.9932	19.5917	0.5720

Figure A76. Experiment 26A

Figure A77. Experiment 26B

Figure A78. Experiment 26C

Table A26. Experiment 26 using open channel flow conditions with 4.5” slotted sill at the end of culvert with 6 FFFBs 2” × 2” at 31” from the toe

H.J.	Run	H	Q	$V_{u/s}$	Y_s	Y_{toe}	Y_1	Y_2	$Y_{d/s}$	F_{r1}	V_1	V_2	$V_{d/s}$	L	X	ΔE	THL	E_2/E_1
Y	26A	0.8d	0.8962	2.2405	2.00	1.50	1.50	8.25	1.50	4.9666	9.9641 P-tube	2.3166 P-tube	3.0646 P-tube	16.00	47.00	6.2131	20.4854	0.5122
Y	26B	1.0d	1.2004	2.4008	2.75	1.75	1.75	9.50	1.75	4.7026	10.1904 P-tube	2.8373 P-tube	3.2762 P-tube	18.00	49.00	6.9998	21.3240	0.5358
Y	26C	1.2d	1.4825	2.4708	3.35	2.00	2.00	10.50	2.25	4.4159	10.2299 P-tube	4.0125 P-tube	3.6629 P-tube	19.00	50.00	7.3110	21.5876	0.5636

Figure A79. Experiment 27A

Figure A80. Experiment 27B

Figure A81. Experiment 27C

Table A27. Experiment 27 using pressure flow conditions with 2.5" slotted sill at the end of culvert

H.J.	Run	H	Q	$V_{u/s}$	Y_s	Y_{toe}	Y_1	Y_2	$Y_{d/s}$	F_{r1}	V_1	V_2	$V_{d/s}$	L	X	ΔE	THL	E_2/E_1
Y	27A	0.8d	0.8917	2.2293	2.00	1.50	1.50	9.60	2.50	4.7610	9.5516 P-tube	3.8417 P-tube	3.1509 P-tube	11.00	13.00	9.1345	19.3760	0.5225
Y	27B	1.0d	1.2038	2.4076	2.75	1.75	1.75	11.50	3.50	4.7809	10.3602 P-tube	3.4749 P-tube	3.6629 P-tube	11.00	16.00	11.5624	19.0801	0.5098
Y	27C	1.2d	1.4958	2.4930	3.25	2.13	2.25	12.00	4.00	4.1633	10.2299 P-tube	3.2762 P-tube	6.9498 P-tube	13.00	20.00	8.5820	13.3581	0.5961

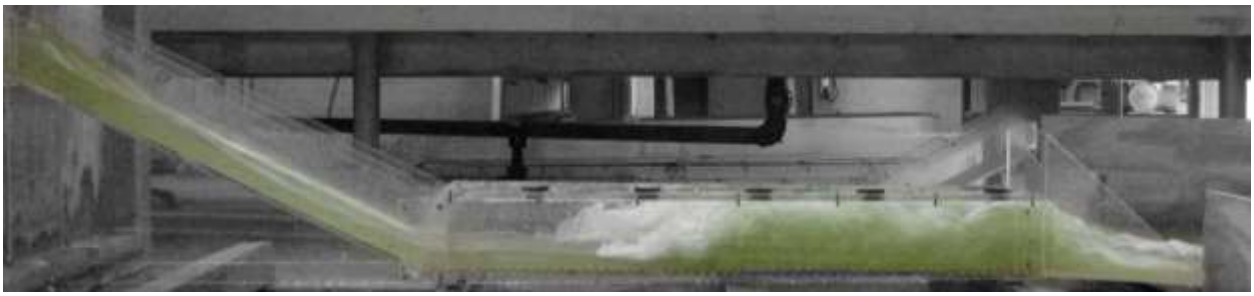

Figure A82. Experiment 28A

Figure A83. Experiment 28B

Figure A84. Experiment 28C

Table A28. Experiment 28 using pressure flow conditions with 2.5” slotted sill at the end of culvert with 6 FFFBs 2” × 2” at 28” from the toe

H.J.	Run	H	Q	$V_{u/s}$	Y_s	Y_{toe}	Y_1	Y_2	$Y_{d/s}$	F_{r1}	V_1	V_2	$V_{d/s}$	L	X	ΔE	THL	E_2/E_1
Y	28A	0.8d	0.9396	1.5660	2.13	1.65	1.50	10.10	1.75	4.9666	9.9641 P-tube	3.0646 P-tube	3.0646 P-tube	12.00	40.00	10.5616	20.3282	0.4999
Y	28B	1.0d	1.2004	2.0007	2.50	2.00	1.85	11.80	2.00	4.6499	10.3602 P-tube	7.6833 P-tube	3.8417 P-tube	12.00	41.00	11.3198	20.3240	0.5218
Y	28C	1.2d	1.4985	2.4975	3.50	2.13	2.25	12.00	2.50	4.3205	10.6160 P-tube	8.1081 P-tube	5.4329 P-tube	16.00	44.00	8.5820	18.3623	0.5961

Figure A85. Experiment 29A

Figure A86. Experiment 29B

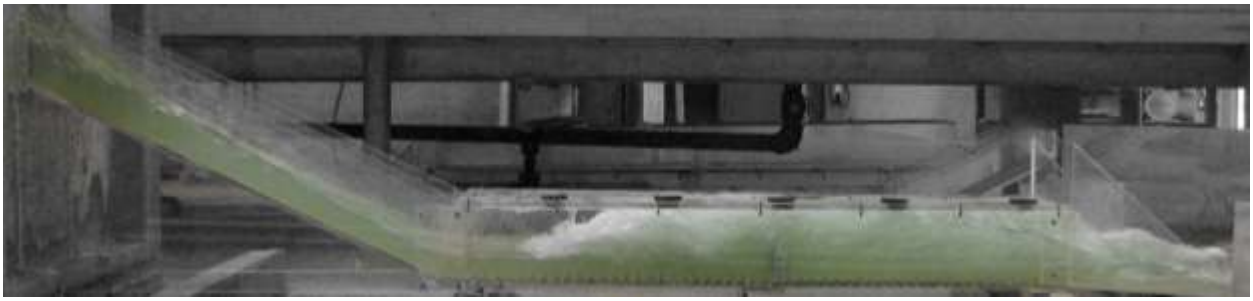

Figure A87. Experiment 29C

Table A29. Experiment 29 using pressure flow conditions with 3” slotted sill 25” from the end of the culvert

H.J.	Run	H	Q	$V_{u/s}$	Y_s	Y_{toe}	Y_1	Y_2	$Y_{d/s}$	F_{r1}	V_1	V_2	$V_{d/s}$	L	X	ΔE	THL	E_2/E_1
Y	29A	0.8d	0.9268	2.3170	2.00	1.50	1.60	10.70	3.00	4.9054	10.1641 P-tube	5.6745 P-tube	3.6629 P-tube	12.00	14.50	11.1143	18.3003	0.5020
Y	29B	1.0d	1.1837	2.3674	2.50	1.85	1.75	11.80	3.00	4.8697	10.5526 P-tube	4.6332 P-tube	3.8417 P-tube	12.00	16.00	12.3653	19.2943	0.4993
Y	29C	1.2d	1.4985	2.4975	3.50	2.00	2.00	12.00	3.50	4.4721	10.3602 P-tube	6.1292 P-tube	3.0646 P-tube	18.00	26.00	10.4167	21.1123	0.5471

Figure A88. Experiment 30A

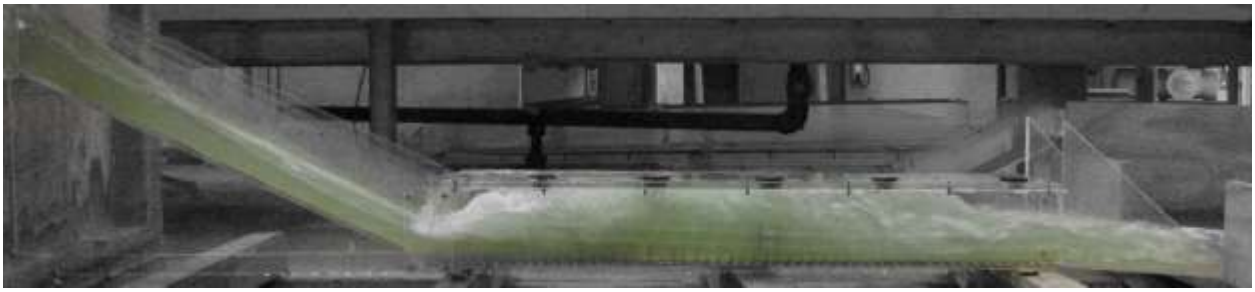

Figure A89. Experiment 30B

Figure A90. Experiment 30C

Table A30. Experiment 30 3” slotted sill 25” from the end of model using pressure flow conditions with 6 FFFBs 2” × 2” at 18” from the toe

H.J.	Run	H	Q	$V_{u/s}$	Y_s	Y_{toe}	Y_1	Y_2	$Y_{d/s}$	F_{r1}	V_1	V_2	$V_{d/s}$	L	X	ΔE	THL	E_2/E_1
Y	30A	0.8d	0.8962	2.2405	2.00	1.85	1.85	11.40	2.75	4.5322	10.0979 P-tube	5.9062 P-tube	4.9143 P-tube	14.00	27.00	10.2995	16.4854	0.5366
Y	30B	1.0d	1.2169	2.4338	2.50	2.00	2.00	11.10	3.00	4.1833	9.6911 P-tube	6.9498 P-tube	5.3080 P-tube	15.00	29.00	8.5088	16.8537	0.5790
Y	30C	1.2d	1.4905	2.4842	3.50	2.25	2.25	12.00	3.50	4.1096	10.0979 P-tube	7.4168 P-tube	4.3340 P-tube	17.00	29.00	8.5820	19.3499	0.5961

Figure A91. Experiment 31A

Figure A92. Experiment 31B

Figure A93. Experiment 31C

Table A31. Experiment 31 using pressure flow conditions with 6 FFFBs 2" × 2" at 18" from the toe

H.J.	Run	H	Q	$V_{u/s}$	Y_s	Y_{toe}	Y_1	Y_2	$Y_{d/s}$	F_{r1}	V_1	V_2	$V_{d/s}$	L	X	ΔE	THL	E_2/E_1
Y	31A	0.8d	0.8962	2.2405	1.75	1.25	1.25	9.70	2.75	5.6569	10.3602 P-tube	4.9143 P-tube	4.6332 P-tube	10.00	12.00	12.5264	16.9854	0.4459
Y	31B	1.0d	1.2267	2.4534	2.50	1.75	1.75	11.80	3.25	4.8697	10.5526 P-tube	4.6332 P-tube	5.0754 P-tube	9.00	12.00	12.3653	17.0716	0.4993
Y	31C	1.2d	1.4958	2.4930	2.50	2.13	2.13	12.00	3.25	4.4669	10.6790 P-tube	2.5900 P-tube	5.6745 P-tube	13.00	14.00	9.4044	16.8581	0.5731

Figure A94. Experiment 32A

Figure A95. Experiment 32B

Figure A96. Experiment 32C

Table A32. Experiment 32 using pressure flow conditions with 2 FFFBs 3” × 3” at the end of culvert

H.J.	Run	H	Q	$V_{u/s}$	Y_s	Y_{toe}	Y_1	Y_2	$Y_{d/s}$	F_{r1}	V_1	V_2	$V_{d/s}$	L	X	ΔE	THL	E_2/E_1
Y	32A	0.8d	0.8962	2.2405	2.00	1.50	1.35	9.26	1.75	5.0918	9.6911 P-tube	2.3166 P-tube	3.0646 P-tube	9.00	9.00	9.8841	19.7157	0.4938
Y	32B	1.0d	1.2332	2.4664	2.50	1.75	1.75	11.66	2.25	4.8226	10.4504 P-tube	3.0646 P-tube	4.1763 P-tube	11.00	13.00	11.9337	19.2872	0.5048
Y	32C	1.2d	1.4958	2.4930	3.50	2.25	2.00	12.00	2.50	4.5277	10.4889 P-tube	4.3340 P-tube	5.6745 P-tube	14.00	22.00	10.4167	17.8581	0.5471

Table A33. Open Channel and Culvert Flow Compared (Source: Singley and Hotchkiss 2010).

Category		Open Channel	Culvert
Geometry	Flow Conditions	Open channel hydraulic principles only.	Open channel, pressurized, orifice, or a combination of multiple flow regimes can be found in culverts.
	Entrance Loss Coefficient	Open channels do not have entrance loss coefficients.	Culverts can have a wide variety of entrance loss coefficients based on shape and size. Current methods are incomplete.
	Aspect Ratio	Typically large aspect ratios.	Smaller aspect ratios that could lead to higher occurrence of dip phenomenon.
Sediment/Debris	Floating Debris	Uniform stream dimensions minimize debris accumulation.	Culvert entrances are prime areas for floating debris to snag.
	Deposition	Uniform stream dimensions during large events reduces the chance of pooling and deposition.	Sediment buildup near a culvert entrance or exit can reduce the effective flow area and in some cases, completely plug a culvert.
	Inlet/Outlet Scour	Open channel does not have an inlet or an outlet.	Often depressions near the edges of the culvert inlet due to the velocity changes as flow is constricted. Deep scour holes are created if mean velocity in the culvert exceeds critical velocity.
	Bed Scour	As flows increase, scoured bed can easily receive sediment from	Higher velocities in culverts potentially makes partial or complete scour of a desinged bed a concern.
Bed Integrity	"Natural" Bed	Stream bed has been formed by stream natrually over time.	Manmade beds created to mimic the natural channel bed have significantly different friction angles when compared to the upstream and downstream reaches.
	Interstitial Flow	Naturally occurring interstitial flow provides habitat for a wide variety of native aquatic life.	Embedded material can be oversized to safeguard against full bed scour. Fines may be scoured out of the culvert through interstitial spaces leaving large volumes of space being filled with water. Flowrates designed for fish passage in a culvert may disappear completely into the interstitial spaces below the surface.
Aquatic Life	Biocomplexity	Natural systems are very complex but each part of the system depends on another.	If a culvert becomes a barrier to any type of plant or animal life, it has potential to change the biological longitudinal connectivity of the river system.
	Vegetation	Vegetation in streams can either increase or decrease the Manning's n value.	Without sunlight, vegetation cannot grow in a long culvert.
	Light	Natural conditions pertaining to light are already acceptable for native aquatic life.	Culvert shade can be an obstacle to some fish species especially in longer culverts.